# NONLINEAR BENDING AND SNAPTHROUGH RESPONSE OF DOUBLY CURVED LAMINATED SHELLS

by

Hooman Aminipour

A Thesis presented to the Faculty of the
American University of Sharjah
College of Engineering
In Partial Fulfillment
of the Requirements
for the Degree of

Master of Science in
Mechanical Engineering

Sharjah, United Arab Emirates

April 2021

**Declaration of Authorship**

I declare that this thesis is my own work and, to the best of my knowledge and belief, it does not contain material published or written by a third party, except where permission has been obtained and/or appropriately cited through full and accurate referencing.

Signed…….Hooman Aminipour…….

Date……22 April 2021……

## Approval Signatures

We, the undersigned, approve the Master's Thesis of Hooman Aminipour.

Thesis Title: Nonlinear Bending and Snapthrough Response of Doubly Curved Laminated Shells.

Date of Defense: 28 April 2021.

| **Name, Title and Affiliation** | **Signature** |
|---|---|
| Dr. Samir Emam<br>Professor, Department of Mechanical Engineering<br>Thesis Advisor | |
| Dr. Maen Alkhader<br>Associate Professor, Department of Mechanical Engineering<br>Thesis Committee Member | |
| Dr. Mohammad AlHamaydeh<br>Professor, Department of Civil Engineering<br>Thesis Committee Member | |
| Dr. Mamoun Abdel-Hafez<br>Head of Department of Mechanical Engineering | |
| Dr. Lotfi Romdhane<br>Associate Dean for Graduate Affairs and Research<br>College of Engineering | |
| Dr. Sameer Al-Asheh<br>Interim Dean<br>College of Engineering | |
| Dr. Mohamed El-Tarhuni<br>Vice Provost for Graduate Studies<br>Office of Graduate Studies | |

**Acknowledgement**

I would like to express my special appreciation to my advisor Dr. Samir Emam who paved my way by providing incredible knowledge, invaluable guidance, tremendous support and patience throughout my research stages. I'm deeply beholden for his great assistance, worthy discussion and suggestions. It has been a great pleasure to have him as an advisor and a professor of two valuable courses.

I would like to thank Dr. Wael Abuzaid, Dr. Maen Alkhader and Dr. Mehdi Ghommem for their valuable courses. A special thanks to Mr. Rami Shunnag and Mr. Wasim Almasri who broadened my knowledge in MATLAB programming and AutoCAD. I would like to thank Mr. Shahid Bux who supported me during my graduate program and guided me through my toughest times. I would like to thank the American University of Sharjah for providing me graduate teaching assistantship as a financial support during my master program.

Most importantly, I appreciate my family who have provided me enormous motivation, endless support and inspiration through all the chapters of my life. My appreciation and admiration are beyond the words for all of the sacrifices that my mother and my father have made for me and my siblings. God bless you my best parents.

Last but not the least, a very special praise to God, the most merciful and compassionate Lord.

به نام خداوند جان و خرد

In the name of God who created the soul and the wisdom

بنی آدم اعضای یکدیگرند — که در آفرینش ز یک گوهرند
چو عضوی به درد آورد روزگار — دگر عضوها را نماند قرار
تو کز محنت دیگران بی غمی — نشاید که نامت نهند آدمی

سعدی شیرازی

Human beings are members of a whole, In creation of one essence and soul.

If one member is afflicted with pain, Other members uneasy will remain.

If you have no sympathy for human pain, The name of “human” you cannot retain!

Saadi Shirazi (Persian poet, 1210-1291). Rhyming translation by M. Aryanpoor.

**Dedication**

To my family,

my Mother and my Father,

with love, admiration, and gratitude.

## Abstract

Shell structures made up of conventional fiber reinforced composite (FRC) laminates find many applications in engineering fields. In contrary to plate structures, shells exhibit two stable equilibrium configurations. Due to excessive loading, shells may largely deform and hence snap from one equilibrium position to the other. Snapthrough or snapback motion involves large deflections and hence it is inherently a nonlinear phenomenon. In this thesis, the nonlinear static response of simply supported doubly curved FRC shells is explored according to the classical laminated theory (CLT) with von Karman geometric nonlinearity. Various types of composites are considered: unidirectional $[0_4]$, symmetric $[0,90]_S$, unsymmetric $[0,0,90,90]$ and antisymmetric $[0,90,0,90]$ laminates. The equations of motion and the associated boundary conditions are derived using the Hamilton's principle. The axial displacements are eliminated from equations of motion by utilizing the Airy stress function and the nonlinear compatibility equation. This reduces the governing equations to two: the compatibility equation and the equation of motion governing the transverse deformation. The Galerkin's approach is used to obtain a reduced-order model (ROM). This discretization leads to a set of nonlinear coupled ordinary differential equations (ODEs). Three modes are retained in the discretization. By setting all time-dependent terms equal to zero, the system of ODEs reduces to a set of nonlinearly coupled algebraic equations which are solved by means of the Newton-Raphson method for the static equilibrium positions and the Jacobian method is used to assess their stability. The effect of the stacking sequence, radii of curvature, curvature ratio and the shell thickness on the nonlinear bending and snapthrough response are investigated.



**Keywords: Nonlinear bending; snapthrough; doubly curved shells; fiber reinforced composite; classical laminated theory; Galerkin's approach.**

## Table of Contents

## List of Figures

## List of Tables

# Chapter 1. Introduction

In this chapter, a brief introduction of the doubly curved FRC shells is provided, the thesis objectives and contribution are outlined, and the thesis organization is presented.

## 1.1. Overview

Cross-ply FRC laminates consist of multiple layers laid down at angles of 0 or 90 degrees. Changing the angle of fibers leads to different material properties of the whole laminate. Therefore, when the laminate is loaded, individual layers deform differently. When shells are transversely loaded, they may largely deform and snap from one equilibrium position to the other if the load exceeds a threshold value. This nonlinear phenomenon is called the snapthrough in the case of loading and snapback in the case of unloading. In the case of nonlinear bending of shells, for a specific range of loadings, there may exist more than one stable equilibrium position. This nonlinear phenomenon is called the bi-stability. If there exists a bi-stable region, the snapthrough and snapback loads are different, the load-deflection curve is discontinuous, and the jump phenomenon occurs between the snapthrough and the snapback loads. On the other hand, in the absence of the bi-stability region, the snapthrough and snapback loads are the same, the load-deflection curve is continuous, and the jump phenomenon disappears. The jump phenomenon may lead to delamination and even the failure of the structure, which makes it important to carefully study the nonlinear bending and snapthrough response of composite shells. There are various parameters such as material properties, stacking sequence of cross ply laminate, radii of curvature, curvature ratio and thickness of the shell which play a significant role in the nonlinear bending of doubly curved shells. The nonlinear bending, the snapthrough, snapback, the jump phenomenon, and the bi-stability highly depend on the material and the geometrical properties of the shell. One of the important aspects that must be considered in the design of FRC shells is to avoid the jump phenomenon by finding out a set of parameters that yields a continuous load-deflection curve and minimize the deflection.

## 1.2. Thesis Objectives

As it is evident from the literature review that will be presented in the next chapter, the nonlinear behavior of doubly curved shells including the nonlinear static

bending, nonlinear dynamics, buckling and postbuckling are investigated by means of different approaches such as the finite element (FE) method, Galerkin's approach, generalized differential quadrature method (GDQM), harmonic differential quadrature method (HDQM) and perturbation technique. A few researchers have utilized the semi-analytical techniques to investigate the nonlinear static bending of doubly curved FRC shells. To the best of the author's knowledge, the nonlinear static bending of simply supported doubly curved FRC shells has not been studied yet on the basis of the classical lamination theory in conjunction with Airy stress function and Galerkin's discretization. The objective of this thesis is to fill this gap by providing a continuum-based model that is capable of capturing the nonlinear bending and snapthrough response of doubly curved FRC shells. Moreover, a parametric study on the influence of the laminate's layup, the shell geometry and thickness on the nonlinear bending and snapthrough response of composite doubly curved shells is presented.

### 1.3. Thesis Contribution

We investigate the nonlinear bending and snapthrough response of simply supported, doubly curved, thin shallow composite shells. Four different cross ply laminates are considered: unidirectional, symmetric, unsymmetric and antisymmetric. The analytical model is based on the extension of the CLT with von Karman geometric nonlinearity. The equations of motion and the associated boundary conditions are derived using the Hamilton's principle. The equations of motion consist of three differential equations that govern the longitudinal displacements in the $x$ and $y$-directions and the lateral deflection in the $z$-direction. The nonlinear compatibility equation along with the Airy stress function are used to eliminate the dependence of the governing equations on the longitudinal displacements. This reduces the governing equations into two: the compatibility equation and the equation of motion in the transverse direction. The Galerkin's approach is used to discretize the equations of motion. The discretized equations are obtained in a general form that is valid for all boundary conditions provided that appropriate trial functions of the stress function and lateral deflection are selected. The nonlinear static bending analysis is studied by solving the nonlinear algebraic equations after neglecting the time-dependent terms. Using the Newton-Raphson method, the algebraic equations are solved and the equilibrium paths are obtained. The stability of the equilibrium solutions is assessed

using the Jacobian method. The model has been validated against the results available in the literature and a good agreement has been obtained. The influence of the laminate's layup, the radii of curvature, the curvature ratio and the thickness on the nonlinear bending, snapthrough, snapback and bi-stability is investigated.

## 1.4. Thesis organization

The remainder of this thesis is organized as follows: Chapter 2 presents the background, a literature review, and the recent developments that are concerned with the nonlinear response of doubly curved FRC shells. Chapter 3 provides the theoretical formulation which includes the kinematic equation, constitutive relations and equations of motion for doubly curved laminated shells. Chapter 4 presents the reduced-order model of the problem that is based on the Galerkin's method. Chapter 5 presents a validation of the proposed model and the results of the nonlinear bending and snapthrough under a variety of material and geometrical parameters. Finally, concluding remarks and future work are presented in Chapter 6.

## Chapter 2. Background and Literature Review

Doubly curved shells find numerous applications in in many engineering fields and industries. Due to their superior properties, shells made up of fiber reinforced laminated composites (FRC) are widely used. In contrary to plate structures, shells exhibit two stable equilibrium configurations. Due to excessive loading, shells may largely deform and hence snap from one equilibrium position to the other. Changing from one stable configuration to the other is called snapthrough in the case of loading and snapback in the case of unloading. Snapthrough or snapback motion involves large deflections and hence it is inherently a nonlinear phenomenon. Many studies were concerned with the nonlinear behavior of doubly curved shells including the nonlinear static bending, nonlinear dynamics, buckling and postbuckling. Various solution methodologies have been proposed to study these nonlinear behaviors which could be categorized to mesh-free and mesh-dependent methods. Next, a brief literature review on the nonlinear bending analysis of shells is presented.

Postbuckling and nonlinear vibration of doubly curved shallow shells were investigated by Chia [1]. He performed his analysis based on Marguerre-type of nonlinearity. The shell with Winkler-Pasternak foundation and an initial imperfection was considered. A method of separation of variables along with the harmonic balance method were used to solve the equations of motion. Chia [2] performed a review on semi-analytical approaches for nonlinear static, postbuckling and nonlinear dynamics of laminated composite plates with various boundary conditions. In the frame work of a shear deformation theory with von Karman nonlinearity, Dennis [3] studied the nonlinear static behavior of laminated shallow cylindrical shells. Galerkin's approach was used to obtain the shells' equilibrium path. On the basis of higher order shear deformations theory, Shen [4] performed a study on the nonlinear bending of simply supported FRC plates under thermomechanical loads. Galerkin's approach coupled with perturbation method were employed to govern the load deflection curve. By utilizing a higher order shear deformation theory in conjunction with perturbation techniques, Shen [5] studied the influence of temperature and moisture on the nonlinear bending behavior of FRC plates. On the basis of an element free approach called reproducing kernel particle method, Chen et al. [6] performed an investigation on the

nonlinear deformation of various structures. Li et al. [7] implemented a combination of Galerkin's approach and reproducing kernel particle method to investigate the large deformation of shell structures. They studied the snapthrough of conical shell, nonlinear deformation of hemispheric, and cylindrical shells. Amabili [8] utilized the Donell's thin shells theory to perform a study on the nonlinear vibration of circular cylindrical panels. The Lagrange equations along with multi-mode method were used to obtain the governing equations which were solved by means of pseudo-arclength continuation technique. The numerical results were presented for both theoretical and experimental approaches. By means of the first-order shear deformation theory with von Karman geometric nonlinearity, Nath et al. [9] studied the nonlinear static and dynamic behavior of FRC plates resting on nonlinear elastic foundation. Chebyshev polynomial series combined with quadratic extrapolation technique of linearization and implicit Houbolt time-marching discretization were employed as a method of solution. Girish and Ramachandra [10] investigated the nonlinear bending and free vibration of doubly curved FRC shells under thermomechanical loading. Reissner's shallow shell theory was employed and discretization was done by the Galerkin's approach. A combination of Newton-Raphson method and Riks technique was used to find the static equilibrium states. Amabili [11] utilized Donnell's and Novozhilov's shell theories to perform an investigation into the nonlinear static and dynamic behavior of simply supported doubly curved shallow shells made of isotropic material. The geometric imperfections were considered and solutions were obtained by implementing the arc-length continuation technique along with the direct time integration. Liew et al. [12] presented a review on the element free (meshless) methods for linear and nonlinear analyses of plates and shells made of FRC and functionally graded materials. Shen [13] presented a two-step perturbation method that can be used to investigate the nonlinear bending, postbuckling and nonlinear dynamics of beams, plates and shells. Alijani and Amabili [14] studied the nonlinear bending and vibration of simply supported rectangular plates taking into account the nonlinearities related to the rotations and thickness deformation. The pseudo arc-length continuation technique and the collocation scheme were implemented to obtain the solution. In the frame work of Donnell's nonlinear shallow shell formulations in conjunction with modified couple stress theory, Ghayesh and Farokhi [15] studied the effect of small scale on the nonlinear bending and free vibration

of doubly curved isotropic microshells. The discretization was done with Galerkin method for fully clamped boundary conditions and a continuation technique was implemented in their study. Farokhi and Ghayesh [16] studied the nonlinear static and forced vibration behavior of doubly curved shallow microshells. The formulation obtained from Novozhilov shell theory and the size dependent behavior was captured by the couple stress theory. Watts et al. [17] adopted the Galerkin's method with moving kriging shape function to study the nonlinear static behavior of corner supported plates and shells. They used a first-order shear deformation theory with von Karman nonlinearity. By making use of Sanders' shell theory with von Karman nonlinearity, Watts et al. [18] analyzed the nonlinear bending of isotropic and FRC conical shells. Discretization was done by the Galerkin's approach and kriging interpolation method was used to estimate the shape functions. The deflection curves were obtained based on Newton-Raphson method along with modified Riks technique. By adopting Reddy's higher order shear deformation theory with von Karman nonlinearity, an analysis was performed on the nonlinear bending of 3-dimensional braided composite cylindrical shells by Zhao et al. [19]. The solution methodology was based on the Galerkin's method along with perturbation technique. Amabili and Reddy [20] introduced a third-order thickness and shear deformation theory with six parameters which is suitable for nonlinear static and dynamic behavior of doubly curved FRC shells. Numerical results were presented for nonlinear static and dynamic behavior of isotropic and FRC circular cylindrical shells which was governed by a software based on the pseudo-arclength continuation and collocation techniques.

Based on the shear deformation theory with von Karman geometric nonlinearity, Reddy and Chao [21] studied the nonlinear bending of simply supported FRC plates. The deflection curves were obtained by the finite element (FE) method. Nonlinear bending of thick laminated FRC plates with different boundary conditions were analyzed based on an extension of Reissner-Mindlin plate theory by Reddy and Chao [22]. The von Karman nonlinearity was taken into consideration and the problem was solved using a FE technique. Reddy and Chao [23] extended their work to investigate the large amplitude vibration, stress distribution as well as linear and nonlinear deflection of thick FRC laminates with various boundary conditions. Noor and Hartley [24] proposed a mixed isoperimetric FE method to deal with nonlinear

bending and postbuckling analysis of FRC shallow shells in which the shear deformation effect was included. Kant and Kommineni [25] employed isoparametric FE to capture the nonlinear static behavior of FRC doubly curved shells. The effect of shear deformation was included in their study. Liao and Reddy [26] implemented degenerated shell element mixed with the beam element to study the nonlinear bending behavior of FRC stiffened shells. The equations were solved by the Newton-Raphson and modified Riks methods. By means of Hellinger-Reissner principle mixed with FE method, a study was performed on the nonlinear static bending and vibration of thin spherical FRC shells by Lee et al. [27]. The static problem solved by using the arc-length technique while the dynamic part was solved based on the Newmark implicit time-integration method. Zhang and Kim [28] established a refined non-conforming triangular plate and shell element. The nonlinear bending analysis of clamped circular plate and postbuckling behavior of hinged cylindrical shell were provided. By reviewing and reproducing the results of more than 40 articles, Sze et al. [29] represented benchmark problems on nonlinear analysis of various structures analyzed by FE method. The selected nonlinear static problems were: deflection of cantilever beams, lifting of slit annular plate, deflection of hemispherical shell with a circular hole at its pole, pulled out open-ended cylindrical shells, pinched cylindrical shell mounted on rigid diaphragms, pinched semi-cylindrical shell, bending and snapthrough of semi-cylindrical roofs. For the last two cases of their analysis, besides the isotropic material, two classes of FRC were taken into consideration. Arciniega and Reddy [30] adopted a tensor based FE method mixed with first order shell theory to study the nonlinear behavior of shells. Most of the investigated structures in this article were presented in the reference [29]. Moreover, postbuckling of plate strips, pinched hyperboloidal FRC shells were studied as well. Besides isotropic and FRC, functionally graded ceramic-metal materials were taken into consideration. In the frame work of a mixed FE method, Urthaler and Reddy [31] studied the nonlinear bending of FRC plate. The first order shear deformation theory with von Karman nonlinearity were employed in that article. Lal et al. [32] implemented a combination of FE method and perturbation technique to study the nonlinear deflection of FRC shell in hygrothermal environment. Higher order shear deformation theory with von Karman nonlinearity were implemented. Rezaiee-Pajand and Arabi [33] proposed a triangular isoparametric FE to examine the nonlinear

behavior of FRC shells under static loads. The shell structures are same as those studied in reference [29]. Shokrieh and Nouri Parkestani [34] proposed a higher order shear deformation theory of doubly curved shells which they used to study the postbuckling and nonlinear bending of isotropic and FRC shells. FE method mixed with arc-length technique were employed to obtain the equilibrium path.

By applying discrete singular convolution technique combined with harmonic differential quadrature method, Civalek [35] studied the nonlinear static and dynamic analysis of simply supported and clamped thin rectangular plate on elastic foundation. Civalek [36] performed a nonlinear dynamic analysis of doubly curved shells made of isotropic material. The proposed method was based on the von Karman-Donnel type equations in which the effect of Winkler-Pasternak elastic foundation was included. Clamped and simply supported boundary conditions were implemented and the governing equations were solved by harmonic differential quadrature method in conjunction with finite difference. In the frame work of first order shear deformation theory with von Karman nonlinearity, Baltacıoglu et al. [37] employed discrete singular convolution technique to analyze large deformation of plate under static load. By means of generalized differential quadrature (GDQ) method, the nonlinear bending of thin isotropic and FRC plates was captured by Bert et al. [38]. Clamped as well as simply supported boundaries were considered and Newton Raphson techniques was implemented to solve the equations of motion. On the basis of first order shear deformation theory with von Karman nonlinearity, Malekzadeh and Setoodeh [39] performed a study about nonlinear deformation of FRC plates. The effect of elastic foundation was examined and GDQ technique was chosen as the solution methodology. Kalbaran and Kurtaran [40] studied the nonlinear static analysis of FRC shells of revolution with variable thickness placed on elastic foundation. The study developed based on the first order shear deformation theory and GDQ method was chosen as the solution analogy. Alamatian and Rezaeepazhand [41] utilized the dynamic relaxation method combined with finite difference discretization to examine the nonlinear bending behavior of FRC plates. The plate has variable cross-section and the analysis was based on the classical lamination theory. On the basis of dynamic relaxation technique and finite difference method, Mehrabian and Golmakani [42] performed an analysis on the nonlinear bending of FRC annular sector plates. First order shear deformation theory

with von Karman nonlinearity was used. Effects of radial stiffener and various boundary conditions were examined.

# Chapter 3. Problem Formulation

In this chapter, we use the Hamilton's principle to derive the equations of motion and the associated boundary conditions of composite thin shallow shells according to the classical lamination theory with von Karman strains.

## 3.1. Kinematic Equations

Consider a doubly curved laminated shallow shell with its orthogonal coordinate system $(x, y, z)$ where the mid-surface curvature lines coincide with $x$ and $y$-directions. The shell is depicted in Figure 3.1, with the dimensions of $L_x, L_y$ and $h$ along the $x, y$ and $z$-directions, respectively, and $R_x$ and $R_y$ are the principal radii of curvature in the $x$ and $y$-directions, respectively. The shell is assumed to have a uniform thickness and constant radii of curvature. According to the classical laminated shell theory, the Kirchhoff hypothesis leads to the following displacement field [43]:

$$u(x, y, z, t) = u_0(x, y, t) - z\,\frac{\partial w_0}{\partial x} + \frac{w_0}{R_x} \tag{3.1}$$

$$v(x, y, z, t) = v_0(x, y, t) - z\,\frac{\partial w_0}{\partial y} + \frac{w_0}{R_y} \tag{3.2}$$

$$w(x, y, z, t) = w_0(x, y, t) \tag{3.3}$$

where $u_0, v_0$ and $w_0$ are the mid-plane displacements in the $x, y$ and $z$-directions, respectively, $\frac{\partial w_0}{\partial x}$ and $\frac{\partial w_0}{\partial y}$ are the rotations of the transverse normal lines. For the sake of clarity, the mid-plane displacements and the rotations are depicted in Figure 3.2. The von Karman strains are defined as

$$\begin{Bmatrix} \varepsilon_{xx} \\ \varepsilon_{yy} \\ \gamma_{xy} \end{Bmatrix} = \begin{Bmatrix} e_{xx} \\ e_{yy} \\ e_{xy} \end{Bmatrix} + z \begin{Bmatrix} \kappa_{xx} \\ \kappa_{yy} \\ \kappa_{xy} \end{Bmatrix} \tag{3.4}$$

where $e_{xx}, e_{yy}$ and $e_{xy}$ are the von Karman membrane strains of the structure's mid-plane and $\kappa_{xx}, \kappa_{yy}$ and $\kappa_{xy}$ are the flexural (bending) strains which are known as the midplane's curvatures defined as

$$\{e\} = \begin{Bmatrix} e_{xx} \\ e_{yy} \\ e_{xy} \end{Bmatrix} = \begin{Bmatrix} \dfrac{\partial u_0}{\partial x} + \dfrac{1}{2}\left(\dfrac{\partial w_0}{\partial x}\right)^2 + \dfrac{w_0}{R_x} \\ \dfrac{\partial v_0}{\partial y} + \dfrac{1}{2}\left(\dfrac{\partial w_0}{\partial y}\right)^2 + \dfrac{w_0}{R_y} \\ \dfrac{\partial u_0}{\partial y} + \dfrac{\partial v_0}{\partial x} + \dfrac{\partial w_0}{\partial x}\dfrac{\partial w_0}{\partial y} \end{Bmatrix} \tag{3.5}$$

$$\{\kappa\} = \begin{Bmatrix} \kappa_{xx} \\ \kappa_{yy} \\ \kappa_{xy} \end{Bmatrix} = \begin{Bmatrix} -\dfrac{\partial^2 w_0}{\partial x^2} \\ -\dfrac{\partial^2 w_0}{\partial y^2} \\ -2\dfrac{\partial^2 w_0}{\partial x \partial y} \end{Bmatrix} \tag{3.6}$$

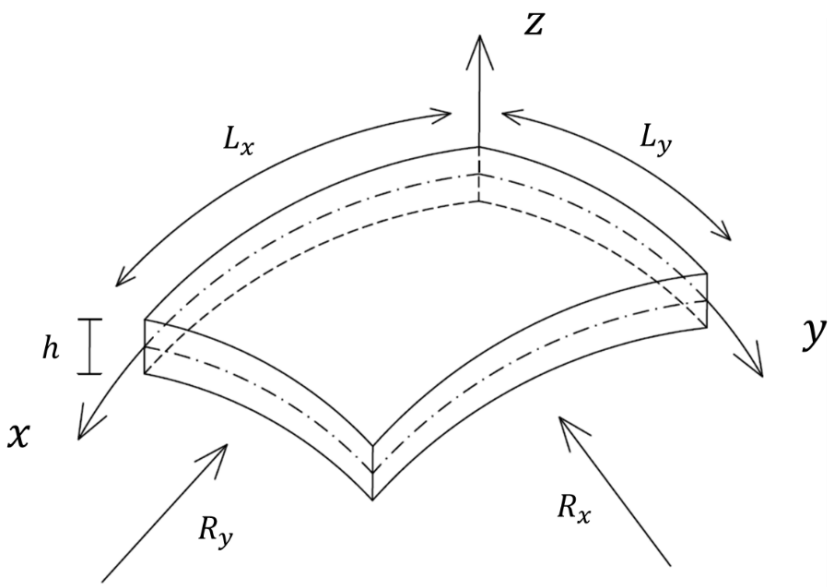


Figure 3.1: A schematic of a doubly curved laminated shell and the associated coordinate system.

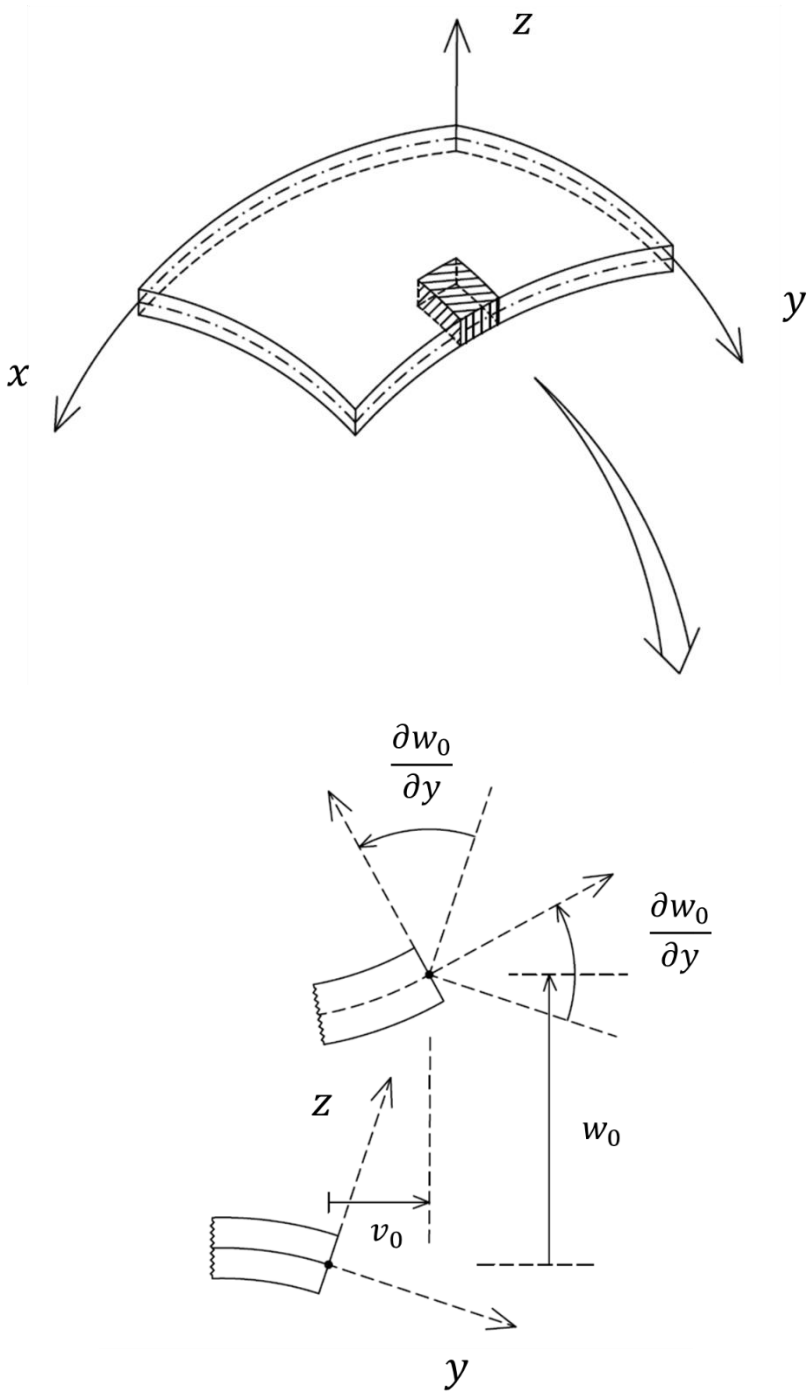


Figure 3.2: An undeformed and deformed elements of doubly curved shell under Kirchhoff hypothesis and the associated mid-plane displacements and rotations of transverse normal lines.

According to the classical shell theory, Love's approximations outlined below are assumed to hold [43-45]

- The shell thickness is small in comparison with the radii of curvature $\left(\frac{h}{R_x} \ll 1\ ,\ \frac{h}{R_y} \ll 1\right)$.
- Normal and shear stresses in the direction normal to the plate mid-surface are negligible compared to other stresses $(\sigma_{zz} = \tau_{xz} = \tau_{yz} = 0)$.
- Due to the infinitesimal strains, the second-order terms in the strain-displacement relations are neglected.
- Straight lines perpendicular to the mid-surface (i.e., transverse normal) before deformation remain straight and perpendicular after deformation.
- There is no change in the length of transverse normal (i.e., they are inextensible).
- Rotation of the transverse normal lines take place in a way that they remain perpendicular to the mid-surface after deformation.

The last three assumptions are known as Kirchhoff's hypothesis. The fourth assumption demonstrates the independency of the transverse displacement $w$ of the transverse coordinate which can be seen in the equation (3.3), whereas the axial displacements $u$ and $v$ vary linearly in the thickness direction (equations (3.1) and (3.2)). The fifth assumption results in zero transverse normal strain $(\varepsilon_{zz} = 0)$. The last assumption implies that the transverse shear strains are zero $(\gamma_{xz} = 0,\ \gamma_{yz} = 0)$.

### 3.2. Lamina Constitutive Equations

The inplane stress-strain relations for the $k^{th}$ lamina in the structure's coordinate system are given by

$$\begin{Bmatrix}\sigma_{xx}\\ \sigma_{yy}\\ \tau_{xy}\end{Bmatrix}^k = \begin{bmatrix}\bar{Q}_{11} & \bar{Q}_{12} & \bar{Q}_{16}\\ \bar{Q}_{12} & \bar{Q}_{22} & \bar{Q}_{26}\\ \bar{Q}_{16} & \bar{Q}_{26} & \bar{Q}_{66}\end{bmatrix}^k \begin{Bmatrix}\varepsilon_{xx}\\ \varepsilon_{yy}\\ \gamma_{xy}\end{Bmatrix}^k \tag{3.7}$$

where $\sigma_{ij}, \tau_{ij}, \varepsilon_{ij}$ and $\gamma_{ij}$ are the normal stresses, shear stresses, normal strains and shear strains, respectively; $\bar{Q}_{ij}$ are the reduced transformed stiffness constants from the material coordinates, $n_1, n_2$ and $n_3$ to the structure coordinates $x, y$ and $z$. Figure 3.3 shows the relation between the material coordinates and the structure coordinates. The reduced transformed stiffness coefficient matrix can be obtained from the plane stress stiffness coefficients as follows [43]:

$$\begin{bmatrix} \bar{Q}_{11} & \bar{Q}_{12} & \bar{Q}_{16} \\ \bar{Q}_{12} & \bar{Q}_{22} & \bar{Q}_{26} \\ \bar{Q}_{16} & \bar{Q}_{26} & \bar{Q}_{66} \end{bmatrix} = T^{-1} \begin{bmatrix} Q_{11} & Q_{12} & 0 \\ Q_{12} & Q_{22} & 0 \\ 0 & 0 & Q_{66} \end{bmatrix} \begin{bmatrix} 1 & 0 & 0 \\ 0 & 1 & 0 \\ 0 & 0 & 2 \end{bmatrix} T \begin{bmatrix} 1 & 0 & 0 \\ 0 & 1 & 0 \\ 0 & 0 & 2 \end{bmatrix}^{-1} \tag{3.8}$$

where $T$ is a transformation matrix that transforms the stresses, strains and the material constants from the material coordinates to the structure coordinates and defined as [43]

$$T = \begin{bmatrix} m^2 & n^2 & 2mn \\ n^2 & m^2 & -2mn \\ -mn & mn & m^2 - n^2 \end{bmatrix} \tag{3.9}$$

where $m = cos\,\theta$ and $n = sin\,\theta$ in which $\theta$ is the angle that the fiber makes with respect to the positive $x$- axis, as shown in Figure 3.3.

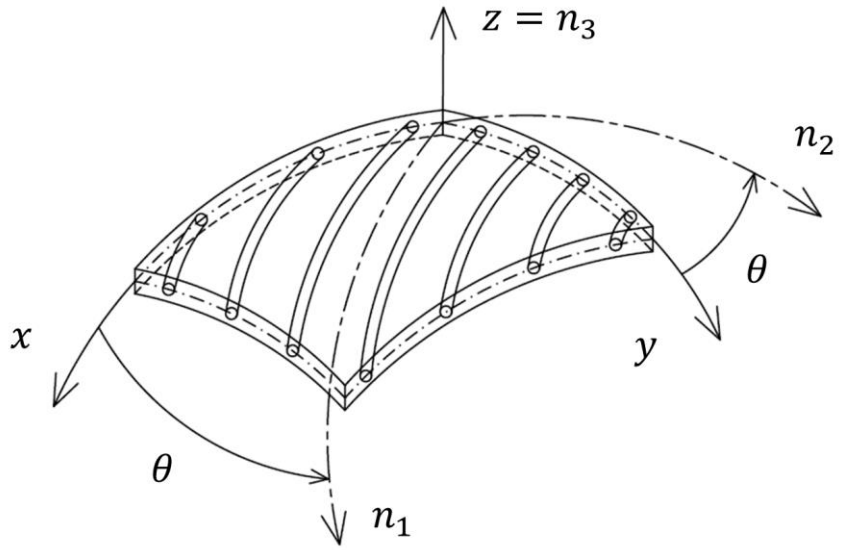


Figure 3.3: Structure coordinates $(x, y, z)$ versus material coordinates $(n_1, n_2, n_3)$. Curved tubes represent the fibers.

The stiffness constants $Q_{ij}$ in equation (3.8) are defined as [43]

$$Q_{11} = \frac{E_{11}}{1 - v_{12}\, v_{21}} \tag{3.10}$$

$$Q_{12} = Q_{21} = \frac{v_{12}\, E_{22}}{1 - v_{12}\, v_{21}} \tag{3.11}$$

$$Q_{22} = \frac{E_{22}}{1 - v_{12}\, v_{21}} \tag{3.12}$$

$$Q_{66} = G_{12} \tag{3.13}$$

$$v_{21} = \frac{E_{22}\, v_{12}}{E_{11}} \tag{3.14}$$

where $E_{11}, E_{22}$ and $G_{12}$ are the longitudinal, transverse and shear modulus respectively, $v_{12}$ and $v_{21}$ are the Poisson's ratios. For an isotropic material, the elastic stiffness constants $Q_{ij}$ reduce to

$$Q_{11} = Q_{22} = \frac{E}{1 - v^2} \tag{3.15}$$

$$Q_{11} = Q_{22} = \frac{E}{1 - v^2} \tag{3.16}$$

$$Q_{33} = \frac{E}{2\,(1 + v)} \tag{3.17}$$

$$Q_{16} = Q_{61} = Q_{26} = Q_{62} = 0 \tag{3.18}$$

### 3.3. Equations of Motion

The equations of motion and the associated boundary conditions are obtained using the Hamilton's principle which states that

$$\int_{t_0}^{t_f} [\delta T - \delta U + \delta W_F]\, dt = 0 \tag{3.19}$$

where $\delta$ is the first variation, $T$ is the kinetic energy, $U$ is the strain energy, $W_F$ is the virtual work done by the nonpotential external forces, and $t_0$ and $t_f$ are two instances of time. The first variation of the kinetic energy, $T$, is defined as

$$\int_{t_0}^{t_f} \delta T \, dt = \delta \int_{t_0}^{t_f} \iiint \frac{1}{2} \rho \left( \frac{\partial w}{\partial t} \right)^2 dV \, dt \tag{3.20}$$

where $\rho$ is the material density and the inplane kinetic energy is ignored. Applying the first variation, we obtain

$$\begin{aligned} \int_{t_0}^{t_f} \delta T \, dt &= \frac{1}{2} \rho \int_{t_0}^{t_f} \iiint \delta \left( \frac{\partial w}{\partial t} \right)^2 dV \, dt = \int_{t_0}^{t_f} \iiint \rho \frac{\partial w}{\partial t} \frac{\partial (\delta w)}{\partial t} dV \, dt \\ &= \iiint \int_{t_0}^{t_f} \rho \frac{\partial w}{\partial t} \frac{\partial (\delta w)}{\partial t} \, dt \, dV \\ &= \iiint \rho \left\{ \left[ \frac{\partial w}{\partial t} \delta w \right]_{t=t_0}^{t=t_f} - \int_{t_0}^{t_f} \frac{\partial^2 w}{\partial t^2} \delta w \, dt \right\} dV \end{aligned} \tag{3.21}$$

The variation takes place over a frozen time thus we have

$$\left( \frac{\partial w}{\partial t} \delta w \right)_{t=t_0} = \left( \frac{\partial w}{\partial t} \delta w \right)_{t=t_f} \tag{3.22}$$

Then equation (3.21) in light of equations (3.3) and (3.20) becomes

$$\begin{aligned} \int_{t_0}^{t_f} \delta T \, dt &= - \int_{t_0}^{t_f} \iiint \rho \frac{\partial^2 w_0}{\partial t^2} \delta w_0 \, dz \, dx \, dy \, dt \\ &= - \int_{t_0}^{t_f} \iint I_0 \frac{\partial^2 w_0}{\partial t^2} \delta w_0 \, dA \, dt \end{aligned} \tag{3.23}$$

where $I_0$ represents the mass moment of inertia defined as

$$I_0 = \int_{\frac{-h}{2}}^{\frac{h}{2}} \rho \, dz = \rho h \tag{3.24}$$

The first variation of strain energy, $U$, is given by

$$\begin{aligned} \delta U &= \iiint \left( \sigma_{xx} \delta \varepsilon_{xx} + \sigma_{yy} \delta \varepsilon_{yy} + \tau_{xy} \delta \gamma_{xy} \right) dV \\ &= \iiint \left[ \sigma_{xx} (\delta e_{xx} + z \, \delta \kappa_{xx}) + \sigma_{yy} \left( \delta e_{yy} + z \, \delta \kappa_{yy} \right) \right. \\ &\left. + \tau_{xy} \left( \delta e_{xy} + z \, \delta \kappa_{xy} \right) \right] dx \, dy \, dz \end{aligned} \tag{3.25}$$

According to equations (3.4)-(3.7), the normal and shear stresses $(\sigma_{xx}, \sigma_{yy}, \tau_{xy})$ are functions of $x, y, z$ and $t$. While on the basis of equations (3.5) and (3.6), membrane strains $(e_{xx}, e_{yy}, e_{xy})$ as well as the midplane's curvatures $(\kappa_{xx}, \kappa_{yy}, \kappa_{xy})$ are only functions of $x, y$ and $t$. By taking these facts into consideration, equation (3.25) could be divided into the following integrals:

$$\begin{aligned}\iiint \sigma_{xx}\delta\varepsilon_{xx}\, dV &= \iint \left\{ \int_{\frac{-h}{2}}^{\frac{h}{2}} \sigma_{xx}(\delta e_{xx} + z\,\delta\kappa_{xx}) dz \right\} dx\, dy \\ &= \iint \left\{ \delta e_{xx} \int_{\frac{-h}{2}}^{\frac{h}{2}} \sigma_{xx}\, dz + \delta\kappa_{xx} \int_{\frac{-h}{2}}^{\frac{h}{2}} z\,\sigma_{xx}\, dz \right\} dx\, dy \\ &= \iint [N_{xx}\delta e_{xx} + M_{xx}\delta\kappa_{xx}] dA \end{aligned} \tag{3.26}$$

$$\begin{aligned}\iiint \sigma_{yy}\delta\varepsilon_{yy}\, dV &= \iint \left\{ \int_{\frac{-h}{2}}^{\frac{h}{2}} \sigma_{yy}(\delta e_{yy} + z\,\delta\kappa_{yy})\, dz \right\} dx\, dy \\ &= \iint \left\{ \delta e_{yy} \int_{\frac{-h}{2}}^{\frac{h}{2}} \sigma_{yy}\, dz + \delta\kappa_{yy} \int_{\frac{-h}{2}}^{\frac{h}{2}} z\,\sigma_{yy}\, dz \right\} dx\, dy \\ &= \iint \left[ N_{yy}\delta e_{yy} + M_{yy}\delta\kappa_{yy} \right] dA \end{aligned} \tag{3.27}$$

$$\begin{aligned}\iiint \tau_{xy}\delta\gamma_{xy}\, dV &= \iint \left\{ \int_{\frac{-h}{2}}^{\frac{h}{2}} \sigma_{xy}(\delta e_{xy} + z\,\delta\kappa_{xy}) dz \right\} dx\, dy \\ &= \iint \left\{ \delta e_{xy} \int_{\frac{-h}{2}}^{\frac{h}{2}} \sigma_{xy}\, dz + \delta\kappa_{xy} \int_{\frac{-h}{2}}^{\frac{h}{2}} z\,\sigma_{xy}\, dz \right\} dx\, dy \\ &= \iint [N_{xy}\delta e_{xy} + M_{xy}\delta\kappa_{xy}] dA \end{aligned} \tag{3.28}$$

where $N_{ij}$ are the inplane force stress resultants and $M_{ij}$ are the moment stress resultants that are defined as

$$\begin{Bmatrix} N_{xx} \\ N_{yy} \\ N_{xy} \end{Bmatrix} = \int_{\frac{-h}{2}}^{\frac{h}{2}} \begin{Bmatrix} \sigma_{xx} \\ \sigma_{yy} \\ \tau_{xy} \end{Bmatrix} dz \tag{3.29}$$

$$\begin{Bmatrix} M_{xx} \\ M_{yy} \\ M_{xy} \end{Bmatrix} = \int_{\frac{-h}{2}}^{\frac{h}{2}} \begin{Bmatrix} \sigma_{xx} \\ \sigma_{yy} \\ \tau_{xy} \end{Bmatrix} z\, dz \tag{3.30}$$

Figure 3.4 demonstrates these stress resultants acting on a shell element where the internal shear and normal forces, and bending moments are shown.

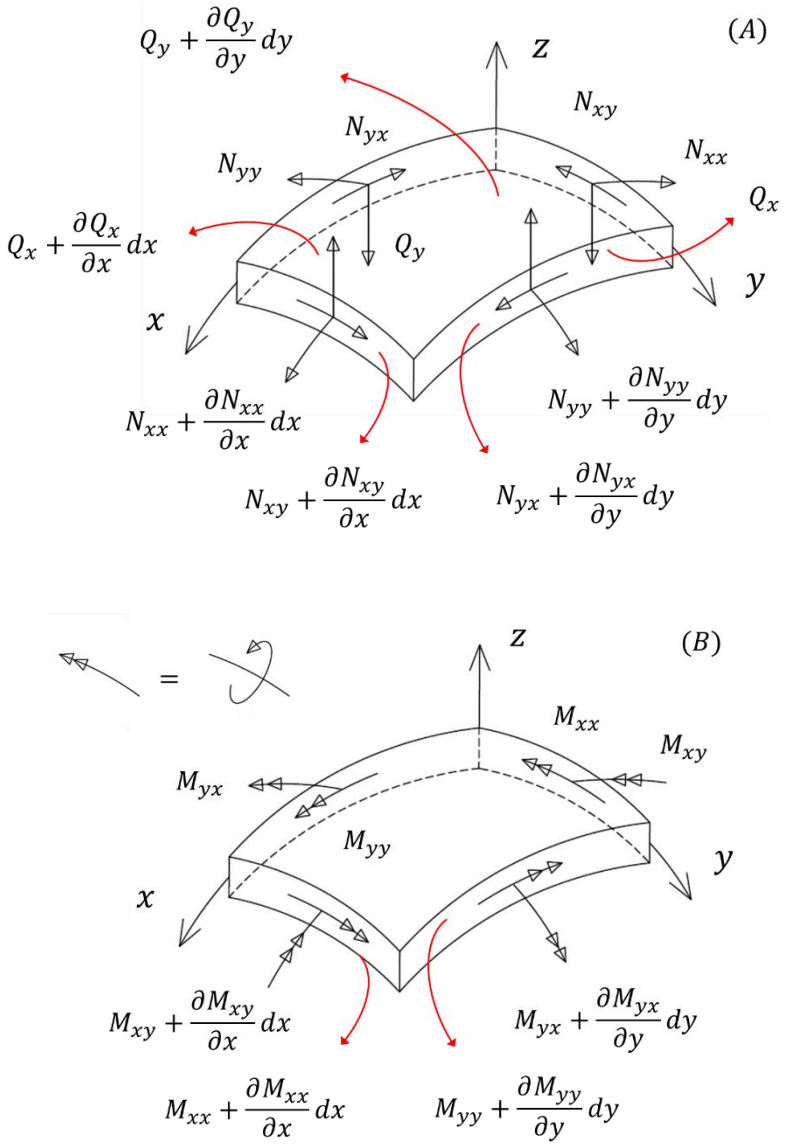


Figure 3.4: (A) Force resultants and (B) moment resultants acting on a shell element.

According to Hook's law, equation (3.7), and the strain-displacement relations, equations (3.4)-(3.6), the force and moment stress resultants, equations (3.29) and (3.30), could be rearranged as

$$\begin{aligned} N_{xx} &= \int_{\frac{-h}{2}}^{\frac{h}{2}} \sigma_{xx}\, dz = \int_{\frac{-h}{2}}^{\frac{h}{2}} \left[\bar{Q}_{11}\, \varepsilon_{xx} + \bar{Q}_{12}\, \varepsilon_{yy} + \bar{Q}_{16}\, \gamma_{xy}\right] dz \\ &= \int_{\frac{-h}{2}}^{\frac{h}{2}} \left[\bar{Q}_{11}\, (e_{xx} + z\, \kappa_{xx}) + \bar{Q}_{12}\, \left(e_{yy} + z\, \kappa_{yy}\right)\right. \\ &\left. + \bar{Q}_{16}\, \left(e_{xy} + z\, \kappa_{xy}\right)\right] dz \\ &= A_{11}\, e_{xx} + B_{11}\, \kappa_{xx} + A_{12}\, e_{yy} + B_{12}\, \kappa_{yy} + A_{16}\, e_{xy} \\ &+ B_{16}\, \kappa_{xy} \end{aligned} \tag{3.31}$$

$$\begin{aligned} N_{yy} &= \int_{\frac{-h}{2}}^{\frac{h}{2}} \sigma_{yy}\, dz = \int_{\frac{-h}{2}}^{\frac{h}{2}} \left[\bar{Q}_{12}\, \varepsilon_{xx} + \bar{Q}_{22}\, \varepsilon_{yy} + \bar{Q}_{26}\, \gamma_{xy}\right] dz \\ &= \int_{\frac{-h}{2}}^{\frac{h}{2}} \left[\bar{Q}_{12}\, (e_{xx} + z\, \kappa_{xx}) + \bar{Q}_{22}\, \left(e_{yy} + z\, \kappa_{yy}\right)\right. \\ &\left. + \bar{Q}_{26}\, \left(e_{xy} + z\, \kappa_{xy}\right)\right] dz \\ &= A_{12}\, e_{xx} + B_{12}\, \kappa_{xx} + A_{22}\, e_{yy} + B_{22}\, \kappa_{yy} + A_{26}\, e_{xy} \\ &+ B_{26}\, \kappa_{xy} \end{aligned} \tag{3.32}$$

$$\begin{aligned} N_{xy} &= \int_{\frac{-h}{2}}^{\frac{h}{2}} \tau_{xy}\, dz = \int_{\frac{-h}{2}}^{\frac{h}{2}} \left[\bar{Q}_{16}\, \varepsilon_{xx} + \bar{Q}_{26}\, \varepsilon_{yy} + \bar{Q}_{66}\, \gamma_{xy}\right] dz \\ &= \int_{\frac{-h}{2}}^{\frac{h}{2}} \left[\bar{Q}_{16}\, (e_{xx} + z\, \kappa_{xx}) + \bar{Q}_{26}\, \left(e_{yy} + z\, \kappa_{yy}\right)\right. \\ &\left. + \bar{Q}_{66}\, \left(e_{xy} + z\, \kappa_{xy}\right)\right] dz \\ &= A_{16}\, e_{xx} + B_{16}\, \kappa_{xx} + A_{26}\, e_{yy} + B_{26}\, \kappa_{yy} + A_{66}\, e_{xy} \\ &+ B_{66}\, \kappa_{xy} \end{aligned} \tag{3.33}$$

$$M_{xx} = \int_{\frac{-h}{2}}^{\frac{h}{2}} \sigma_{xx}\, z\, dz = \int_{\frac{-h}{2}}^{\frac{h}{2}} \left[\bar{Q}_{11}\, \varepsilon_{xx} + \bar{Q}_{12}\, \varepsilon_{yy} + \bar{Q}_{16}\, \gamma_{xy}\right] z\, dz$$

$$= \int_{\frac{-h}{2}}^{\frac{h}{2}} \left[\bar{Q}_{11}\, (e_{xx} + z\, \kappa_{xx}) + \bar{Q}_{12}\, \left(e_{yy} + z\, \kappa_{yy}\right)\right.$$

$$\left. + \bar{Q}_{16}\, \left(e_{xy} + z\, \kappa_{xy}\right)\right] z\, dz$$

$$= B_{11}\, e_{xx} + D_{11}\, \kappa_{xx} + B_{12}\, e_{yy} + D_{12}\, \kappa_{yy} + B_{16}\, e_{xy}$$

$$+ D_{16}\, \kappa_{xy} \tag{3.34}$$

$$M_{yy} = \int_{\frac{-h}{2}}^{\frac{h}{2}} \sigma_{yy}\, z\, dz = \int_{\frac{-h}{2}}^{\frac{h}{2}} \left[\bar{Q}_{12}\, \varepsilon_{xx} + \bar{Q}_{22}\, \varepsilon_{yy} + \bar{Q}_{26}\, \gamma_{xy}\right] z\, dz$$

$$= \int_{\frac{-h}{2}}^{\frac{h}{2}} \left[\bar{Q}_{12}\, (e_{xx} + z\, \kappa_{xx}) + \bar{Q}_{22}\, \left(e_{yy} + z\, \kappa_{yy}\right)\right.$$

$$\left. + \bar{Q}_{26}\, \left(e_{xy} + z\, \kappa_{xy}\right)\right] z\, dz$$

$$= B_{12}\, e_{xx} + D_{12}\, \kappa_{xx} + B_{22}\, e_{yy} + D_{22}\, \kappa_{yy} + B_{26}\, e_{xy}$$

$$+ D_{26}\, \kappa_{xy} \tag{3.35}$$

$$M_{xy} = \int_{\frac{-h}{2}}^{\frac{h}{2}} \tau_{xy}\, z\, dz = \int_{\frac{-h}{2}}^{\frac{h}{2}} \left[\bar{Q}_{16}\, \varepsilon_{xx} + \bar{Q}_{26}\, \varepsilon_{yy} + \bar{Q}_{66}\, \gamma_{xy}\right] z\, dz$$

$$= \int_{\frac{-h}{2}}^{\frac{h}{2}} \left[\bar{Q}_{16}\, (e_{xx} + z\, \kappa_{xx}) + \bar{Q}_{26}\, \left(e_{yy} + z\, \kappa_{yy}\right)\right.$$

$$\left. + \bar{Q}_{66}\, \left(e_{xy} + z\, \kappa_{xy}\right)\right] z\, dz$$

$$= B_{16}\, e_{xx} + D_{16}\, \kappa_{xx} + B_{26}\, e_{yy} + D_{26}\, \kappa_{yy} + B_{66}\, e_{xy}$$

$$+ D_{66}\, \kappa_{xy} \tag{3.36}$$

where $A_{ij}, B_{ij}$ and $D_{ij}$ denote the extensional, bending-extensional coupling, and bending stiffness constants, respectively, defined as

$$A_{ij} = \sum_{k=1}^{N_c} \int_{z_k}^{z_{k+1}} \bar{Q}_{ij}^{k}\, dz = \sum_{k=1}^{N_c} \bar{Q}_{ij}^{k}\, (z_{k+1} - z_k) \tag{3.37}$$

$$B_{ij} = \sum_{k=1}^{N_c} \int_{z_k}^{z_{k+1}} \bar{Q}_{ij}^k \, z \, dz = \sum_{k=1}^{N_c} \frac{1}{2} \bar{Q}_{ij}^k \, (z_{k+1}^2 - z_k^2) \tag{3.38}$$

$$D_{ij} = \sum_{k=1}^{N_c} \int_{z_k}^{z_{k+1}} \bar{Q}_{ij}^k \, z^2 \, dz = \sum_{k=1}^{N_c} \frac{1}{3} \bar{Q}_{ij}^k \, (z_{k+1}^3 - z_k^3) \tag{3.39}$$

where $N_c$ is the number of layers of the composite shell.

Equations (3.31)-(3.36) could be written in a matrix form as

$$\begin{Bmatrix} N_{xx} \\ N_{yy} \\ N_{xy} \end{Bmatrix} = \begin{bmatrix} A_{11} & A_{12} & A_{16} \\ A_{12} & A_{22} & A_{26} \\ A_{16} & A_{26} & A_{66} \end{bmatrix} \begin{Bmatrix} e_{xx} \\ e_{yy} \\ e_{xy} \end{Bmatrix} + \begin{bmatrix} B_{11} & B_{12} & B_{16} \\ B_{12} & B_{22} & B_{26} \\ B_{16} & B_{26} & B_{66} \end{bmatrix} \begin{Bmatrix} \kappa_{xx} \\ \kappa_{yy} \\ \kappa_{xy} \end{Bmatrix} \tag{3.40}$$

$$\begin{Bmatrix} M_{xx} \\ M_{yy} \\ M_{xy} \end{Bmatrix} = \begin{bmatrix} B_{11} & B_{12} & B_{16} \\ B_{12} & B_{22} & B_{26} \\ B_{16} & B_{26} & B_{66} \end{bmatrix} \begin{Bmatrix} e_{xx} \\ e_{yy} \\ e_{xy} \end{Bmatrix} + \begin{bmatrix} D_{11} & D_{12} & D_{16} \\ D_{12} & D_{22} & D_{26} \\ D_{16} & D_{26} & D_{66} \end{bmatrix} \begin{Bmatrix} \kappa_{xx} \\ \kappa_{yy} \\ \kappa_{xy} \end{Bmatrix} \tag{3.41}$$

The first variation of the normal and shear strains are defined as

$$\begin{Bmatrix} \delta e_{xx} \\ \delta e_{yy} \\ \delta e_{xy} \end{Bmatrix} = \begin{Bmatrix} \dfrac{\partial(\delta u_0)}{\partial x} + \dfrac{\partial(\delta w_0)}{\partial x}\dfrac{\partial w_0}{\partial x} + \dfrac{\delta w_0}{R_x} \\ \dfrac{\partial(\delta v_0)}{\partial y} + \dfrac{\partial(\delta w_0)}{\partial y}\dfrac{\partial w_0}{\partial y} + \dfrac{\delta w_0}{R_y} \\ \dfrac{\partial(\delta u_0)}{\partial y} + \dfrac{\partial(\delta v_0)}{\partial x} + \dfrac{\partial(\delta w_0)}{\partial x}\dfrac{\partial w_0}{\partial y} + \dfrac{\partial w_0}{\partial x}\dfrac{\partial(\delta w_0)}{\partial y} \end{Bmatrix} \tag{3.42}$$

$$\begin{Bmatrix} \delta\kappa_{xx} \\ \delta\kappa_{yy} \\ \delta\kappa_{xy} \end{Bmatrix} = \begin{Bmatrix} -\dfrac{\partial^2(\delta w_0)}{\partial x^2} \\ -\dfrac{\partial^2(\delta w_0)}{\partial y^2} \\ -2\dfrac{\partial^2(\delta w_0)}{\partial x \partial y} \end{Bmatrix} \tag{3.43}$$

Substituting equations (3.42) and (3.43) into equations (3.26)-(3.28) and applying the integration by parts, one may find the following equations:

$$\iiint \sigma_{xx}\delta\varepsilon_{xx}\,dV = \iint [N_{xx}\delta e_{xx} + M_{xx}\delta\kappa_{xx}]\,dA$$

$$= \int_0^{L_y}\int_0^{L_x}\left[N_{xx}\left(\frac{\partial(\delta u_0)}{\partial x} + \frac{\partial(\delta w_0)}{\partial x}\frac{\partial w_0}{\partial x} + \frac{\delta w_0}{R_x}\right) - M_{xx}\frac{\partial^2(\delta w_0)}{\partial x^2}\right]dx\,dy$$

$$= \int_0^{L_y}\left\{\left[N_{xx}\delta u_0 + N_{xx}\frac{\partial w_0}{\partial x}\delta w_0 - M_{xx}\frac{\partial(\delta w_0)}{\partial x}\right]_{x=0}^{x=L_x} - \int_0^{L_x}\left[\frac{\partial N_{xx}}{\partial x}\delta u_0 + \delta w_0\frac{\partial}{\partial x}\left(N_{xx}\frac{\partial w_0}{\partial x}\right) - \frac{\partial M_{xx}}{\partial x}\frac{\partial(\delta w_0)}{\partial x} - \frac{1}{R_x}N_{xx}\delta w_0\right]dx\right\}dy$$

$$= \int_0^{L_y}\left\{\left[N_{xx}\delta u_0 + N_{xx}\frac{\partial w_0}{\partial x}\delta w_0 - M_{xx}\frac{\partial(\delta w_0)}{\partial x} + \frac{\partial M_{xx}}{\partial x}\delta w_0\right]_{x=0}^{x=L_x} - \int_0^{L_x}\left[\frac{\partial N_{xx}}{\partial x}\delta u_0 + \delta w_0\frac{\partial}{\partial x}\left(N_{xx}\frac{\partial w_0}{\partial x}\right) + \frac{\partial^2 M_{xx}}{\partial x^2}\delta w_0 - \frac{1}{R_x}N_{xx}\delta w_0\right]dx\right\}dy \qquad (3.44)$$

$$\iiint \sigma_{yy}\delta\varepsilon_{yy}\,dV = \iint \left[N_{yy}\delta e_{yy} + M_{yy}\delta\kappa_{yy}\right]dA$$

$$= \int_0^{L_x}\int_0^{L_y}\left[N_{yy}\left(\frac{\partial(\delta v_0)}{\partial y} + \frac{\partial(\delta w_0)}{\partial y}\frac{\partial w_0}{\partial y} + \frac{\delta w_0}{R_y}\right) - M_{yy}\frac{\partial^2(\delta w_0)}{\partial y^2}\right]dy\,dx$$

$$= \int_0^{L_x}\left[N_{yy}\delta v_0 + N_{yy}\frac{\partial w_0}{\partial y}\delta w_0 - M_{yy}\frac{\partial(\delta w_0)}{\partial y}\right]_{y=0}^{y=L_y}dx$$

$$
\begin{aligned}
-\int_0^{L_x}\int_0^{L_y}\Bigg[&\frac{\partial N_{yy}}{\partial y}\delta v_0+\delta w_0\frac{\partial}{\partial y}\left(N_{yy}\frac{\partial w_0}{\partial y}\right)-\frac{\partial M_{yy}}{\partial y}\frac{\partial(\delta w_0)}{\partial y}\\
&-\frac{1}{R_y}N_{yy}\delta w_0\Bigg]dy\,dx\\
&=\int_0^{L_x}\Bigg\{\Bigg[N_{yy}\delta v_0+N_{yy}\frac{\partial w_0}{\partial y}\delta w_0-M_{yy}\frac{\partial(\delta w_0)}{\partial y}\\
&+\frac{\partial M_{yy}}{\partial y}\delta w_0\Bigg]_{y=0}^{y=L_y}\\
&-\int_0^{L_y}\Bigg[\frac{\partial N_{yy}}{\partial y}\delta v_0+\delta w_0\frac{\partial}{\partial y}\left(N_{yy}\frac{\partial w_0}{\partial y}\right)+\frac{\partial^2 M_{yy}}{\partial y^2}\delta w_0\\
&-\frac{1}{R_y}N_{yy}\delta w_0\Bigg]dy\Bigg\}\,dx
\end{aligned}
\tag{3.45}
$$

$$
\begin{aligned}
\iiint \tau_{xy}\delta\gamma_{xy}\,dV&=\iint\left[N_{xy}\delta e_{xy}+M_{xy}\delta\kappa_{xy}\right]dA\\
&=\int_0^{L_y}\int_0^{L_x}\Bigg[N_{xy}\Bigg(\frac{\partial(\delta u_0)}{\partial y}+\frac{\partial(\delta v_0)}{\partial x}+\frac{\partial(\delta w_0)}{\partial x}\frac{\partial w_0}{\partial y}\\
&+\frac{\partial w_0}{\partial x}\frac{\partial(\delta w_0)}{\partial y}\Bigg)-M_{xy}\frac{\partial^2(\delta w_0)}{\partial x\partial y}-M_{xy}\frac{\partial^2(\delta w_0)}{\partial x\partial y}\Bigg]\,dx\,dy\\
&=\int_0^{L_y}\Bigg\{\Bigg[N_{xy}\delta v_0+N_{xy}\frac{\partial w_0}{\partial y}\delta w_0-M_{xy}\frac{\partial(\delta w_0)}{\partial y}\Bigg]_{x=0}^{x=L_x}\\
&-\int_0^{L_x}\Bigg[\frac{\partial N_{xy}}{\partial x}\delta v_0+\delta w_0\frac{\partial}{\partial x}\left(N_{xy}\frac{\partial w_0}{\partial y}\right)\\
&-\frac{\partial M_{xy}}{\partial x}\frac{\partial(\delta w_0)}{\partial y}\Bigg]dx\Bigg\}\,dy\\
&+\int_0^{L_x}\Bigg\{\Bigg[N_{xy}\delta u_0+N_{xy}\frac{\partial w_0}{\partial x}\delta w_0-M_{xy}\frac{\partial(\delta w_0)}{\partial x}\Bigg]_{y=0}^{y=L_y}\\
&-\int_0^{L_y}\Bigg[\frac{\partial N_{xy}}{\partial y}\delta u_0+\delta w_0\frac{\partial}{\partial y}\left(N_{xy}\frac{\partial w_0}{\partial x}\right)\\
&-\frac{\partial M_{xy}}{\partial y}\frac{\partial(\delta w_0)}{\partial x}\Bigg]dy\Bigg\}\,dx
\end{aligned}
$$

$$= \int_0^{L_y} \left[ N_{xy}\delta v_0 + N_{xy}\frac{\partial w_0}{\partial y}\delta w_0 - M_{xy}\frac{\partial(\delta w_0)}{\partial y} + \frac{\partial M_{xy}}{\partial y}\delta w_0 \right]_{x=0}^{x=L_x} dy$$

$$+ \int_0^{L_x} \left[ N_{xy}\delta u_0 + N_{xy}\frac{\partial w_0}{\partial x}\delta w_0 - M_{xy}\frac{\partial(\delta w_0)}{\partial x} \right.$$

$$\left. + \frac{\partial M_{xy}}{\partial x}\delta w_0 \right]_{y=0}^{y=L_y} dx$$

$$- \int_0^{L_y}\int_0^{L_x} \left[ \frac{\partial N_{xy}}{\partial x}\delta v_0 + \delta w_0 \frac{\partial}{\partial x}\left( N_{xy}\frac{\partial w_0}{\partial y} \right) + \frac{\partial N_{xy}}{\partial y}\delta u_0 \right.$$

$$\left. + \delta w_0 \frac{\partial}{\partial y}\left( N_{xy}\frac{\partial w_0}{\partial x} \right) + 2\frac{\partial^2 M_{xy}}{\partial x \partial y}\delta w_0 \right] dx\, dy \qquad (3.46)$$

Now in the light of equations (3.44)-(3.46), one may rewrite the first variation of the strain energy, equation (3.25), as follows:

$$\delta U = \iiint \left( \sigma_{xx}\delta\varepsilon_{xx} + \sigma_{yy}\delta\varepsilon_{yy} + \tau_{xy}\delta\gamma_{xy} \right) dV$$

$$= \iint \left[ N_{xx}\delta e_{xx} + M_{xx}\delta\kappa_{xx} + N_{yy}\delta e_{yy} + M_{yy}\delta\kappa_{yy} \right.$$

$$\left. + N_{xy}\delta e_{xy} + M_{xy}\delta\kappa_{xy} \right] dA$$

$$= \int_0^{L_y} \left[ N_{xx}\delta u_0 + N_{xy}\delta v_0 + N_{xy}\frac{\partial w_0}{\partial y}\delta w_0 + N_{xx}\frac{\partial w_0}{\partial x}\delta w_0 \right.$$

$$+ \frac{\partial M_{xx}}{\partial x}\delta w_0 - M_{xy}\frac{\partial(\delta w_0)}{\partial y} + \frac{\partial M_{xy}}{\partial y}\delta w_0$$

$$\left. - M_{xx}\frac{\partial(\delta w_0)}{\partial x} \right]_{x=0}^{x=L_x} dy$$

$$+ \int_0^{L_x} \left[ N_{xy}\delta u_0 + N_{yy}\delta v_0 + N_{yy}\frac{\partial w_0}{\partial y}\delta w_0 + N_{xy}\frac{\partial w_0}{\partial x}\delta w_0 \right.$$

$$+ \frac{\partial M_{yy}}{\partial y}\delta w_0 - M_{xy}\frac{\partial(\delta w_0)}{\partial x} + \frac{\partial M_{xy}}{\partial x}\delta w_0$$

$$\left. - M_{yy}\frac{\partial(\delta w_0)}{\partial y} \right]_{y=0}^{y=L_y} dx$$

$$-\int_0^{L_y}\int_0^{L_x}\left\{\left[\frac{\partial N_{xx}}{\partial x}+\frac{\partial N_{xy}}{\partial y}\right]\delta u_0+\left[\frac{\partial N_{yy}}{\partial y}+\frac{\partial N_{xy}}{\partial x}\right]\delta v_0\right.$$
$$+\left[\frac{\partial}{\partial x}\left(N_{xy}\frac{\partial w_0}{\partial y}+N_{xx}\frac{\partial w_0}{\partial x}\right)+\frac{\partial}{\partial y}\left(N_{xy}\frac{\partial w_0}{\partial x}+N_{yy}\frac{\partial w_0}{\partial y}\right)\right.$$
$$\left.\left.+\frac{\partial^2 M_{xx}}{\partial x^2}+\frac{\partial^2 M_{yy}}{\partial y^2}+2\frac{\partial^2 M_{xy}}{\partial x\partial y}-\frac{N_{xx}}{R_x}-\frac{N_{yy}}{R_y}\right]\delta w_0\right\}dx\,dy \qquad (3.47)$$

The virtual work done by the nonpotential external forces, $W_F$, can be written as

$$\delta W_F=\iint f(x,y)\,\delta w_0\,dA \qquad (3.48)$$

where $f(x,y)$ is the distributed transverse force acting on either the top or the bottom surface of the laminate.

According to equations (3.23), (3.47), (3.48) and (3.19), the Hamilton's principle becomes

$$\int_{t_0}^{t_f}[\delta T-\delta U+\delta W_F]\,dt$$
$$=\int_{t_0}^{t_f}\int_0^{L_x}\left[-N_{xy}\delta u_0-N_{yy}\delta v_0\right.$$
$$-\left(N_{yy}\frac{\partial w_0}{\partial y}+N_{xy}\frac{\partial w_0}{\partial x}+\frac{\partial M_{yy}}{\partial y}+\frac{\partial M_{xy}}{\partial x}\right)\delta w_0$$
$$\left.+M_{xy}\frac{\partial(\delta w_0)}{\partial x}+M_{yy}\frac{\partial(\delta w_0)}{\partial y}\right]_{y=0}^{y=L_y}dx\,dt$$
$$+\int_{t_0}^{t_f}\int_0^{L_y}\left[-N_{xx}\delta u_0-N_{xy}\delta v_0\right.$$
$$-\left(N_{xy}\frac{\partial w_0}{\partial y}+N_{xx}\frac{\partial w_0}{\partial x}+\frac{\partial M_{xx}}{\partial x}+\frac{\partial M_{xy}}{\partial y}\right)\delta w_0$$
$$\left.+M_{xy}\frac{\partial(\delta w_0)}{\partial y}+M_{xx}\frac{\partial(\delta w_0)}{\partial x}\right]_{x=0}^{x=L_x}dy\,dt$$

$$-\int_{t_0}^{t_f}\iint\left\{\left[-\frac{\partial N_{xx}}{\partial x}-\frac{\partial N_{xy}}{\partial y}\right]\delta u_0+\left[-\frac{\partial N_{yy}}{\partial y}-\frac{\partial N_{xy}}{\partial x}\right]\delta v_0\right.$$
$$+\left[-\frac{\partial}{\partial x}\left(N_{xy}\frac{\partial w_0}{\partial y}+N_{xx}\frac{\partial w_0}{\partial x}\right)-\frac{\partial}{\partial y}\left(N_{xy}\frac{\partial w_0}{\partial x}+N_{yy}\frac{\partial w_0}{\partial y}\right)\right.$$
$$-\frac{\partial^2 M_{xx}}{\partial x^2}-\frac{\partial^2 M_{yy}}{\partial y^2}-2\frac{\partial^2 M_{xy}}{\partial x\partial y}+\frac{1}{R_x}N_{xx}+\frac{1}{R_y}N_{yy}$$
$$\left.\left.-f(x,y)+I_0\frac{\partial^2 w_0}{\partial t^2}\right]\delta w_0\right\}dA\,dt=0 \tag{3.49}$$

Equating the coefficients of each of the virtual displacements $\delta u_0, \delta v_0$ and $\delta w_0$ to zero, the following equilibrium equations are obtained:

$$\delta u_0:\ \frac{\partial N_{xx}}{\partial x}+\frac{\partial N_{xy}}{\partial y}=0 \tag{3.50}$$

$$\delta v_0:\ \frac{\partial N_{yy}}{\partial y}+\frac{\partial N_{xy}}{\partial x}=0 \tag{3.51}$$

$$\delta w_0:\ \frac{\partial}{\partial x}\left(N_{xy}\frac{\partial w_0}{\partial y}+N_{xx}\frac{\partial w_0}{\partial x}\right)+\frac{\partial}{\partial y}\left(N_{xy}\frac{\partial w_0}{\partial x}+N_{yy}\frac{\partial w_0}{\partial y}\right)-\frac{1}{R_x}N_{xx}$$
$$-\frac{1}{R_y}N_{yy}+\frac{\partial^2 M_{xx}}{\partial x^2}+\frac{\partial^2 M_{yy}}{\partial y^2}+2\frac{\partial^2 M_{xy}}{\partial x\partial y}+f(x,y)$$
$$=I_0\frac{\partial^2 w_0}{\partial t^2} \tag{3.52}$$

The associated boundary conditions are

$$\int_0^{L_x}\left[-N_{xy}\delta u_0-N_{yy}\delta v_0-\left(N_{yy}\frac{\partial w_0}{\partial y}+N_{xy}\frac{\partial w_0}{\partial x}+\frac{\partial M_{yy}}{\partial y}+\frac{\partial M_{xy}}{\partial x}\right)\delta w_0\right.$$
$$\left.+M_{xy}\frac{\partial(\delta w_0)}{\partial x}+M_{yy}\frac{\partial(\delta w_0)}{\partial y}\right]_{y=0}^{y=L_y}dx=0 \tag{3.53}$$

$$\int_0^{L_y}\left[-N_{xx}\delta u_0-N_{xy}\delta v_0-\left(N_{xy}\frac{\partial w_0}{\partial y}+N_{xx}\frac{\partial w_0}{\partial x}+\frac{\partial M_{xx}}{\partial x}+\frac{\partial M_{xy}}{\partial y}\right)\delta w_0\right.$$
$$\left.+M_{xy}\frac{\partial(\delta w_0)}{\partial y}+M_{xx}\frac{\partial(\delta w_0)}{\partial x}\right]_{x=0}^{x=L_x}dy=0 \tag{3.54}$$

Which results in

$$\text{Either } \left(N_{yy} = 0\right) \text{ or } (v_0 = 0) \text{ at } y = L_y \text{ and } y = 0 \tag{3.55}$$

$$\text{Either } \left(N_{xy} = 0\right) \text{ or } (u_0 = 0) \text{ at } y = L_y \text{ and } y = 0 \tag{3.56}$$

$$\text{Either } \left[\left(N_{yy}\frac{\partial w_0}{\partial y} + N_{xy}\frac{\partial w_0}{\partial x} + \frac{\partial M_{yy}}{\partial y} + \frac{\partial M_{xy}}{\partial x}\right) = 0\right] \text{ or } (w_0 = 0) \text{ at } y = L_y \text{ and } y = 0 \tag{3.57}$$

$$\text{Either } \left(M_{yy} = 0\right) \text{ or } \left(\frac{\partial w_0}{\partial y} = 0\right) \text{ at } y = L_y \text{ and } y = 0 \tag{3.58}$$

$$\text{Either } \left(M_{xy} = 0\right) \text{ or } \left(\frac{\partial w_0}{\partial x} = 0\right) \text{ at } y = L_y \text{ and } y = 0 \tag{3.59}$$

$$\text{Either } (N_{xx} = 0) \text{ or } (u_0 = 0) \text{ at } x = L_x \text{ and } x = 0 \tag{3.60}$$

$$\text{Either } \left(N_{xy} = 0\right) \text{ or } (v_0 = 0) \text{ at } x = L_x \text{ and } x = 0 \tag{3.61}$$

$$\text{Either } \left[\left(N_{xy}\frac{\partial w_0}{\partial y} + N_{xx}\frac{\partial w_0}{\partial x} + \frac{\partial M_{xx}}{\partial x} + \frac{\partial M_{xy}}{\partial y}\right) = 0\right] \text{ or } (w_0 = 0) \text{ at } x = L_x \text{ and } x = 0 \tag{3.62}$$

$$\text{Either } \left(M_{xy} = 0\right) \text{ or } \left(\frac{\partial w_0}{\partial y} = 0\right) \text{ at } x = L_x \text{ and } x = 0 \tag{3.63}$$

$$\text{Either } (M_{xx} = 0) \text{ or } \left(\frac{\partial w_0}{\partial x} = 0\right) \text{ at } x = L_x \text{ and } x = 0 \tag{3.64}$$

In this study, the transverse displacement $w_0$ is of the main interest. It is possible to reduce the force stress resultants by introducing the stress function and the compatibility equation. The compatibility equation is given by [46, 47]

$$\frac{\partial^2 \varepsilon_{xx}}{\partial y^2} + \frac{\partial^2 \varepsilon_{yy}}{\partial x^2} = \frac{\partial^2 \varepsilon_{xy}}{\partial x \partial y} \tag{3.65}$$

Based on the equations (3.5) and (3.6), one may gain the following derivatives of strain:

$$\frac{\partial^2 e_{xx}}{\partial y^2} = \frac{\partial^3 u_0}{\partial x \partial y^2} + \frac{\partial^3 w_0}{\partial x \partial y^2}\frac{\partial w_0}{\partial x} + \left(\frac{\partial^2 w_0}{\partial x \partial y}\right)^2 + \frac{1}{R_x}\frac{\partial^2 w_0}{\partial y^2} \tag{3.66}$$

$$\frac{\partial^2 e_{yy}}{\partial x^2} = \frac{\partial^3 v_0}{\partial x^2 \partial y} + \frac{\partial^3 w_0}{\partial x^2 \partial y}\frac{\partial w_0}{\partial y} + \left(\frac{\partial^2 w_0}{\partial x \partial y}\right)^2 + \frac{1}{R_y}\frac{\partial^2 w_0}{\partial x^2} \tag{3.67}$$

$$\frac{\partial^2 e_{xy}}{\partial x \partial y} = \frac{\partial^3 u_0}{\partial x \partial y^2} + \frac{\partial^3 v_0}{\partial x^2 \partial y} + \frac{\partial^3 w_0}{\partial x^2 \partial y}\frac{\partial w_0}{\partial y} + \frac{\partial w_0}{\partial x}\frac{\partial^3 w_0}{\partial x \partial y^2} + \frac{\partial^2 w_0}{\partial x^2}\frac{\partial^2 w_0}{\partial y^2} + \left(\frac{\partial^2 w_0}{\partial x \partial y}\right)^2 \tag{3.68}$$

$$\frac{\partial^2 \kappa_{xx}}{\partial y^2} = -\frac{\partial^4 w_0}{\partial x^2 \partial y^2} \tag{3.69}$$

$$\frac{\partial^2 \kappa_{yy}}{\partial x^2} = -\frac{\partial^4 w_0}{\partial x^2 \partial y^2} \tag{3.70}$$

$$\frac{\partial^2 \kappa_{xy}}{\partial x \partial y} = -2\frac{\partial^4 w_0}{\partial x^2 \partial y^2} \tag{3.71}$$

In the light of equation (3.4) and by substituting equations (3.66)-(3.71) into equation (3.65), the compatibility equation could be simplified to the following form:

$$\frac{\partial^2 e_{xx}}{\partial y^2} + \frac{\partial^2 e_{yy}}{\partial x^2} = \frac{\partial^2 e_{xy}}{\partial x \partial y} \tag{3.72}$$

Which after the substitution of the derivatives, it takes the following form:

$$\frac{\partial^2 e_{xx}}{\partial y^2} + \frac{\partial^2 e_{yy}}{\partial x^2} - \frac{\partial^2 e_{xy}}{\partial x \partial y} = \left(\frac{\partial^2 w_0}{\partial x \partial y}\right)^2 - \frac{\partial^2 w_0}{\partial x^2}\frac{\partial^2 w_0}{\partial y^2} + \frac{1}{R_x}\frac{\partial^2 w_0}{\partial y^2} + \frac{1}{R_y}\frac{\partial^2 w_0}{\partial x^2} \tag{3.73}$$

Since the transverse displacement $w_0$ is the main interest, the axial displacement $u_0$ and $v_0$ could be eliminated from the strain-displacement relations (equation (3.5)) by using the compatibility equation (equation (3.73)).

Based on equation (3.40), the membrane strain could be defined as follows:

$$\begin{Bmatrix} e_{xx} \\ e_{yy} \\ e_{xy} \end{Bmatrix} = \begin{bmatrix} A_{11} & A_{12} & A_{16} \\ A_{12} & A_{22} & A_{26} \\ A_{16} & A_{26} & A_{66} \end{bmatrix}^{-1} \left( \begin{Bmatrix} N_{xx} \\ N_{yy} \\ N_{xy} \end{Bmatrix} - \begin{bmatrix} B_{11} & B_{12} & B_{16} \\ B_{12} & B_{22} & B_{26} \\ B_{16} & B_{26} & B_{66} \end{bmatrix} \begin{Bmatrix} \kappa_{xx} \\ \kappa_{yy} \\ \kappa_{xy} \end{Bmatrix} \right) \tag{3.74}$$

Substituting equation (3.74) into the moment stress resultant (equation (3.41)) yields

$$\begin{Bmatrix} M_{xx} \\ M_{yy} \\ M_{xy} \end{Bmatrix} = \begin{bmatrix} B_{11} & B_{12} & B_{16} \\ B_{12} & B_{22} & B_{26} \\ B_{16} & B_{26} & B_{66} \end{bmatrix} \begin{bmatrix} A_{11} & A_{12} & A_{16} \\ A_{12} & A_{22} & A_{26} \\ A_{16} & A_{26} & A_{66} \end{bmatrix}^{-1} \left( \begin{Bmatrix} N_{xx} \\ N_{yy} \\ N_{xy} \end{Bmatrix} - \begin{bmatrix} B_{11} & B_{12} & B_{16} \\ B_{12} & B_{22} & B_{26} \\ B_{16} & B_{26} & B_{66} \end{bmatrix} \begin{Bmatrix} \kappa_{xx} \\ \kappa_{yy} \\ \kappa_{xy} \end{Bmatrix} \right) + \begin{bmatrix} D_{11} & D_{12} & D_{16} \\ D_{12} & D_{22} & D_{26} \\ D_{16} & D_{26} & D_{66} \end{bmatrix} \begin{Bmatrix} \kappa_{xx} \\ \kappa_{yy} \\ \kappa_{xy} \end{Bmatrix} \tag{3.75}$$

Next, we introduce the stress function $\phi(x, y)$ such that

$$N_{xx} = \frac{\partial^2 \phi}{\partial y^2} \quad , \quad N_{yy} = \frac{\partial^2 \phi}{\partial x^2} \quad , \quad N_{xy} = -\frac{\partial^2 \phi}{\partial x \partial y} \tag{3.76}$$

Equation (3.76) identically satisfies the first and second equations of motion (equations (3.50) and (3.51)). Next, we substitute equation (3.76) into equations (3.74) and (3.75) and obtain

$$\begin{Bmatrix} e_{xx} \\ e_{yy} \\ e_{xy} \end{Bmatrix} = \begin{bmatrix} A_{11} & A_{12} & A_{16} \\ A_{12} & A_{22} & A_{26} \\ A_{16} & A_{26} & A_{66} \end{bmatrix}^{-1} \left( \begin{Bmatrix} \frac{\partial^2 \phi}{\partial y^2} \\ \frac{\partial^2 \phi}{\partial x^2} \\ -\frac{\partial^2 \phi}{\partial x \partial y} \end{Bmatrix} - \begin{bmatrix} B_{11} & B_{12} & B_{16} \\ B_{12} & B_{22} & B_{26} \\ B_{16} & B_{26} & B_{66} \end{bmatrix} \begin{Bmatrix} \kappa_{xx} \\ \kappa_{yy} \\ \kappa_{xy} \end{Bmatrix} \right) \tag{3.77}$$

$$\begin{Bmatrix} M_{xx} \\ M_{yy} \\ M_{xy} \end{Bmatrix} = \begin{bmatrix} B_{11} & B_{12} & B_{16} \\ B_{12} & B_{22} & B_{26} \\ B_{16} & B_{26} & B_{66} \end{bmatrix} \begin{bmatrix} A_{11} & A_{12} & A_{16} \\ A_{12} & A_{22} & A_{26} \\ A_{16} & A_{26} & A_{66} \end{bmatrix}^{-1} \left\{ \begin{Bmatrix} \frac{\partial^2 \phi}{\partial y^2} \\ \frac{\partial^2 \phi}{\partial x^2} \\ -\frac{\partial^2 \phi}{\partial x \partial y} \end{Bmatrix} - \begin{bmatrix} B_{11} & B_{12} & B_{16} \\ B_{12} & B_{22} & B_{26} \\ B_{16} & B_{26} & B_{66} \end{bmatrix} \begin{Bmatrix} \kappa_{xx} \\ \kappa_{yy} \\ \kappa_{xy} \end{Bmatrix} \right\} + \begin{bmatrix} D_{11} & D_{12} & D_{16} \\ D_{12} & D_{22} & D_{26} \\ D_{16} & D_{26} & D_{66} \end{bmatrix} \begin{Bmatrix} \kappa_{xx} \\ \kappa_{yy} \\ \kappa_{xy} \end{Bmatrix} \tag{3.78}$$

When the matrices $A, B$ and $D$ are full, the algebra becomes involved. However, for unidirectional, symmetric, unsymmetric and antisymmetric cross ply laminates, which are the laminates under investigation, the $A, B$ and $D$ matrices take the following forms:

$$A = \begin{bmatrix} A_{11} & A_{12} & 0 \\ A_{12} & A_{22} & 0 \\ 0 & 0 & A_{66} \end{bmatrix}, \; B = \begin{bmatrix} B_{11} & 0 & 0 \\ 0 & B_{22} & 0 \\ 0 & 0 & 0 \end{bmatrix}, \; D = \begin{bmatrix} D_{11} & D_{12} & 0 \\ D_{12} & D_{22} & 0 \\ 0 & 0 & D_{66} \end{bmatrix} \tag{3.79}$$

Meanwhile, for the unidirectional and symmetric laminates, the $B$ matrix vanishes. In the light of equations (3.79) and (3.6), equations (3.77) and (3.78) reduce to

$$\begin{Bmatrix} e_{xx} \\ e_{yy} \\ e_{xy} \end{Bmatrix} = \begin{bmatrix} \frac{A_{22}}{\Delta} & -\frac{A_{12}}{\Delta} & 0 \\ -\frac{A_{12}}{\Delta} & \frac{A_{11}}{\Delta} & 0 \\ 0 & 0 & \frac{1}{A_{66}} \end{bmatrix} \left\{ \begin{Bmatrix} \frac{\partial^2 \phi}{\partial y^2} \\ \frac{\partial^2 \phi}{\partial x^2} \\ -\frac{\partial^2 \phi}{\partial x \partial y} \end{Bmatrix} - \begin{bmatrix} B_{11} & 0 & 0 \\ 0 & B_{22} & 0 \\ 0 & 0 & 0 \end{bmatrix} \begin{Bmatrix} -\frac{\partial^2 w_0}{\partial x^2} \\ -\frac{\partial^2 w_0}{\partial y^2} \\ -2\frac{\partial^2 w_0}{\partial x \partial y} \end{Bmatrix} \right\}$$

$$= \begin{bmatrix} \frac{A_{22}}{\Delta} & -\frac{A_{12}}{\Delta} & 0 \\ -\frac{A_{12}}{\Delta} & \frac{A_{11}}{\Delta} & 0 \\ 0 & 0 & \frac{1}{A_{66}} \end{bmatrix} \begin{Bmatrix} \frac{\partial^2 \phi}{\partial y^2} \\ \frac{\partial^2 \phi}{\partial x^2} \\ -\frac{\partial^2 \phi}{\partial x \partial y} \end{Bmatrix}$$

$$- \begin{bmatrix} \frac{A_{22}B_{11}}{\Delta} & -\frac{A_{12}B_{22}}{\Delta} & 0 \\ -\frac{A_{12}B_{11}}{\Delta} & \frac{A_{11}B_{22}}{\Delta} & 0 \\ 0 & 0 & 0 \end{bmatrix} \begin{Bmatrix} -\frac{\partial^2 w_0}{\partial x^2} \\ -\frac{\partial^2 w_0}{\partial y^2} \\ -2\frac{\partial^2 w_0}{\partial x \partial y} \end{Bmatrix} \tag{3.80}$$

$$\begin{Bmatrix} M_{xx} \\ M_{yy} \\ M_{xy} \end{Bmatrix} = \begin{bmatrix} B_{11} & 0 & 0 \\ 0 & B_{22} & 0 \\ 0 & 0 & 0 \end{bmatrix} \left( \begin{bmatrix} \frac{A_{22}}{\Delta} & -\frac{A_{12}}{\Delta} & 0 \\ -\frac{A_{12}}{\Delta} & \frac{A_{11}}{\Delta} & 0 \\ 0 & 0 & \frac{1}{A_{66}} \end{bmatrix} \left\{ \begin{Bmatrix} \frac{\partial^2 \phi}{\partial y^2} \\ \frac{\partial^2 \phi}{\partial x^2} \\ -\frac{\partial^2 \phi}{\partial x \partial y} \end{Bmatrix} \right\} - \begin{bmatrix} B_{11} & 0 & 0 \\ 0 & B_{22} & 0 \\ 0 & 0 & 0 \end{bmatrix} \left\{ \begin{Bmatrix} -\frac{\partial^2 w_0}{\partial x^2} \\ -\frac{\partial^2 w_0}{\partial y^2} \\ -2\frac{\partial^2 w_0}{\partial x \partial y} \end{Bmatrix} \right\} \right)$$

$$+ \begin{bmatrix} D_{11} & D_{12} & 0 \\ D_{12} & D_{22} & 0 \\ 0 & 0 & D_{66} \end{bmatrix} \begin{Bmatrix} -\frac{\partial^2 w_0}{\partial x^2} \\ -\frac{\partial^2 w_0}{\partial y^2} \\ -2\frac{\partial^2 w_0}{\partial x \partial y} \end{Bmatrix}$$

$$= \begin{bmatrix} \frac{A_{22}B_{11}}{\Delta} & -\frac{A_{12}B_{11}}{\Delta} & 0 \\ -\frac{A_{12}B_{22}}{\Delta} & \frac{A_{11}B_{22}}{\Delta} & 0 \\ 0 & 0 & 0 \end{bmatrix} \begin{Bmatrix} \frac{\partial^2 \phi}{\partial y^2} \\ \frac{\partial^2 \phi}{\partial x^2} \\ -\frac{\partial^2 \phi}{\partial x \partial y} \end{Bmatrix}$$

$$+\begin{bmatrix} D_{11}-\frac{A_{22}B_{11}^2}{\Delta} & D_{12}+\frac{A_{12}B_{11}B_{22}}{\Delta} & 0 \\ D_{12}+\frac{A_{12}B_{11}B_{22}}{\Delta} & D_{22}-\frac{A_{11}B_{22}^2}{\Delta} & 0 \\ 0 & 0 & D_{66} \end{bmatrix}\begin{Bmatrix} -\frac{\partial^2 w_0}{\partial x^2} \\ -\frac{\partial^2 w_0}{\partial y^2} \\ -2\frac{\partial^2 w_0}{\partial x \partial y} \end{Bmatrix} \tag{3.81}$$

where $\Delta = A_{11}A_{22} - A_{12}^2$. The expanded form of equations (3.80) and (3.81) could be expressed as

$$e_{xx} = \frac{A_{22}}{\Delta}\frac{\partial^2 \phi}{\partial y^2} - \frac{A_{12}}{\Delta}\frac{\partial^2 \phi}{\partial x^2} + \frac{A_{22}B_{11}}{\Delta}\frac{\partial^2 w_0}{\partial x^2} - \frac{A_{12}B_{22}}{\Delta}\frac{\partial^2 w_0}{\partial y^2} \tag{3.82}$$

$$e_{yy} = -\frac{A_{12}}{\Delta}\frac{\partial^2 \phi}{\partial y^2} + \frac{A_{11}}{\Delta}\frac{\partial^2 \phi}{\partial x^2} - \frac{A_{12}B_{11}}{\Delta}\frac{\partial^2 w_0}{\partial x^2} + \frac{A_{11}B_{22}}{\Delta}\frac{\partial^2 w_0}{\partial y^2} \tag{3.83}$$

$$e_{xy} = -\frac{1}{A_{66}}\frac{\partial^2 \phi}{\partial x \partial y} \tag{3.84}$$

$$M_{xx} = +\frac{A_{22}B_{11}}{\Delta}\frac{\partial^2 \phi}{\partial y^2} - \frac{A_{12}B_{11}}{\Delta}\frac{\partial^2 \phi}{\partial x^2} - \left(D_{11} - \frac{A_{22}B_{11}^2}{\Delta}\right)\frac{\partial^2 w_0}{\partial x^2} - \left(D_{12} + \frac{A_{12}B_{11}B_{22}}{\Delta}\right)\frac{\partial^2 w_0}{\partial y^2} \tag{3.85}$$

$$M_{yy} = -\frac{A_{12}B_{22}}{\Delta}\frac{\partial^2 \phi}{\partial y^2} + \frac{A_{11}B_{22}}{\Delta}\frac{\partial^2 \phi}{\partial x^2} - \left(D_{12} + \frac{A_{12}B_{11}B_{22}}{\Delta}\right)\frac{\partial^2 w_0}{\partial x^2} - \left(D_{22} - \frac{A_{11}B_{22}^2}{\Delta}\right)\frac{\partial^2 w_0}{\partial y^2} \tag{3.86}$$

$$M_{xy} = -2D_{66}\frac{\partial^2 w_0}{\partial x \partial y} \tag{3.87}$$

According to equations (3.82)-(3.87), the derivatives of the membrane strains ($e_{xx}, e_{yy}, e_{xy}$) and the moment stress resultants ($M_{xx}, M_{yy}, M_{xy}$) that appear in the left-

hand side of the compatibility equation, equation (3.73), and the left-hand side of the lateral deflection equation, equation (3.52), are defined as

$$\frac{\partial^2 e_{xx}}{\partial y^2} = \frac{A_{22}}{\Delta}\frac{\partial^4 \phi}{\partial y^4} - \frac{A_{12}}{\Delta}\frac{\partial^4 \phi}{\partial x^2 \partial y^2} + \frac{A_{22}B_{11}}{\Delta}\frac{\partial^4 w_0}{\partial x^2 \partial y^2} - \frac{A_{12}B_{22}}{\Delta}\frac{\partial^4 w_0}{\partial y^4} \tag{3.88}$$

$$\frac{\partial^2 e_{yy}}{\partial x^2} = -\frac{A_{12}}{\Delta}\frac{\partial^4 \phi}{\partial x^2 \partial y^2} + \frac{A_{11}}{\Delta}\frac{\partial^4 \phi}{\partial x^4} - \frac{A_{12}B_{11}}{\Delta}\frac{\partial^4 w_0}{\partial x^4} + \frac{A_{11}B_{22}}{\Delta}\frac{\partial^4 w_0}{\partial x^2 \partial y^2} \tag{3.89}$$

$$\frac{\partial^2 e_{xy}}{\partial x \partial y} = -\frac{1}{A_{66}}\frac{\partial^4 \phi}{\partial x^2 \partial y^2} \tag{3.90}$$

$$\frac{\partial^2 M_{xx}}{\partial x^2} = +\frac{A_{22}B_{11}}{\Delta}\frac{\partial^4 \phi}{\partial x^2 \partial y^2} - \frac{A_{12}B_{11}}{\Delta}\frac{\partial^4 \phi}{\partial x^4} - \left(D_{11} - \frac{A_{22}B_{11}^2}{\Delta}\right)\frac{\partial^4 w_0}{\partial x^4} - \left(D_{12} + \frac{A_{12}B_{11}B_{22}}{\Delta}\right)\frac{\partial^4 w_0}{\partial x^2 \partial y^2} \tag{3.91}$$

$$\frac{\partial^2 M_{yy}}{\partial y^2} = -\frac{A_{12}B_{22}}{\Delta}\frac{\partial^4 \phi}{\partial y^4} + \frac{A_{11}B_{22}}{\Delta}\frac{\partial^4 \phi}{\partial x^2 \partial y^2} - \left(D_{12} + \frac{A_{12}B_{11}B_{22}}{\Delta}\right)\frac{\partial^4 w_0}{\partial x^2 \partial y^2} - \left(D_{22} - \frac{A_{11}B_{22}^2}{\Delta}\right)\frac{\partial^4 w_0}{\partial y^4} \tag{3.92}$$

$$\frac{\partial^2 M_{xy}}{\partial x \partial y} = -2D_{66}\frac{\partial^4 w_0}{\partial x^2 \partial y^2} \tag{3.93}$$

Substituting equations (3.88)-(3.90) into equation (3.73) and plugging equations (3.91)-(3.93) and (3.76) into equation (3.52), one could find two equations of motion: the compatibility equation and the equation governing the transverse deflection as

$$\frac{A_{11}}{\Delta}\frac{\partial^4 \phi}{\partial x^4} + \frac{A_{22}}{\Delta}\frac{\partial^4 \phi}{\partial y^4} - \left(\frac{2A_{12}}{\Delta} - \frac{1}{A_{66}}\right)\frac{\partial^4 \phi}{\partial x^2 \partial y^2} - \frac{A_{12}B_{11}}{\Delta}\frac{\partial^4 w_0}{\partial x^4} - \frac{A_{12}B_{22}}{\Delta}\frac{\partial^4 w_0}{\partial y^4} + \left(\frac{A_{11}B_{22}}{\Delta} + \frac{A_{22}B_{11}}{\Delta}\right)\frac{\partial^4 w_0}{\partial x^2 \partial y^2} - \left(\frac{\partial^2 w_0}{\partial x \partial y}\right)^2 + \frac{\partial^2 w_0}{\partial x^2}\frac{\partial^2 w_0}{\partial y^2} - \frac{1}{R_x}\frac{\partial^2 w_0}{\partial y^2} - \frac{1}{R_y}\frac{\partial^2 w_0}{\partial x^2} = 0 \tag{3.94}$$

$$
\begin{aligned}
&-\frac{A_{12}B_{11}}{\Delta}\frac{\partial^4\phi}{\partial x^4}-\frac{A_{12}B_{22}}{\Delta}\frac{\partial^4\phi}{\partial y^4}+\left(\frac{A_{22}B_{11}}{\Delta}+\frac{A_{11}B_{22}}{\Delta}\right)\frac{\partial^4\phi}{\partial x^2\partial y^2}\\
&\quad-\left(D_{11}-\frac{A_{22}B_{11}^2}{\Delta}\right)\frac{\partial^4 w_0}{\partial x^4}-\left(D_{22}-\frac{A_{11}B_{22}^2}{\Delta}\right)\frac{\partial^4 w_0}{\partial y^4}\\
&\quad-2\left(2D_{66}+D_{12}+\frac{A_{12}B_{11}B_{22}}{\Delta}\right)\frac{\partial^4 w_0}{\partial x^2\partial y^2}+\frac{\partial^2\phi}{\partial y^2}\frac{\partial^2 w_0}{\partial x^2}\\
&\quad+\frac{\partial^2\phi}{\partial x^2}\frac{\partial^2 w_0}{\partial y^2}-2\frac{\partial^2\phi}{\partial x\partial y}\frac{\partial^2 w_0}{\partial x\partial y}-\frac{1}{R_x}\frac{\partial^2\phi}{\partial y^2}-\frac{1}{R_y}\frac{\partial^2\phi}{\partial x^2}+f(x,y)\\
&\quad=I_0\frac{\partial^2 w_0}{\partial t^2}
\end{aligned}
\tag{3.95}
$$

It can be seen that by means of the stress function and the compatibility equation, the three equations of motion, equations (3.50)-(3.51), are reduced to two equations: (3.50)-(3.51). These equations are the two governing equations that will be used in this study to explore the nonlinear behavior of the doubly curved FRC shells. These two equations are coupled and must be solved simultaneously. To do that, they will be discretized using the Galerkin's method and get a set of ordinary differential equations, as will be shown in the next chapter.

# Chapter 4. Reduced-Order Model

In this chapter, a reduced-order model of the problem is developed using the Galerkin's discretization. In order to apply the Galerkin's discretization technique, a set of basis or shape functions that is consistent with the boundary conditions is needed. For the sake of generality, let us assume that the functions $w_0(x,y,t)$ and $\phi(x,y,t)$ can be expressed in the following forms:

$$w_0(x,y,t) = \sum_{m=1}^{N}\sum_{n=1}^{N} X_m(x)\, Y_n(y)\, q_{mn}(t) \tag{4.1}$$

$$\phi(x,y,t) = \sum_{m=1}^{N}\sum_{n=1}^{N} \psi_m(x)\, \psi_n(y)\, F_{mn}(t) \tag{4.2}$$

where $N$ designates the number of modes retained in the discretization; $X(x)$ and $Y(y)$ are the shape functions of the lateral deflection in the $x$ and $y$-directions; $\psi(x)$ and $\psi(y)$ are the trial function of the stress function in the $x$ and $y$-directions, respectively; and $q_{mn}(t)$ and $F_{mn}(t)$ are generalized coordinates to be determined. We note that the shape functions and the trial functions must satisfy the boundary conditions that are imposed on the $w_0$ and $\phi$, respectively. Plugging equations (4.1) and (4.2) into equations (3.94) and (3.95), multiplying the equation of compatibility, equation (3.94), by the arbitrary trial functions $\psi_i(x)\,\psi_j(y)$ and multiplying the equation of the lateral deflection, equation (3.95), by the arbitrary mode shapes $X_i(x)Y_j(y)$ and integrating over the shell geometry, the discretized equations are obtained. The discretization of one term is shown below and the discretization of the remaining terms are presented in the Appendix.

$$\int_0^{L_x}\int_0^{L_y} \frac{\partial^2 w_0}{\partial x \partial y}\frac{\partial^2 w_0}{\partial x \partial y}\psi_i(x)\,\psi_j(y)\,dy\,dx$$

$$= \int_0^{L_x} \int_0^{L_y} \left[ \sum_{m=1}^{N} \sum_{n=1}^{N} X'_m(x)\, Y'_n(y)\, q_{mn}(t) \right]$$

$$\times \left[ \sum_{p=1}^{N} \sum_{q=1}^{N} X'_p(x)\, Y'_q(y)\, q_{pq}(t) \right] \psi_i(x)\, \psi_j(y)\, dy\, dx$$

$$= \left[ \int_0^{L_x} \sum_{m=1}^{N} \sum_{p=1}^{N} X'_m(x)\, X'_p(x)\, \psi_i(x)\, dx \right]$$

$$\times \left[ \int_0^{L_y} \sum_{n=1}^{N} \sum_{q=1}^{N} Y'_n(y)\, Y'_q(y)\, \psi_j(y)\, dy \right] q_{mn}(t)\, q_{pq}(t) \tag{4.3}$$

$$\int_0^{L_x} X'_m(x)\, X'_p(x)\, \psi_i(x)\, dx = c_{mpi}^{\phi x} \tag{4.4}$$

$$\int_0^{L_y} Y'_n(y)\, Y'_q(y)\, \psi_j(y)\, dy = c_{nqj}^{\phi y} \tag{4.5}$$

Thus we have

$$\int_0^{L_x} \int_0^{L_y} \frac{\partial^2 w_0}{\partial x \partial y} \frac{\partial^2 w_0}{\partial x \partial y} \psi_i(x)\, \psi_j(y)\, dy\, dx$$

$$= \sum_{m=1}^{N} \sum_{n=1}^{N} \sum_{p=1}^{N} \sum_{q=1}^{N} c_{mpi}^{\phi x}\, c_{nqj}^{\phi y}\, q_{mn}(t)\, q_{pq}(t) \tag{4.6}$$

The last term of the discretization is the load projection that is defined as

$$\int_0^{L_x} \int_0^{L_y} f(x,y)\, X_i(x)\, Y_j(y)\, dy\, dx = f_{ij} \tag{4.7}$$

At this step, substituting the discretized terms presented in the Appendix into the equations (3.94) and (3.95), the discretized equations of motion are obtained as follows:

$$\sum_{m=1}^{N}\sum_{n=1}^{N}\left[\frac{A_{11}}{\Delta}\,k_{mi}^{\phi x}\,d_{nj}^{\phi y}+\frac{A_{22}}{\Delta}\,d_{mi}^{\phi x}\,k_{nj}^{\phi y}-\left(\frac{2A_{12}}{\Delta}-\frac{1}{A_{66}}\right)r_{mi}^{\phi x}\,r_{nj}^{\phi y}\right]F_{mn}(t)$$
$$+\sum_{m=1}^{N}\sum_{n=1}^{N}\left[-\frac{A_{12}B_{11}}{\Delta}\,e_{mi}^{\phi x}\,g_{nj}^{\phi y}-\frac{A_{12}B_{22}}{\Delta}\,g_{mi}^{\phi x}\,e_{nj}^{\phi y}\right.$$
$$+\left(\frac{A_{11}B_{22}}{\Delta}+\frac{A_{22}B_{11}}{\Delta}\right)h_{mi}^{\phi x}\,h_{nj}^{\phi y}-\frac{1}{R_x}g_{mi}^{\phi x}\,h_{nj}^{\phi y}$$
$$\left.-\frac{1}{R_y}h_{mi}^{\phi x}\,g_{nj}^{\phi y}\right]q_{mn}(t)$$
$$+\sum_{m=1}^{N}\sum_{n=1}^{N}\sum_{p=1}^{N}\sum_{q=1}^{N}\left[a_{mpi}^{\phi x}\,a_{qnj}^{\phi y}-c_{mpi}^{\phi x}\,c_{nqj}^{\phi y}\right]q_{mn}(t)\,q_{pq}(t)=0 \qquad (4.8)$$

$$I_0\sum_{m=1}^{N}\sum_{n=1}^{N}d_{mi}^{wx}\,d_{nj}^{wy}\,\ddot{q}_{mn}(t)$$
$$+\sum_{m=1}^{N}\sum_{n=1}^{N}\left[\frac{A_{12}B_{11}}{\Delta}\,e_{mi}^{wx}\,g_{nj}^{wy}+\frac{A_{12}B_{22}}{\Delta}\,g_{mi}^{wx}\,e_{nj}^{wy}\right.$$
$$-\left(\frac{A_{22}B_{11}}{\Delta}+\frac{A_{11}B_{22}}{\Delta}\right)h_{mi}^{wx}\,h_{nj}^{wy}+\frac{1}{R_x}\,g_{mi}^{wx}\,h_{nj}^{wy}$$
$$\left.+\frac{1}{R_y}h_{mi}^{wx}\,g_{nj}^{wy}\right]F_{mn}(t)$$
$$+\sum_{m=1}^{N}\sum_{n=1}^{N}\left[\left(D_{11}-\frac{A_{22}B_{11}^2}{\Delta}\right)k_{mi}^{wx}\,d_{nj}^{wy}\right.$$
$$+\left(D_{22}-\frac{A_{11}B_{22}^2}{\Delta}\right)d_{mi}^{wx}\,k_{nj}^{wy}$$
$$\left.+2\left(2D_{66}+D_{12}+\frac{A_{12}B_{11}B_{22}}{\Delta}\right)r_{mi}^{wx}\,r_{nj}^{wy}\right]\,q_{mn}(t)$$
$$-\sum_{m=1}^{N}\sum_{n=1}^{N}\sum_{p=1}^{N}\sum_{q=1}^{N}\left(a_{mpi}^{wx}\,b_{qnj}^{wy}-2c_{mpi}^{wx}\,c_{nqj}^{wy}\right.$$
$$\left.+\,b_{pmi}^{wx}\,a_{nqj}^{wy}\right)q_{mn}(t)\,F_{pq}(t)=f_{ij} \qquad (4.9)$$

Simplifying equations (4.8) and (4.9), one can obtain the compact form of the two discretized equations of motion as below:

$$\sum_{m=1}^{N}\sum_{n=1}^{N}\eta_{mnij}\,F_{mn}(t)-\sum_{m=1}^{N}\sum_{n=1}^{N}\theta_{mnij}\,q_{mn}(t)+\sum_{m=1}^{N}\sum_{n=1}^{N}\sum_{p=1}^{N}\sum_{q=1}^{N}\gamma_{mnpqij}\,q_{mn}(t)\,q_{pq}(t)=0 \tag{4.10}$$

$$\sum_{m=1}^{N}\sum_{n=1}^{N}\Omega_{mnij}\,\ddot{q}_{mn}(t)+\sum_{m=1}^{N}\sum_{n=1}^{N}\xi_{mnij}\,F_{mn}(t)+\sum_{m=1}^{N}\sum_{n=1}^{N}\mu_{mnij}\,q_{mn}(t)-\sum_{m=1}^{N}\sum_{n=1}^{N}\sum_{p=1}^{N}\sum_{q=1}^{N}\beta_{mnpqij}\,q_{mn}(t)\,F_{pq}(t)=f_{ij} \tag{4.11}$$

where

$$\eta_{mnij}=\frac{A_{11}}{\Delta}\,k_{mi}^{\phi x}\,d_{nj}^{\phi y}+\frac{A_{22}}{\Delta}\,d_{mi}^{\phi x}\,k_{nj}^{\phi y}-\left(\frac{2A_{12}}{\Delta}-\frac{1}{A_{66}}\right)r_{mi}^{\phi x}\,r_{nj}^{\phi y} \tag{4.12}$$

$$\theta_{mnij}=\frac{A_{12}B_{11}}{\Delta}\,e_{mi}^{\phi x}\,g_{nj}^{\phi y}+\frac{A_{12}B_{22}}{\Delta}\,g_{mi}^{\phi x}\,e_{nj}^{\phi y}-\left(\frac{A_{11}B_{22}}{\Delta}+\frac{A_{22}B_{11}}{\Delta}\right)h_{mi}^{\phi x}\,h_{nj}^{\phi y}+\frac{1}{R_x}g_{mi}^{\phi x}\,h_{nj}^{\phi y}+\frac{1}{R_y}h_{mi}^{\phi x}\,g_{nj}^{\phi y} \tag{4.13}$$

$$\gamma_{mnpqij}=a_{mpi}^{\phi x}\,a_{qnj}^{\phi y}-c_{mpi}^{\phi x}\,c_{nqj}^{\phi y} \tag{4.14}$$

$$\Omega_{mnij}=I_0\,d_{mi}^{wx}\,d_{nj}^{wy} \tag{4.15}$$

$$\xi_{mnij}=\frac{A_{12}B_{11}}{\Delta}\,e_{mi}^{wx}\,g_{nj}^{wy}+\frac{A_{12}B_{22}}{\Delta}\,g_{mi}^{wx}\,e_{nj}^{wy}-\left(\frac{A_{22}B_{11}}{\Delta}+\frac{A_{11}B_{22}}{\Delta}\right)h_{mi}^{wx}\,h_{nj}^{wy}+\frac{1}{R_x}\,g_{mi}^{wx}\,h_{nj}^{wy}+\frac{1}{R_y}h_{mi}^{wx}\,g_{nj}^{wy} \tag{4.16}$$

$$\mu_{mnij} = \left(D_{11} - \frac{A_{22}B_{11}^2}{\Delta}\right) k_{mi}^{wx}\, d_{nj}^{wy} + \left(D_{22} - \frac{A_{11}B_{22}^2}{\Delta}\right) d_{mi}^{wx}\, k_{nj}^{wy} + 2\left(2D_{66} + D_{12} + \frac{A_{12}B_{11}B_{22}}{\Delta}\right) r_{mi}^{wx}\, r_{nj}^{wy} \tag{4.17}$$

$$\beta_{mnpqij} = a_{mpi}^{wx}\, b_{qnj}^{wy} - 2c_{mpi}^{wx}\, c_{nqj}^{wy} + b_{pmi}^{wx}\, a_{nqj}^{wy} \tag{4.18}$$

where the $a_{mpi}^{wx}, b_{pmi}^{wx}, c_{mpi}^{\phi x}, a_{mpi}^{\phi x}$, etc. are constants defined in the Appendix. The discretized equations of motion, equations (4.10) and (4.11), are valid for all boundary conditions provided that the appropriate shape functions of lateral deflection ($X(x)$ and $Y(y)$) and the trial function of stress function ($\psi(x)$ and $\psi(y)$) are used. Solving the static part of the discretized equations yields the equilibrium positions. The stability of the equilibrium positions is identified by using Jacobian matrix which is defined as:

$$J = \frac{\partial EQ_{ij}}{\partial r_{mn}}\,; \quad i, j, m, n = 1,2, \dots, N \tag{4.19}$$

where $J$ is the Jacobian matrix, $EQ_{ij}$ is an algebraic equation, $r_{mn}$ is the generalized coordinate and $N$ is the number of modes retained in the discretization. An equilibrium position is called stable if all eigenvalues of the Jacobian matrix are positive, otherwise it is unstable. Next, the discretized equations are used to solve the nonlinear bending and snapthrough response of doubly curved FRC shells.

## Chapter 5. Results and Discussion

In this chapter, the nonlinear static bending and snapthrough behavior of doubly curved FRC shells is presented. First, the present model is validated against the available results in the literature. Then the nonlinear static response of simply supported doubly curved shells under uniformly distributed loads is investigated. For a simply supported shell with the dimensions of $L_x, L_y$ and $h$ in the $x, y$ and $z$-directions respectively, the lateral deflection $w_0(x, y, t)$ and the stress function $\phi(x, y, t)$ could be expanded as the following double trigonometric series which satisfy the boundary conditions [44, 48]:

$$w_0(x, y, t) = \sum_{m=1}^{N} \sum_{n=1}^{N} \sin\left(\frac{m\pi x}{L_x}\right) \sin\left(\frac{n\pi y}{L_y}\right) q_{mn}(t) \tag{5.1}$$

$$\phi(x, y, t) = \sum_{m=1}^{N} \sum_{n=1}^{N} \sin\left(\frac{m\pi x}{L_x}\right) \sin\left(\frac{n\pi y}{L_y}\right) F_{mn}(t) \tag{5.2}$$

where $m$ and $n$ are the number of half-waves (mode numbers) in the $x$ and $y$-directions, respectively [49]. According to the equations (3.55)-(3.64), the simply supported boundary conditions associated with the three equations of motion, equations (3.50)-(3.52), are

$$w_0 = v_0 = \frac{\partial w_0}{\partial y} = N_{xx} = M_{xx} = 0 \quad at \quad x = L_x \quad and \quad x = 0 \tag{5.3}$$

$$w_0 = u_0 = \frac{\partial w_0}{\partial x} = N_{yy} = M_{yy} = 0 \quad at \quad y = L_y \quad and \quad y = 0 \tag{5.4}$$

Using the Airy stress function, equation (3.76), and the definition of the moment stress resultants with respect to the stress function and $w_0$, equations (3.85)-(3.87), the simply supported boundary conditions, equations (5.3) and (5.4), can be rearranged as

$$at \quad x = L_x \quad and \quad x = 0:$$

$$w_0 = \frac{\partial w_0}{\partial y} = 0,$$

$$N_{xx} = \frac{\partial^2 \phi}{\partial y^2} = 0,$$

$$M_{xx} = \frac{A_{22}B_{11}}{\Delta}\frac{\partial^2 \phi}{\partial y^2} - \frac{A_{12}B_{11}}{\Delta}\frac{\partial^2 \phi}{\partial x^2} - \left(D_{11} - \frac{A_{22}B_{11}^2}{\Delta}\right)\frac{\partial^2 w_0}{\partial x^2}$$
$$- \left(D_{12} + \frac{A_{12}B_{11}B_{22}}{\Delta}\right)\frac{\partial^2 w_0}{\partial y^2} = 0 \tag{5.5}$$

$$at \quad y = L_y \quad and \quad y = 0:$$

$$w_0 = \frac{\partial w_0}{\partial x} = 0,$$

$$N_{yy} = \frac{\partial^2 \phi}{\partial x^2} = 0,$$

$$M_{yy} = -\frac{A_{12}B_{22}}{\Delta}\frac{\partial^2 \phi}{\partial y^2} + \frac{A_{11}B_{22}}{\Delta}\frac{\partial^2 \phi}{\partial x^2} - \left(D_{12} + \frac{A_{12}B_{11}B_{22}}{\Delta}\right)\frac{\partial^2 w_0}{\partial x^2}$$
$$- \left(D_{22} - \frac{A_{11}B_{22}^2}{\Delta}\right)\frac{\partial^2 w_0}{\partial y^2} = 0 \tag{5.6}$$

The first three symmetric mode shapes $(i, j = 1,3,5)$ of lateral deflection of a simply supported plate that are used in this thesis are shown in Figure 5.1.

Let the simply supported shell be subjected to a distributed load $f(x, y)$. The Fourier series expansion for the load is given as [50]

$$f(x, y) = \sum_{m=1}^{\infty}\sum_{n=1}^{\infty} p_{mn} \sin\left(\frac{m\pi x}{L_x}\right)\sin\left(\frac{n\pi y}{L_y}\right) \tag{5.7}$$

Multiplying both sides of equation (5.7) by an arbitrary mode shape of the lateral deflection of simply supported shell and integrating over the domain, the Fourier series coefficients $p_{mn}$ can be determined as follows:

$$\int_0^{L_x}\int_0^{L_y} f(x, y) \sin\left(\frac{m\pi x}{L_x}\right)\sin\left(\frac{n\pi y}{L_y}\right) dy\, dx =$$

$$\int_0^{L_x}\int_0^{L_y}\sum_{m=1}^{\infty}\sum_{n=1}^{\infty} p_{mn}\sin\left(\frac{m\pi x}{L_x}\right)\sin\left(\frac{n\pi y}{L_y}\right)\sin\left(\frac{r\pi x}{L_x}\right)\sin\left(\frac{s\pi y}{L_y}\right)dy\,dx \qquad (5.8)$$

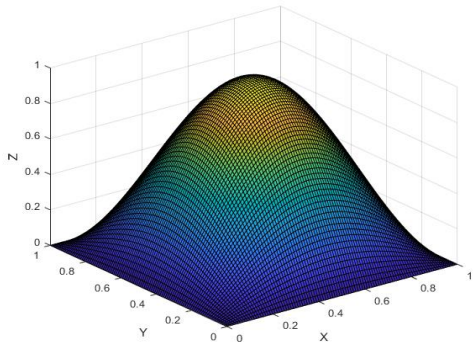


Mode (1,1)

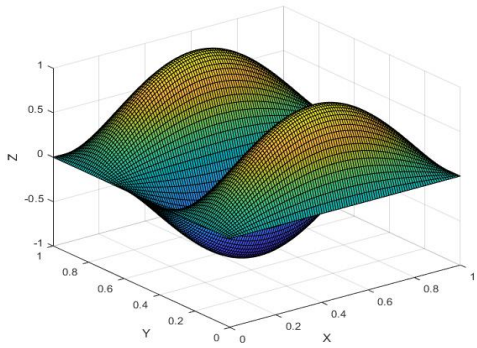


Mode (1,3)

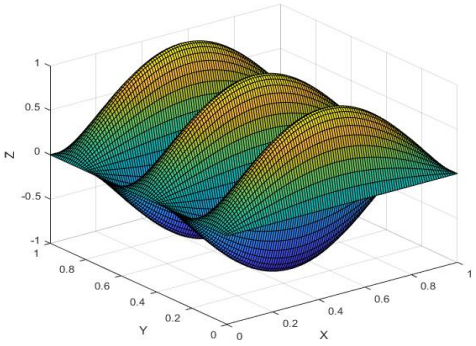


Mode (1,5)

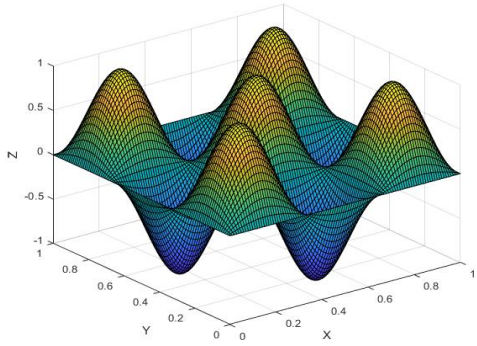


Mode (3,3)

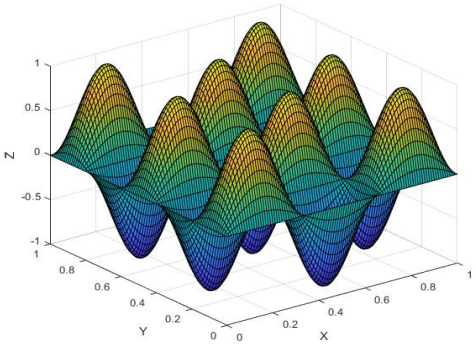


Mode (3,5)

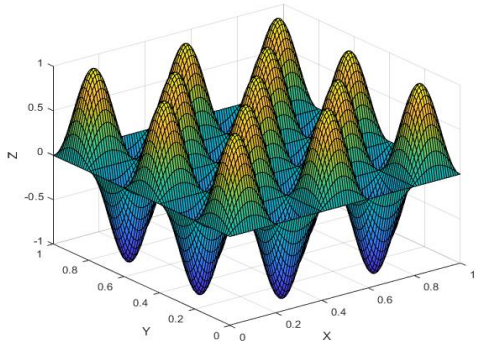


Mode (5,5)

Figure 5.1: The first three symmetric mode shapes of lateral deflection of a simply supported plate.

The orthogonality conditions for the lateral deflection mode shapes are

$$\int_0^{L_x} \sin\left(\frac{m\pi x}{L_x}\right) \sin\left(\frac{r\pi x}{L_x}\right) dx = \begin{cases} 0 & m \neq r \\ \frac{L_x}{2} & m = r \end{cases} \tag{5.9}$$

$$\int_0^{L_y} \sin\left(\frac{n\pi y}{L_y}\right) \sin\left(\frac{s\pi y}{L_y}\right) dy = \begin{cases} 0 & n \neq s \\ \frac{L_y}{2} & n = s \end{cases} \tag{5.10}$$

In the light of equations (5.9) and (5.10), equation (5.8) can be solved for coefficients $p_{mn}$ as

$$p_{mn} = \frac{4}{L_x\, L_y} \int_0^{L_x} \int_0^{L_y} f(x,y) \sin\left(\frac{m\pi x}{L_x}\right) \sin\left(\frac{n\pi y}{L_y}\right) dy\, dx \tag{5.11}$$

According to equations (4.7) and (5.1), the projection of a distributed load for a simply supported shell is defined as

$$f_{ij} = \int_0^{L_x} \int_0^{L_y} f(x,y) \sin\left(\frac{i\pi x}{L_x}\right) \sin\left(\frac{j\pi y}{L_y}\right) dy\, dx \tag{5.12}$$

One may notice that for a concentrated load with magnitude of $p_0$ that acts on a point with a coordinate of $(x_0, y_0)$, still equations (5.7) and (5.12) are valid, while in this case the $p_{mn}$ is defined as [50]

$$p_{mn} = \frac{4\, p_0}{L_x\, L_y} \sin\left(\frac{m\pi x_0}{L_x}\right) \sin\left(\frac{n\pi y_0}{L_y}\right) \tag{5.13}$$

It is worth mentioning that, all results are based on the three-mode discretization, i.e. $(i, j = 1,3,5)$, which results in eighteen generalized coordinates: $q_{11}, q_{13}, q_{15}, q_{31}, q_{33}, q_{35}, q_{51}, q_{53}, q_{55}, F_{11}, F_{13}, F_{15}, F_{31}, F_{33}, F_{35}, F_{51}, F_{53}$ and $F_{55}$. Note that due to the geometry of the shell, stacking sequence of laminate, boundary conditions and the applied load, only the symmetric modes are contributing. For linear and nonlinear static analysis, the time dependent terms in the discretized model of the shell must be set to zero. As a result, the nonlinear ordinary differential equations reduce to a set of nonlinear coupled algebraic equations. Afterwards, these algebraic equations

are solved by means of a modified Newton-Raphson method for the equilibrium positions. It is worth mentioning that in all figures and tables related to the nonlinear bending of shells and plates, the center deflection of the structure is considered.

### 5.1. Model Verification

Before presenting the results, it is crucial to validate the present model against the results available in the literature. Three different types of loading are taken into account: uniform distributed load (UDL), sinusoidal distributed load (SDL), and central point load (CPL). Based on the Navier solution, Ugural [50] suggested the following closed form solutions for deflection of simply supported isotropic plates under three different loading. The dimensions of plate are $L_x$, $L_y$ and $h$ in the $x, y$ and $z$ -directions, respectively. Under a uniform distributed load, the deflection of the plate at a point with a coordinate of $(x, y)$ is [50]

$$w_{UDL}(x,y) = \frac{16\, p_0}{\pi^6 D} \sum_{i}^{\infty} \sum_{j}^{\infty} \frac{\sin\left(\frac{i\pi x}{L_x}\right) \sin\left(\frac{j\pi y}{L_y}\right)}{i\, j \left[\left(\frac{i}{L_x}\right)^2 + \left(\frac{j}{L_y}\right)^2\right]^2}\ , \qquad i,j = 1,3,5,\ldots\ , \tag{5.14}$$

$$f(x,y) = p_0$$

For a square plate, i.e. $L_x = L_y$, and considering the deflection of plate's center, the summation converges to the following formula [50]:

$$w_{UDL}\left(\frac{L_x}{2}, \frac{L_y}{2}\right) = \frac{0.00406\, p_0\, L_x^4}{D}\ , \qquad f(x,y) = p_0 \tag{5.15}$$

Under a concentrated load that acts at a point with $(x_0, y_0)$ coordinates, the deflection of the plate at a point with a coordinate of $(x, y)$ is [50]

$$w_{CPL}(x,y) = \frac{4\, p_0}{\pi^4 D\, L_x\, L_y} \sum_{i}^{\infty} \sum_{j}^{\infty} \frac{\sin\left(\frac{i\pi x_0}{L_x}\right) \sin\left(\frac{j\pi y_0}{L_y}\right)}{\left[\left(\frac{i}{L_x}\right)^2 + \left(\frac{j}{L_y}\right)^2\right]^2} \sin\left(\frac{i\pi x}{L_x}\right) \sin\left(\frac{j\pi y}{L_y}\right), \tag{5.16}$$

$$i,j = 1,3,5,\ldots\ , \qquad f(x_0, y_0) = p_0$$

For a square plate, i.e. $L_x = L_y$, with a concentrated load at its center (central point load) and considering the deflection of plate's center, the summation converges to the following formula [50]:

$$w_{CPL}\left(\frac{L_x}{2},\frac{L_y}{2}\right)=\frac{0.01159\,p_0\,L_x^2}{D}\quad,\qquad f\left(\frac{L_x}{2},\frac{L_y}{2}\right)=p_0 \tag{5.17}$$

Under a sinusoidal distributed load, the deflection of the plate at a point with a coordinate $(x,y)$ is [50]:

$$w_{SDL}(x,y)=\frac{1}{\pi^4 D}\sum_{i}^{\infty}\sum_{j}^{\infty}\frac{p_{ij}}{\left[\left(\frac{i}{L_x}\right)^2+\left(\frac{j}{L_y}\right)^2\right]^2}\sin\left(\frac{i\pi x}{L_x}\right)\sin\left(\frac{j\pi y}{L_y}\right),$$

$$i,j=1,2,3,\ldots\ ,\ f(x,y)=p_0\sin\left(\frac{m\pi x}{L_x}\right)\sin\left(\frac{n\pi y}{L_y}\right) \tag{5.18}$$

$$p_{ij}=\frac{4}{L_x\,L_y}\int_0^{L_x}\int_0^{L_y}f(x,y)\sin\left(\frac{i\pi x}{L_x}\right)\sin\left(\frac{j\pi y}{L_y}\right)dy\,dx \tag{5.19}$$

where in all cases D is the flexural rigidity of the plate and defined as [50]

$$D=\frac{E\,h^3}{12\,(1-v^2)} \tag{5.20}$$

The present model is verified against reference [50] for the linear static analysis of simply supported isotropic plate made of Aluminum with material and geometrical properties listed in Table 5.1. The results of this comparison are shown in Table 5.2. To find out the effective number of modes which must be retained in the Galerkin's discretization, a sensitivity analysis is performed and results are listed in Table 5.3. In this table, the results of the present model is compared with reference [50] by making use of equations (5.14) and (5.16). Table 5.3 illustrates that increasing the number of modes improves the accuracy of the solution.

For simply supported doubly curved FRC shells under a uniform distributed load, a comparison is made with the analytical results of Reddy [43]. The material properties and dimensions of the shell are $E_{11}=25E_{22}$, $G_{12}=G_{13}=0.5E_{22}$, $G_{23}=0.2E_{22}$, $E_{22}=10^6 Pa$, $v_{12}=0.25$, $L_x/h=L_y/h=100$, $R_x=R_y, h=0.1\,m$. The nondimensional linear deflection of the shell center is presented in Table 5.4 for various values of $R_x/L_x$ and different layups. Under a uniform loading, the nondimensional deflection is defined as [43]

$$\bar{w}\left(\frac{L_x}{2},\frac{L_y}{2}\right)=\frac{w\,E_{22}\,h^3\,1000}{L_x^4\,p_0}\quad,\qquad f(x,y)=p_0 \tag{5.21}$$

Table 5.1: Mechanical and geometrical properties of an isotropic plate.

| $E\ (GPa)$ | $\rho\ (kg/m^3)$ | $v$ | $L_x\ (cm)$ | $L_y\ (cm)$ | $h\ (mm)$ |
|---|---|---|---|---|---|
| 71 | 2770 | 0.33 | 60 | 60 | 4 |

Table 5.2: Comparison of linear center deflection (mm) of simply supported isotropic square plate under various loading.

| | UDL | SDL | CPL |
|---|---|---|---|
| | $f(x,y)=100\ \ Pa$ | $f(x,y)=100\sin\left(\frac{\pi x}{L_x}\right)\sin\left(\frac{\pi y}{L_y}\right)\ Pa$ | $f\left(\frac{L_x}{2},\frac{L_y}{2}\right)=100\ \ N$ |
| Present | 0.123932 | 0.0782735 | 0.967722 |
| [50] | 0.123823 | 0.0782735 | 0.981873 |

Table 5.3: Convergence analysis for linear center deflection (mm) of simply supported isotropic square plate under various loading.

| | UDL | | CPL | |
|---|---|---|---|---|
| | $f(x,y)=100\ \ Pa$ | | $f\left(\frac{L_x}{2},\frac{L_y}{2}\right)=100\ \ N$ | |
| Modes' number | Present | [50] | Present | [50] |
| $i,j=1$ | 0.1268923 | 0.1268923 | 0.8697058 | 0.8697058 |
| $i,j=1,2$ | 0.1268923 | 0.1268923 | 0.8697058 | 0.8697058 |
| $i,j=1,2,3$ | 0.1236825 | 0.1236825 | 0.9500194 | 0.9500194 |
| $i,j=1,2,3,4$ | 0.1236825 | 0.1236825 | 0.9500194 | 0.9500194 |
| $i,j=1,2,3,4,5$ | 0.1239324 | 0.1239324 | 0.9677220 | 0.9677220 |

Table 5.4: Comparison of the nondimensional linear center deflection of simply supported doubly curved FRC shells under a uniform distributed load.

| | Layup | | | | | |
|---|---|---|---|---|---|---|
| | [0,90] | | [0,90,0] | | [0,90,90,0] | |
| $\frac{R_x}{L_x}$ | Present | [43] | Present | [43] | Present | [43] |
| 1 | 0.073078 | 0.0718 | 0.072604 | 0.0718 | 0.072309 | 0.0715 |
| 2 | 0.287606 | 0.2855 | 0.287645 | 0.2858 | 0.285679 | 0.2844 |
| 3 | 0.646385 | 0.6441 | 0.624469 | 0.6224 | 0.625585 | 0.6246 |
| 4 | 1.143434 | 1.1412 | 1.045579 | 1.0443 | 1.055936 | 1.0559 |
| 5 | 1.755355 | 1.7535 | 1.511719 | 1.5118 | 1.534433 | 1.5358 |
| 10 | 5.540495 | 5.5428 | 3.634492 | 3.6445 | 3.709345 | 3.7208 |
| ∞ | 16.957866 | 16.980 | 6.664467 | 6.6970 | 6.798859 | 6.8331 |

Table 5.5 presents the sensitivity of the linear bending solution against the even modes retained in the discretization of simply supported doubly curved FRC shells with layups [0,90]. It can be seen that only the symmetric modes are contributing. Therefore, the first three odd modes are used in the discretization.

Figure 5.2, presents a comparison between the current model and the analytical results of Reddy [43] for linear static bending of simply supported composite plates under a uniform distributed load taking into account the influence of the aspect ratio and staking sequence. As the figure shows, a good agreement has been reported. The material properties and dimensions of plate are $E_{11} = 25E_{22}$, $G_{12} = G_{13} = 0.5E_{22}$, $G_{23} = 0.2E_{22}$, $v_{12} = 0.25$, $L_x/h = L_y/h = 100$. The nondimensional center deflection of the plate in this figure is based on the following equation [43]:

$$\widehat{w}\left(\frac{L_x}{2}, \frac{L_y}{2}\right) = \frac{w\, E_{22}\, h^3}{p_0\, L_y^4} \quad , \qquad f(x,y) = p_0 \tag{5.22}$$

Table 5.5: Sensitivity analysis of the nondimensional linear center deflection of simply supported FRC shell with layup [0,90] under a uniform distributed load.

| | $\frac{R_x}{L_x}$ | | |
|---|---|---|---|
| Modes' number | 5 | 10 | ∞ |
| $i,j = 1$ | 1.934504 | 5.789371 | 17.242061 |
| $i,j = 1,2$ | 1.934504 | 5.789371 | 17.242061 |
| $i,j = 1,2,3$ | 1.737121 | 5.520424 | 16.937108 |
| $i,j = 1,2,3,4$ | 1.737121 | 5.520424 | 16.937108 |
| $i,j = 1,2,3,4,5$ | 1.755355 | 5.540495 | 16.957866 |

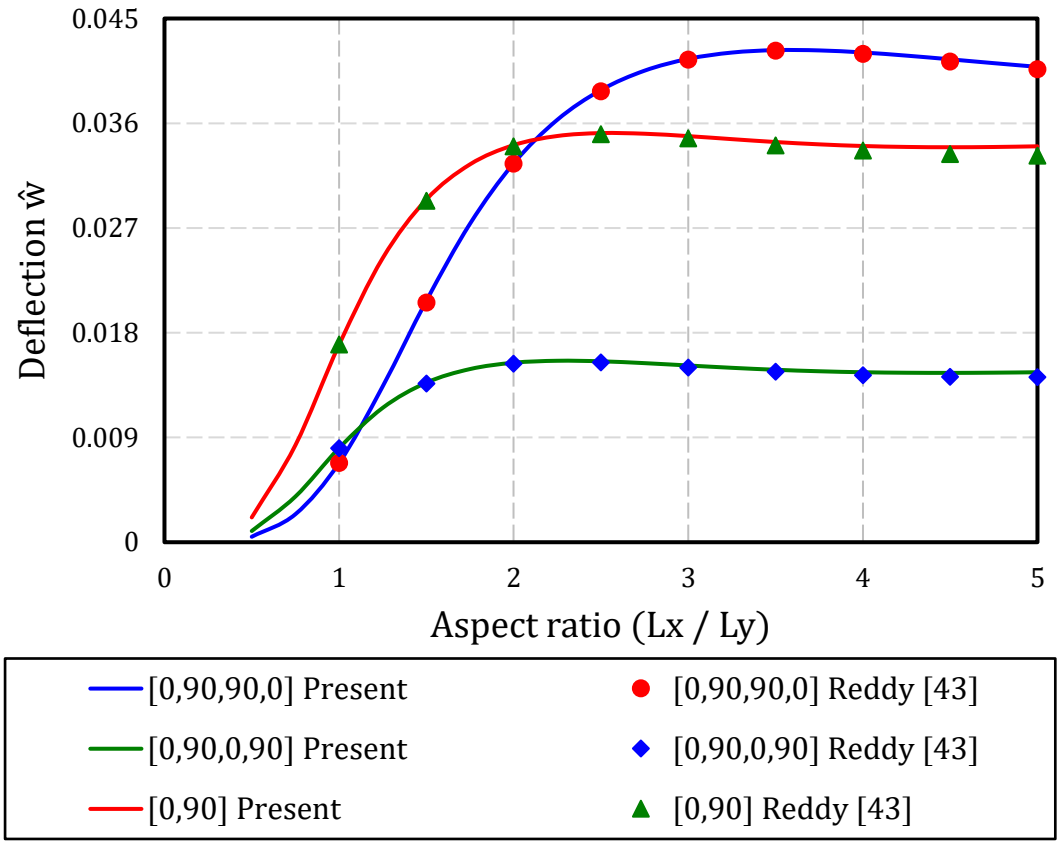


Figure 5.2: Comparison of nondimensional linear center deflection of simply supported composite plate with different layups and aspect ratios under a uniform distributed load.

Figure 5.3 presents the nonlinear static bending and snapthrough of simply supported FRC shell under a uniform distributed load using the current model and the FE results reported by Noor and Hartely [24] and Reddy [43]. As it is evident from the figure, an excellent agreement has been obtained. The shell is made of a nine-layer cross ply laminate [0,90,0,90,0,90,0,90,0] with material and geometrical properties of $E_{11} = 40E_{22},\ E_{22} = 10^6\ psi,\ G_{12} = G_{13} = 0.6E_{22},\ G_{23} = 0.5E_{22},\ v_{12} = 0.25,\ h = 1\ in, L_x = L_y = 100\ in, R_x = R_y = R = -1000\ in.$

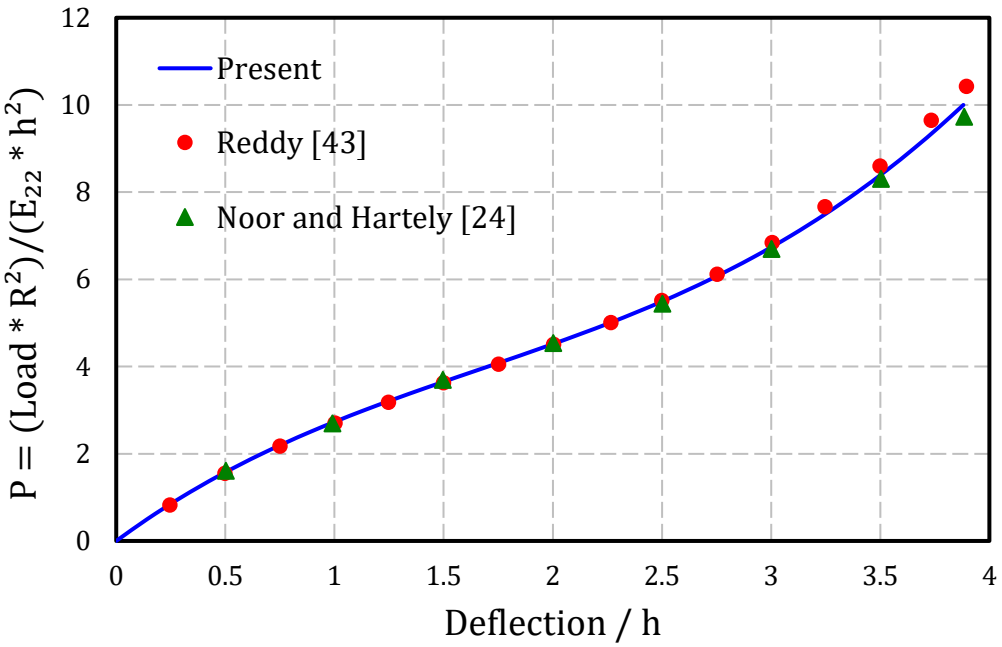


Figure 5.3: A comparison of the nonlinear load-deflection curve of simply supported doubly curved composite shell with layup [0,90,0,90,0,90,0,90,0] under a uniform distributed load.

Having the model validated, we present the numerical results for the nonlinear bending and snapthrough behavior of doubly curved shells made up of two types of materials, Aluminum as an isotropic material with properties $E = 71\ GPa,\ \rho = 2770\ kg/m^3,\ v = 0.33$ [15] and FRC with material properties of $E_{11} = 181\ GPa, E_{22} = 10.3\ GPa, G_{12} = 7.17\ GPa, \rho = 1579\ kg/m^3, v_{12} = 0.28$ [52].

## 5.2. Nonlinear Bending of Shells: The Jump Phenomenon

This section addresses the snapthrough and jump phenomena that may occur during the nonlinear bending of doubly curved shells. Figure 5.4 illustrates the nonlinear bending behavior of an isotropic doubly curved shell under a uniform distributed load. The shell dimensions are $h = 4\ mm, L_x = L_y = 60\ cm, R_x = R_y = -10L_x$. In the loading process, the red dashed line, the load deflection curve is monotonic, from A to C, before the shell jumps, from C to E. After the jump, increasing the load causes the shell to follow the deflection path from point E to F. Now in the unloading process, the green dashed line, as the load decreases, the shell follows the path from point F to point D. Then, decreasing the load further causes the shell to jump from point D to point B. After this jump, the shell follows the path from point B to point A as the load decreases. The loads related to points C and D are called the snapthrough and snapback load, respectively. In the snapthrough/snapback motion, the shell changes its configuration from concave to convex and vice versa.

In the case that there exist jumps, points C and D are also called the limit points. The states between points C and D are unstable solutions which are shown by dotted points. The region between the two vertical lines (CE and DB) which is the region between the snapthrough and snapback loads is called the bi-stability region. The name comes from the fact that in this area for each specific load, there exist two stable equilibrium states.

To define the snapthrough and snapback loads, one will face two different scenarios, either the jumps occur in the load-deflection curve or the curve is continuous (without jump). If there are jumps, the snapthrough and snapback loads must be calculated according to the stability analysis of the solutions and the jump phenomenon. We notice that due to the three-mode contribution, the Jacobian matrix in this study is an 18 by 18 matrix. For the load-deflection curves that are continuous and do not include the jump phenomenon, the snapthrough loads must be found by means of the first and second derivatives of the load-deflection curve. The first derivative of the load-deflection curve defines the slope while the second derivative defines the curvature. When the second derivative changes its sign from positive to negative or vice versa, the snapthrough or snapback occurs. In the case of a continuous load-deflection curve, the

snapthrough and snapback loads become identical and the bi-stability region and the jump phenomenon vanish.

It is worth mentioning that in this thesis, in all cases it is assumed that the material behaves elastically through the loading and unloading process and it does not reach to the plastic deformation. As an evidence, the von Mises stress for a simply supported isotropic shell under uniformly distributed load is shown in Figure 5.5. The results of this figure are related to a point with coordinates of $(L_x/2\,, L_y/2\,, 0)$ and the shell dimensions are $h = 4\ mm,\ L_x = L_y = 60\ cm,\ R_x = R_y = -10L_x$. The von Mises stress is defined as

$$\sigma_y = \sqrt{\frac{1}{2}\left[\left(\sigma_{xx} - \sigma_{yy}\right)^2 + \left(\sigma_{yy} - \sigma_{zz}\right)^2 + (\sigma_{zz} - \sigma_{xx})^2\right] + 3\left(\tau_{xy}^2 + \tau_{xz}^2 + \tau_{yz}^2\right)} \qquad (5.23)$$

In the case of plane stress ($\sigma_{zz} = \tau_{xz} = \tau_{yz} = 0$), equation (5.23) reduces to

$$\sigma_y = \sqrt{\sigma_{xx}^2 + \sigma_{yy}^2 + 3\tau_{xy}^2 - \sigma_{xx}\sigma_{yy}} \qquad (5.24)$$

The yielding stress for aluminum is reported as 169 MPa, while according to the Figure 5.5 the maximum von Mises stress that may occur during the snapthrough motion and beyond the snapthrough motion is around 20 MPa. In other words, the snapthrough and snapback motions are in the region of elastic deformation.

### 5.3. Sensitivity Analysis versus the Number of Modes

In order to assess the significance of the number of modes retained in the discretization, the results for the nonlinear bending of simply supported symmetric $[0,90]_S$ spherical shell under a uniform distributed load using a single, two, and three modes are presented in Figure 5.6. The shell dimensions are $h = 4\ mm,\ L_x = L_y = 60\ cm,\ R_x = R_y = -10\,L_x$. It can be seen that a single-mode discretization underestimates the snapback load and overestimates the deflection afterwards. Nevertheless, the results are similar in the pre snapthrough region where the deflection is small. Therefore, all results of our analysis are based on the three-mode discretization. It is worth mentioning that due to the geometry and type of loading only the symmetric modes are contributing $(i, j = 1,3,5)$ which resulted in eighteen generalized coordinates, as outlined earlier.

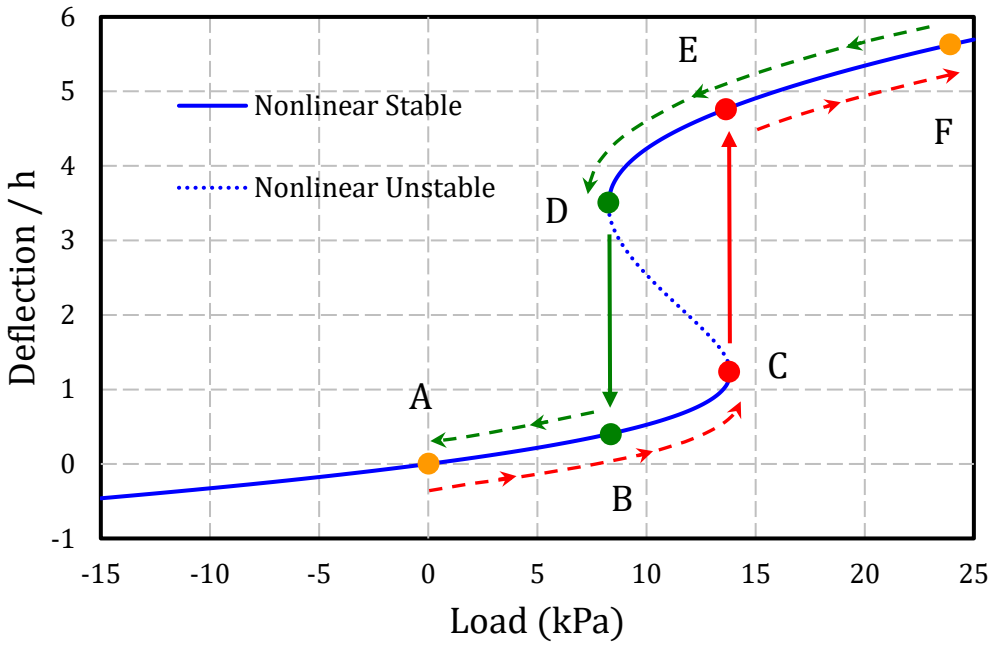


Figure 5.4: Nonlinear load-deflection curve of simply supported isotropic spherical shell under a uniform distributed load and illustration of the snapthrough, snapback, stable and unstable solutions, bi-stability region and jump phenomena.

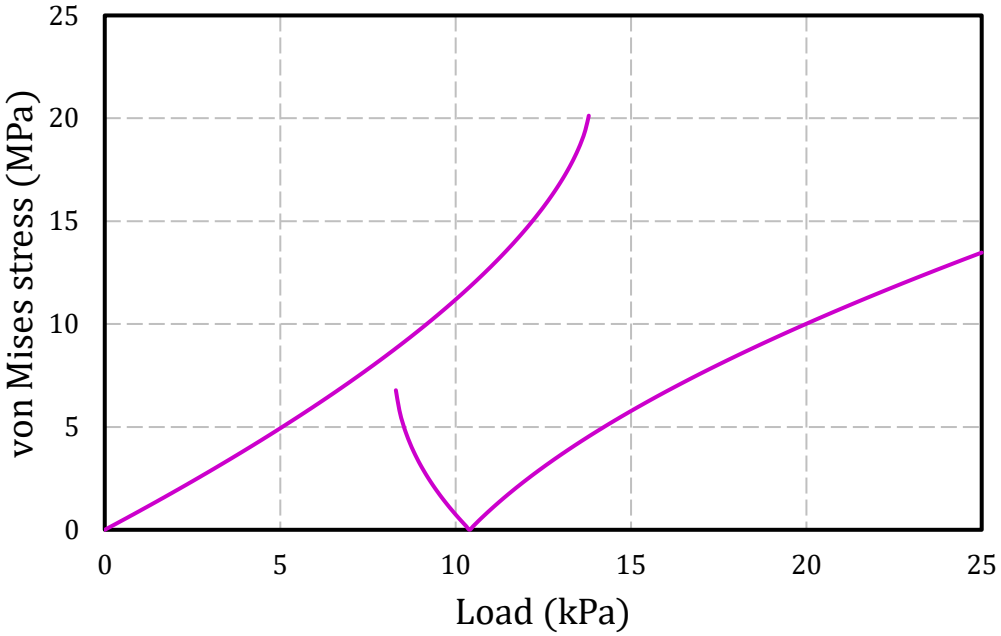


Figure 5.5: Load-stress curve for simply supported aluminum spherical shell under uniformly distributed load for a point with coordinates of $(L_x/2\,,L_y/2\,,0)$.

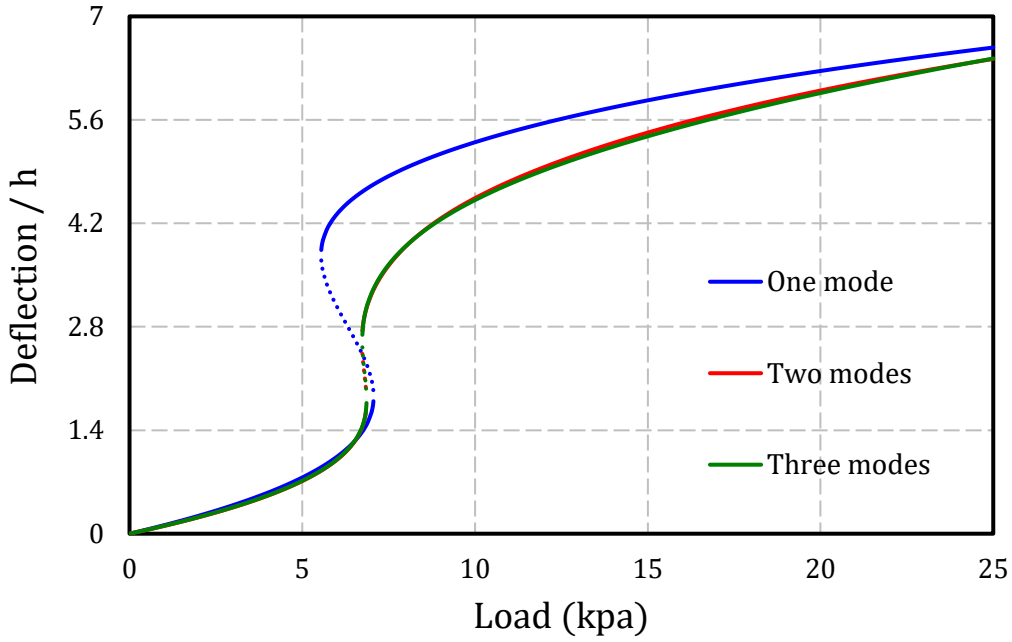


Figure 5.6: The nonlinear load-deflection curve of simply supported symmetric $[0,90]_S$ spherical shells under a uniform distributed load using one, two and three modes.

Next, a parametric study of nonlinear static bending of doubly curved FRC shells is presented. The influence of the curvature-to-length ratio, curvature ratio, length-to-thickness ratio and stacking sequence of laminate on the nonlinear bending, snapthrough/snapback loads, bi-stability region and the jumps phenomena will be examined.

### 5.4. Effect of the Curvature-to-Length Ratio $R_x/L_x$

The first set of the numerical results is concerned with the nonlinear bending behavior of composite spherical shells with varying the curvature-to-length ratio $R_x/L_x$. Here the length of the shell is kept constant while the radius of curvature is varied. For the sake of comparison, the nonlinear static bending behavior of a metallic shell made up of Aluminum is presented as a baseline. Figure 5.7 illustrates the nondimensional lateral deflection of the center of a simply supported isotropic spherical shell under a uniformly distributed load. The shell dimensions are $h = 4\ mm$, $L_x = L_y = 60\ cm$, $R_x = R_y$ that will be kept fixed while the layup and the $R_x/L_x$ are varied. The radius of curvature is varied from 10 times the shell's length to infinity. As it is evident from the figure, by increasing the radius of curvature, the snapthrough and

snapback load decreases. One can also note that as the shell's radius increases, the shell shows softening behavior (more deflection under the same load) before the snapthrough while the hardening behavior (less deflection under the same load) is obvious after the snapthrough. Moreover, as the radius of curvature increases, the magnitude of the jump decreases and the bi-stability region diminishes. The stable branches are represented by solid lines while the unstable branches are represented by the dashed lines. At $R_x/L_x = -20$, the load-deflection curve is continuous and there are no jumps. We vary the shell parameters such as the material properties, the curvature-to-length ratio $R_x/L_x$, the curvature ratio $R_y/R_x$, and the thickness and investigate their impact on the nonlinear bending response and the snapthrough and snapback values. One of the objectives is to find out a set of parameters that yields a continuous load-deflection curve and minimize the deflection.

Figures 5.8-5.11 present the nonlinear bending and snapthrough response of a simply supported composite spherical shell under a uniform distributed load with the following layups: unidirectional $[0_4]$, symmetric $[0,90]_S$, unsymmetric $[0,0,90,90]$ and antisymmetric $[0,90,0,90]$, respectively. It is evident from Figure 5.8 that the load-deflection curves are continuous and there are no jumps, which means that the snapthrough and snapback loads are identical. The results show that the material properties represented by the laminate's layup strongly affect the nonlinear bending response, the jump phenomenon, and the snapthrough/snapback loads. In all cases, as the radius of curvature increases, the snapthrough and snapback loads decrease.

Table 5.6 presents the snapthrough and snapback loads for simply supported spherical shells with a variety of materials and curvature-to-length ratio $R_x/L_x$. The numerical results for isotropic and composite shells of $R_x/L_x = -10, -12, -15$ and $-20$ are presented. The lowest snapthrough loads are reported for the unsymmetric $[0,0,90,90]$ laminates. When the snapthrough and snapback loads are different, the shell becomes bi-stable, i.e. it exhibits two stable equilibrium positions and the jump phenomenon exists.

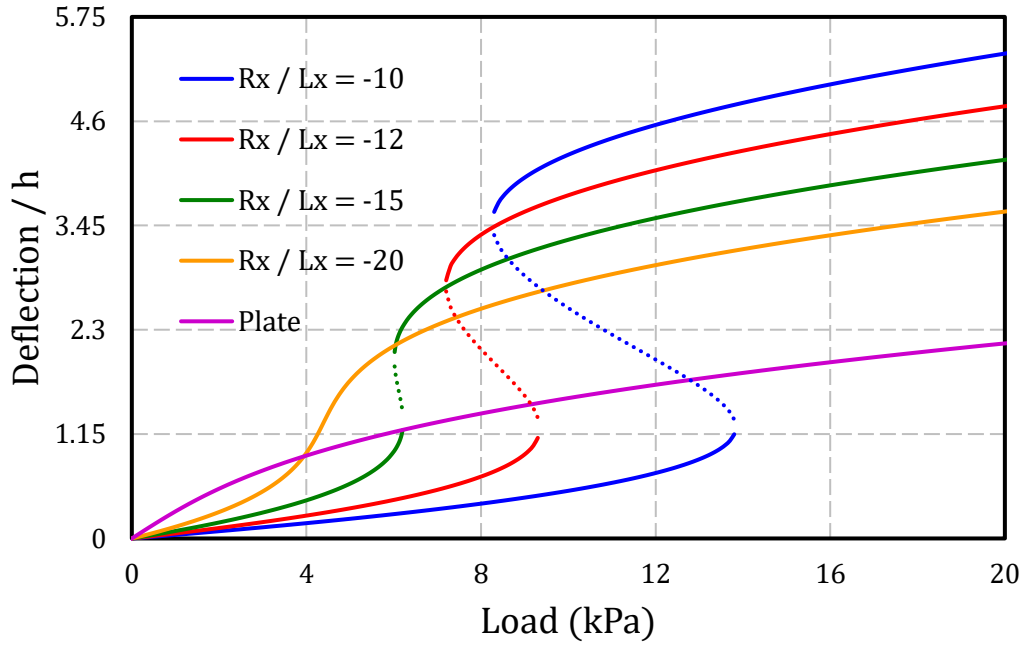


Figure 5.7: The nonlinear load-deflection curves of simply supported isotropic spherical shells under a uniformly distributed load with varying $R_x/L_x$.

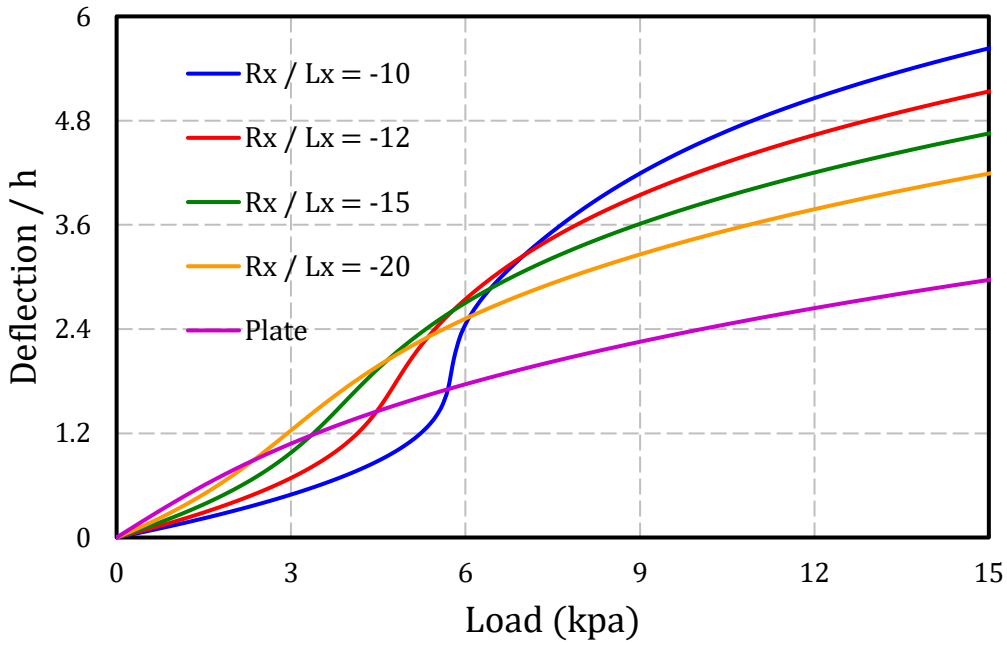


Figure 5.8: The nonlinear load-deflection curves of simply supported unidirectional $[0_4]$ spherical shells under a uniformly distributed load with varying $R_x/L_x$.

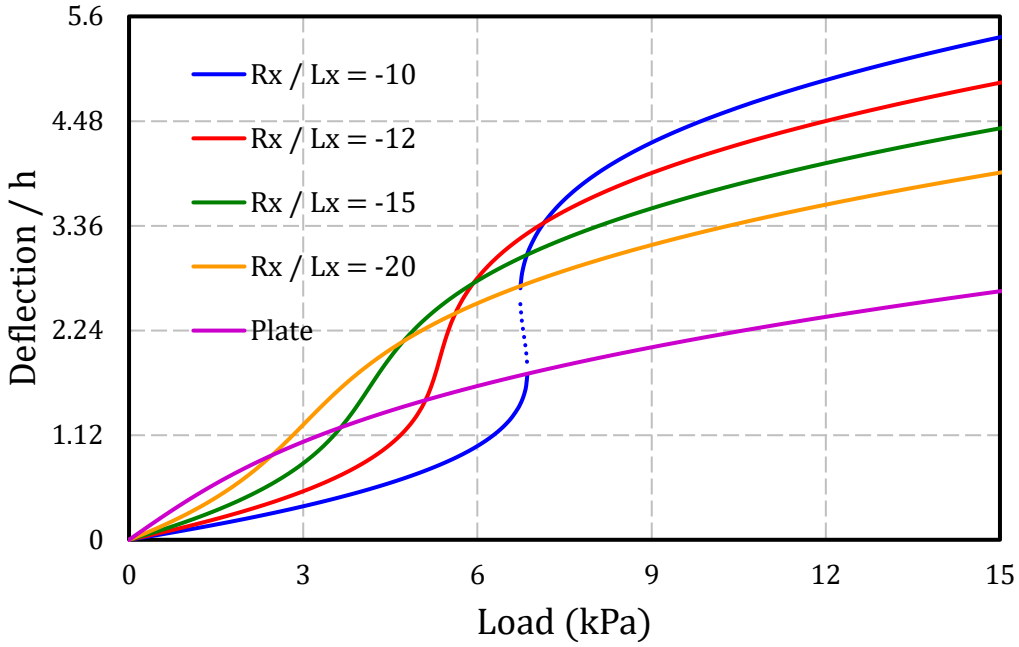


Figure 5.9: The nonlinear load-deflection curves of simply supported symmetric $[0,90]_S$ spherical shells under a uniformly distributed load with varying $R_x/L_x$.

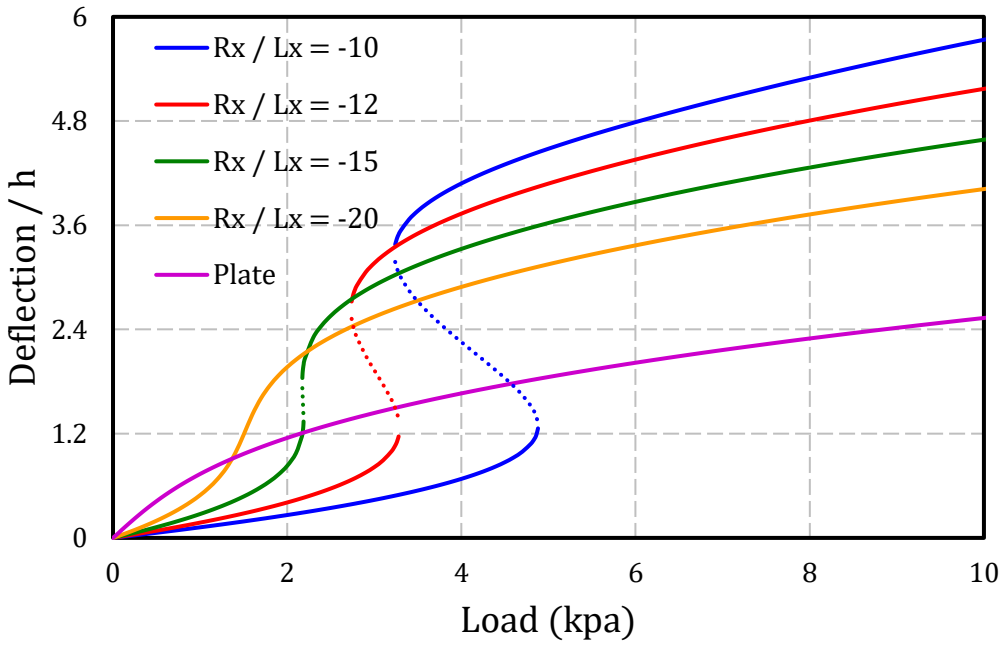


Figure 5.10: The nonlinear load-deflection curves of simply supported unsymmetric [0,0,90,90] spherical shells under a uniformly distributed load with varying $R_x/L_x$.

Table 5.6: The snapthrough and snapback loads of simply supported spherical shells with dimensions of $h = 4\ mm, L_x = L_y = 60\ cm, R_x = R_y$ under a uniform distributed load for a variety of materials and curvature-to-length ratio.

| Material | $R_x/L_x$ | Snapthrough load (Pa) | Snapback load (Pa) |
|---|---|---|---|
| Aluminum | -10 | 13835 | 8258 |
| | -12 | 9341 | 7193 |
| | -15 | 6214 | 6013 |
| | -20 | 4387 | 4387 |
| Unidirectional | -10 | 5763 | 5763 |
| $[0_4]$ | -12 | 4791 | 4791 |
| | -15 | 3909 | 3909 |
| | -20 | 2993 | 2993 |
| Symmetric | -10 | 6861 | 6737 |
| $[0,90]_S$ | -12 | 5353 | 5353 |
| | -15 | 4130 | 4130 |
| | -20 | 3031 | 3031 |
| Unsymmetric | -10 | 4881 | 3230 |
| [0,0,90,90] | -12 | 3290 | 2733 |
| | -15 | 2188 | 2174 |
| | -20 | 1520 | 1520 |
| Antisymmetric | -10 | 6463 | 5987 |
| [0,90,0,90] | -12 | 4855 | 4855 |
| | -15 | 3687 | 3687 |
| | -20 | 2665 | 2665 |

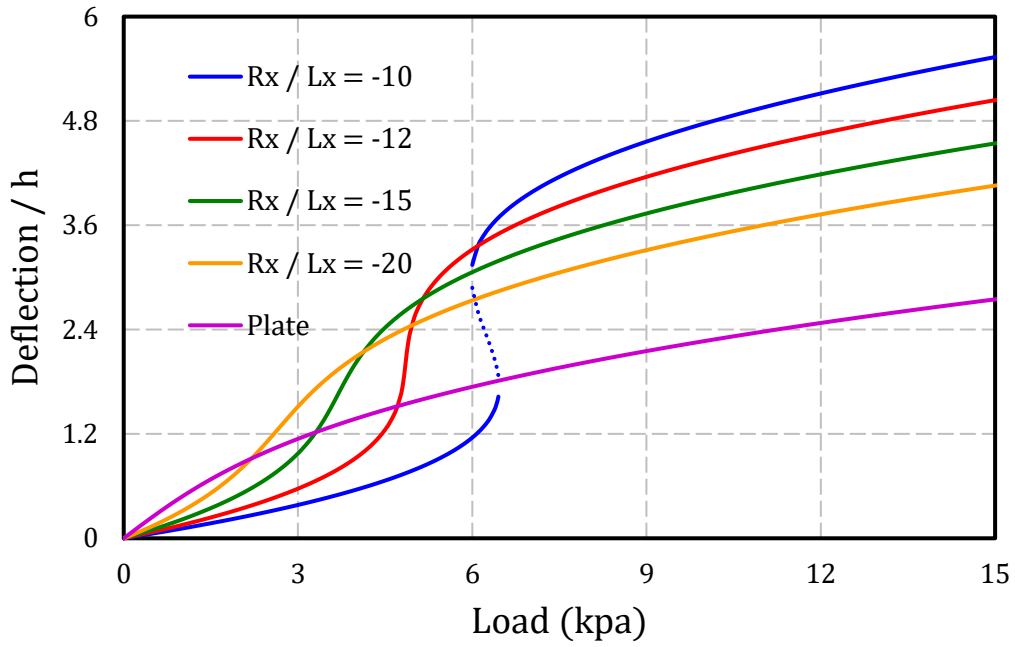


Figure 5.11: The nonlinear load-deflection curves of simply supported antisymmetric [0,90,0,90] spherical shells under a uniform distributed load with varying $R_x/L_x$.

### 5.5. Effect of the Curvature Ratio $R_y/R_x$

Here, the effect of curvature ratio $R_y/R_x$ on the nonlinear bending and snapthrough of simply supported doubly curved shells under a uniformly distributed load is investigated. The shell has the following geometrical properties: $h = 4\ mm$, $L_x = L_y = 60\ cm, R_x = -10L_x$. Figures 5.12-5.16 present the nonlinear bending behavior of isotropic and composite simply supported shells for $R_y/R_x = 1, 1.5$, and 2.5. The results show that as the curvature ratio increases, the snapthrough and snapback loads decrease and the region of bi-stability diminishes. Moreover, in all cases, as the curvature ratio increases, two effects can be observed: softening behavior (more deflection under the same load) before the snapthrough and hardening behavior (less deflection under the same load) after the snapthrough. The laminate's layup is found to significantly affect the snapthrough response. The results reveal that the curvature ratio $R_y/R_x$ and the laminate's layup are key parameters that can be manipulated for a desired response.

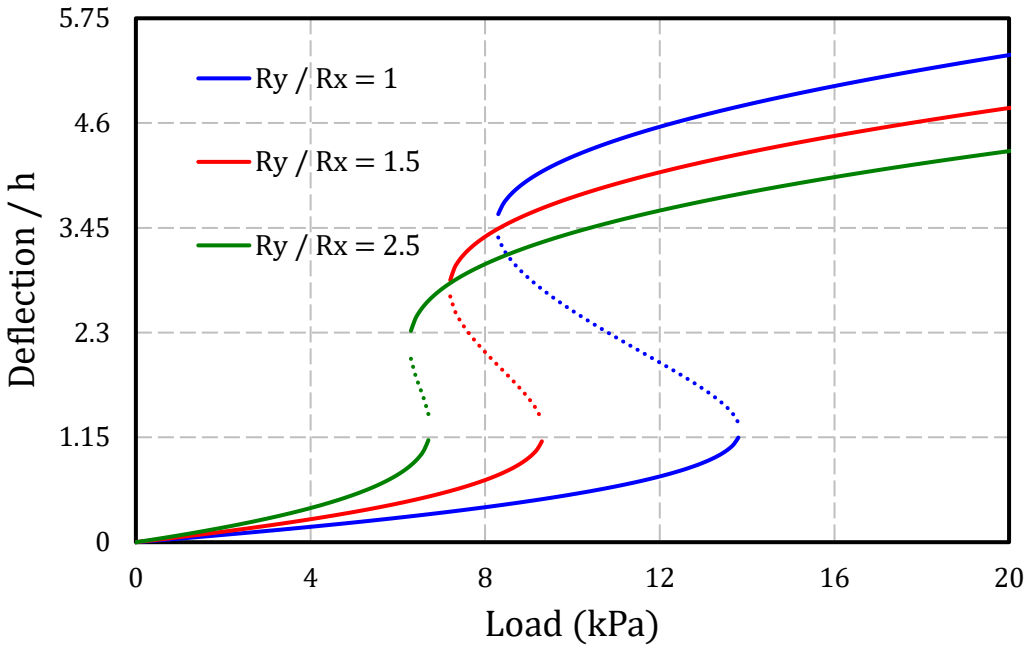


Figure 5.12: The nonlinear load-deflection curves of simply supported isotropic doubly curved shells under a uniformly distributed load with varying $R_y/R_x$.

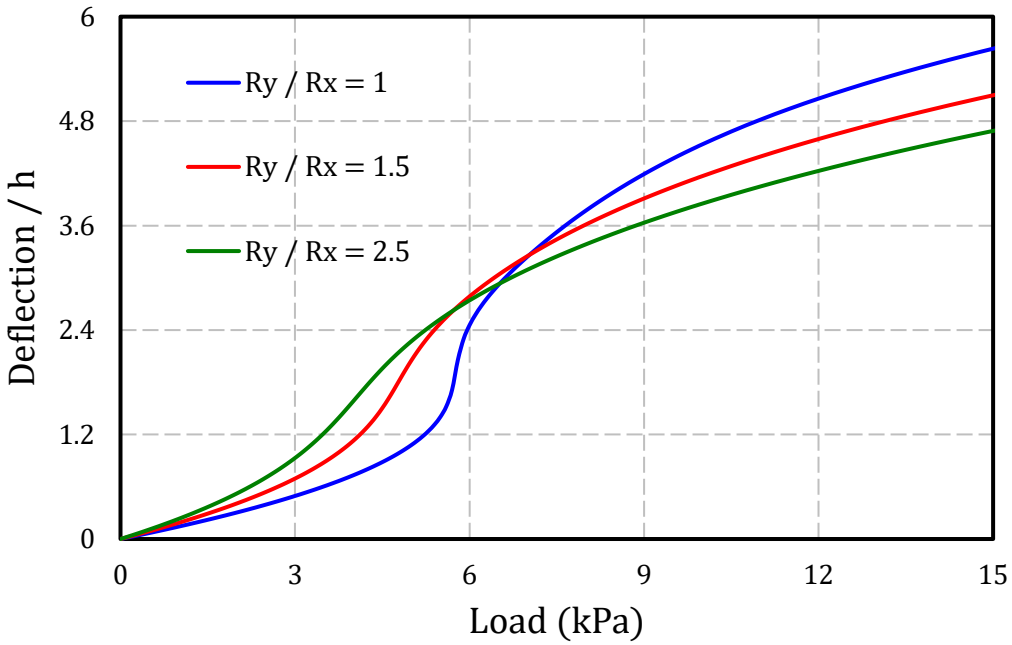


Figure 5.13: The nonlinear load-deflection curves of simply supported unidirectional $[0_4]$ doubly curved shells under a uniformly distributed load with varying $R_y/R_x$.

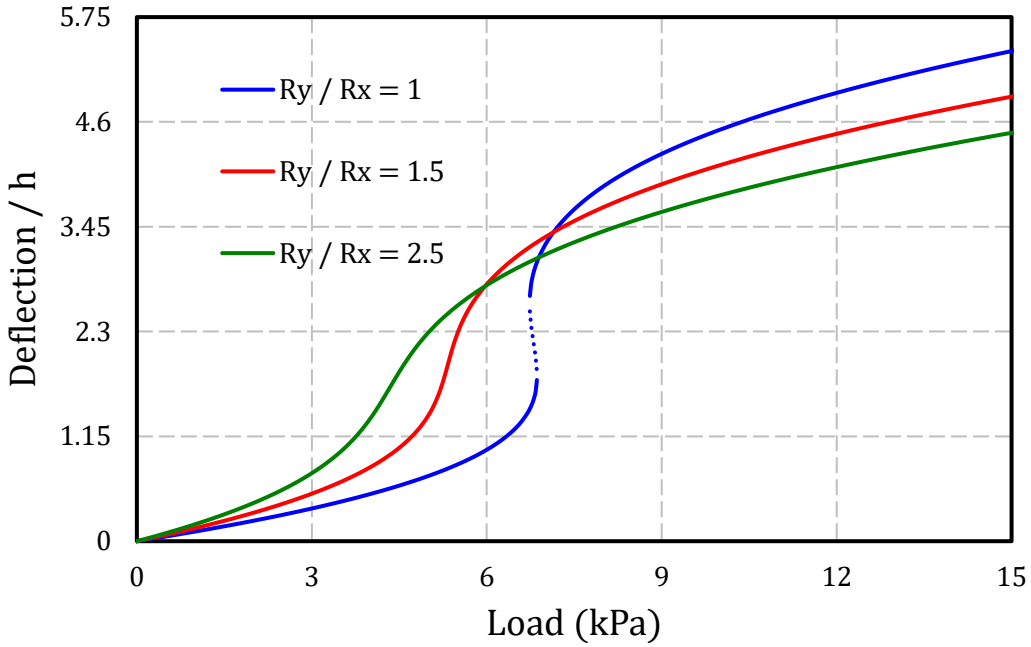


Figure 5.14: The nonlinear load-deflection curves of simply supported symmetric $[0,90]_S$ doubly curved shells under uniformly distributed load with varying $R_y/R_x$.

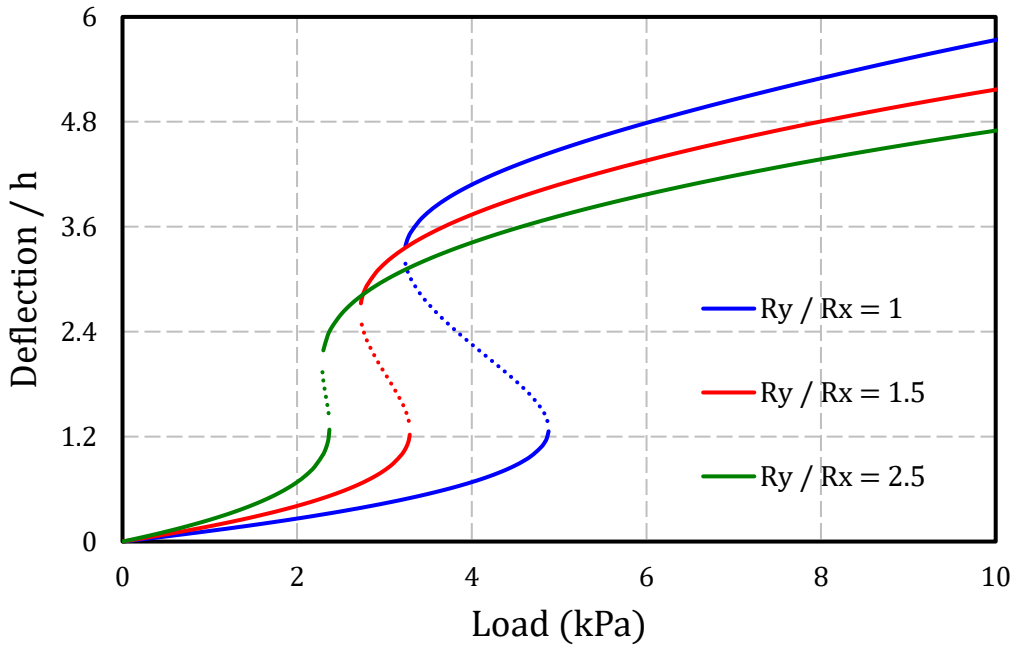


Figure 5.15: The nonlinear load-deflection curves of simply supported unsymmetric [0,0,90,90] doubly curved shells under a uniformly distributed load with varying $R_y/R_x$.

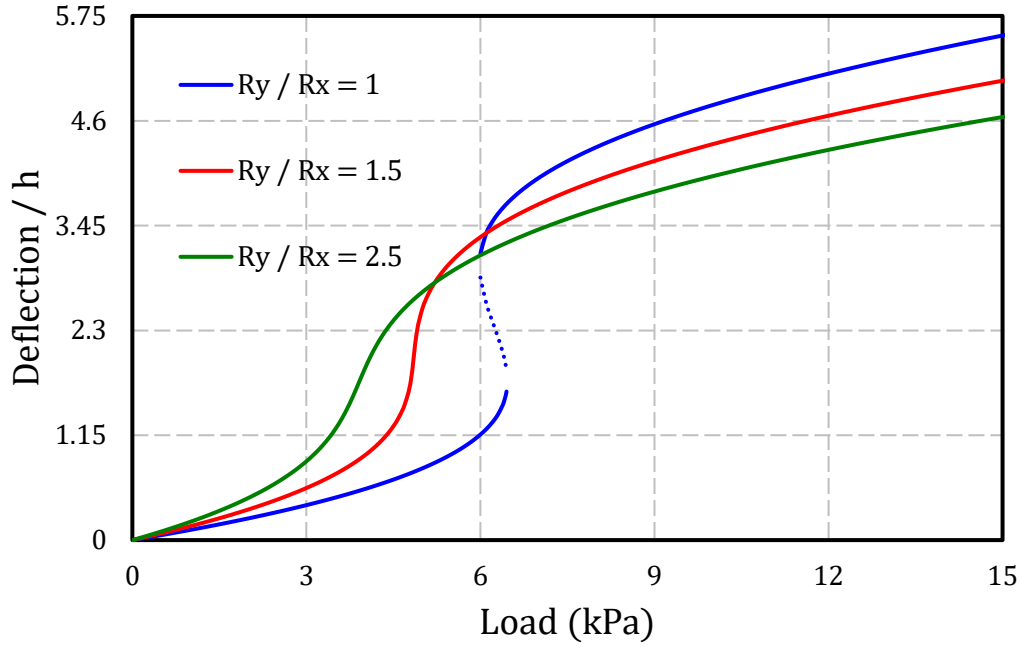


Figure 5.16: The nonlinear load-deflection curves of simply supported antisymmetric [0,90,0,90] doubly curved shells under a uniformly distributed load with varying $R_y/R_x$.

Table 5.7 presents the snapthrough and snapback loads for simply supported shells under a uniformly distributed load with various curvature ratio and material properties. The lowest snapthrough load is reported for the unsymmetric laminates while the symmetric laminate shows the highest snapthrough load of all composites considered in this study.

Next, the influence of the thickness on the snapthrough response of doubly curved composite shells will be examined taking into account the limits of the length-to-thickness ratio for the validity of the model used in this study.

Table 5.7: The snapthrough and snapback loads of simply supported doubly curved shells with dimensions of $h = 4\ mm, L_x = L_y = 60\ cm, R_x/L_x = -10$ under a uniformly distributed load for various materials and curvature ratio $R_y/R_x$.

| Material | $R_y/R_x$ | Snapthrough load (Pa) | Snapback load (Pa) |
|---|---|---|---|
| Aluminum | 1 | 13835 | 8258 |
| | 1.5 | 9343 | 7183 |
| | 2.5 | 6737 | 6266 |
| Unidirectional | 1 | 5763 | 5763 |
| $[0_4]$ | 1.5 | 4781 | 4781 |
| | 2.5 | 4056 | 4056 |
| Symmetric | 1 | 6861 | 6737 |
| $[0,90]_S$ | 1.5 | 5334 | 5334 |
| | 2.5 | 4342 | 4342 |
| Unsymmetric | 1 | 4881 | 3230 |
| [0,0,90,90] | 1.5 | 3291 | 2724 |
| | 2.5 | 2370 | 2287 |
| Antisymmetric | 1 | 6463 | 5987 |
| [0,90,0,90] | 1.5 | 4854 | 4854 |
| | 2.5 | 3907 | 3907 |

## 5.6. Effect of the Shell Thickness

The significance of the shell thickness on the nonlinear bending and snapthrough response of simply supported spherical shell is investigated. Figures 5.17-5.21 demonstrate the nonlinear bending, snapthrough and snapback of simply supported spherical shells under a uniformly distributed load while the thickness of the shell is varied. The geometrical properties of the shell are $L_x = L_y = 60\ cm,\ R_x = R_y =$

$-10L_x$. For the metallic shell, the jump has been reported for the thicknesses considered in this study, as shown in Figure 5.17. On the other hand, the shells with unidirectional layup exhibit a continuous load-deflection curve where there are no jumps, as shown in Figure 5.18. The nonlinear bending, snapthrough and snapback for the symmetric, unsymmetric, and antisymmetric are shown in Figures 5.19-5.21. In all of these figures, before and after the snapthrough, the stiffening behavior is witnessed as the shell becomes thicker. As it is evident from the figures, the shell thickness plays an important role on the nonlinear bending of composite shells.

Table 5.8 presents the snapthrough and snapback uniform loads for spherical isotropic, unidirectional, symmetric, unsymmetric, and antisymmetric shells with various thickness. For continuous load-deflection curves, the snapthrough and the snapback loads are identical. When jumps are involved, the shell exhibits the bi-stability property under loads that lie between the snapthrough and snapback loads. The unsymmetric laminates exhibit the lowest snapthrough and snapback loads while the highest snapthrough and snapback loads are reported for symmetric laminates.

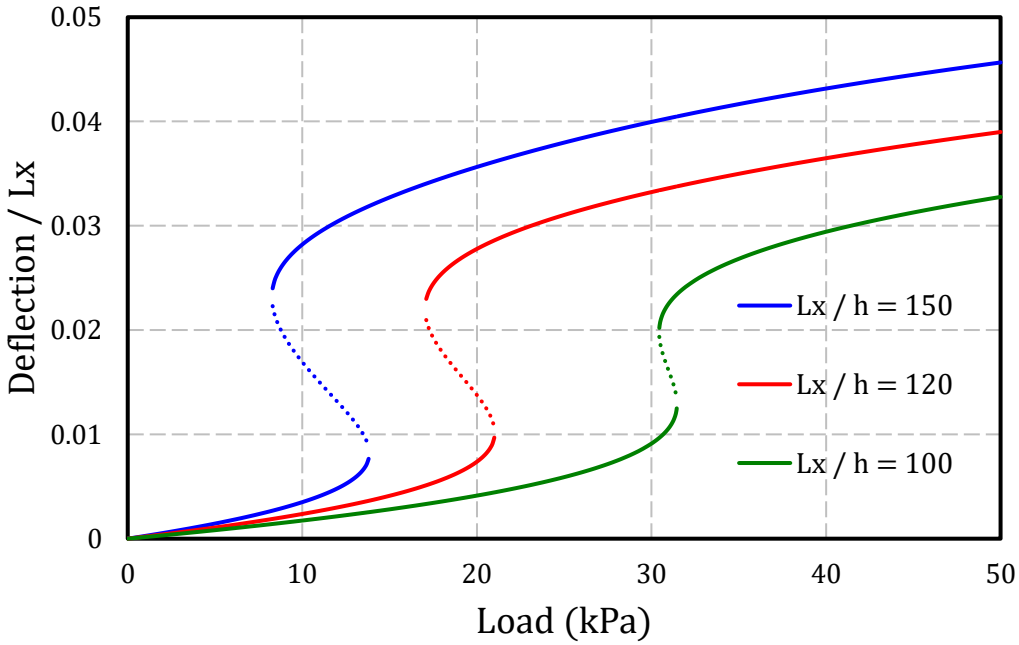


Figure 5.17: The nonlinear load-deflection curves of simply supported isotropic spherical shells under a uniformly distributed load for various $L_x/h$.

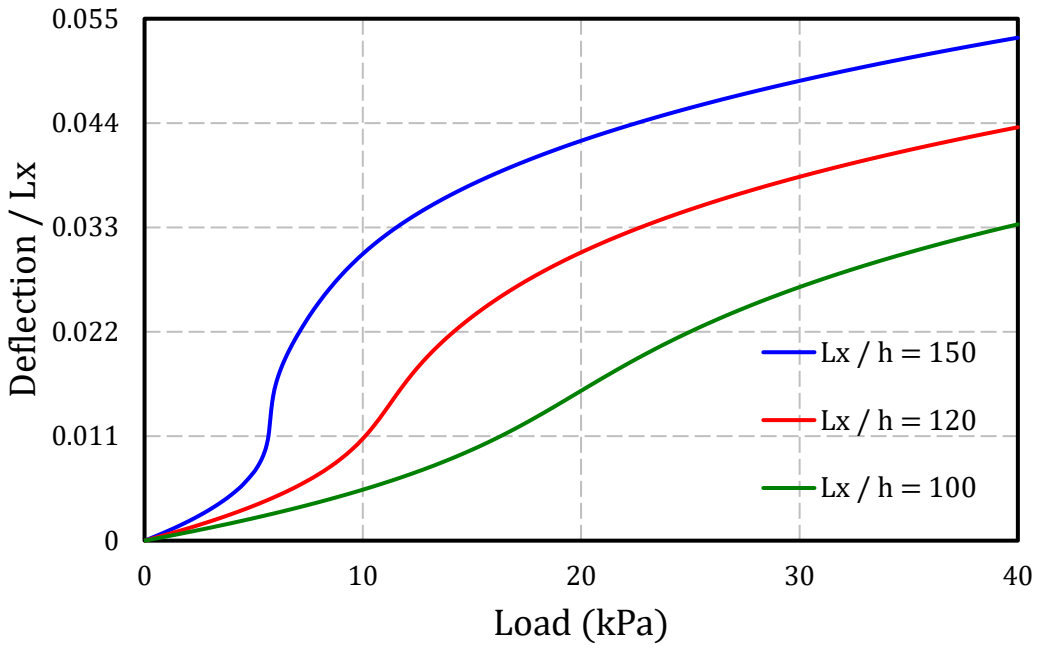


Figure 5.18: The nonlinear load-deflection curves of simply supported unidirectional $[0_4]$ spherical shells under a uniformly distributed load for various $L_x/h$.

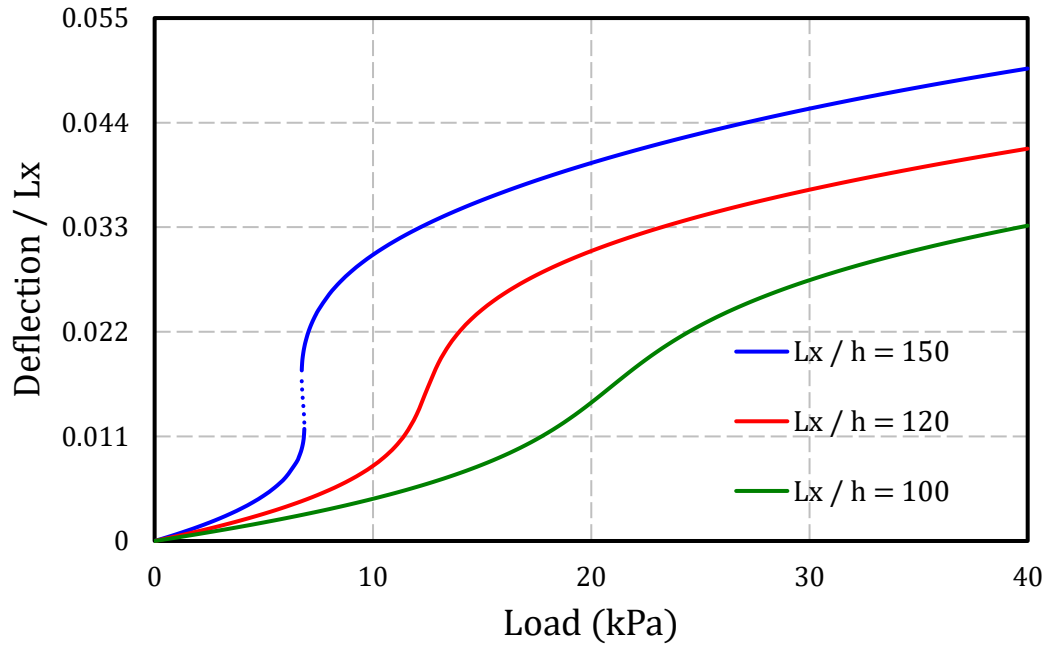


Figure 5.19: The nonlinear load-deflection curves of simply supported symmetric $[0,90]_S$ spherical shells under a uniformly distributed load for various $L_x/h$.

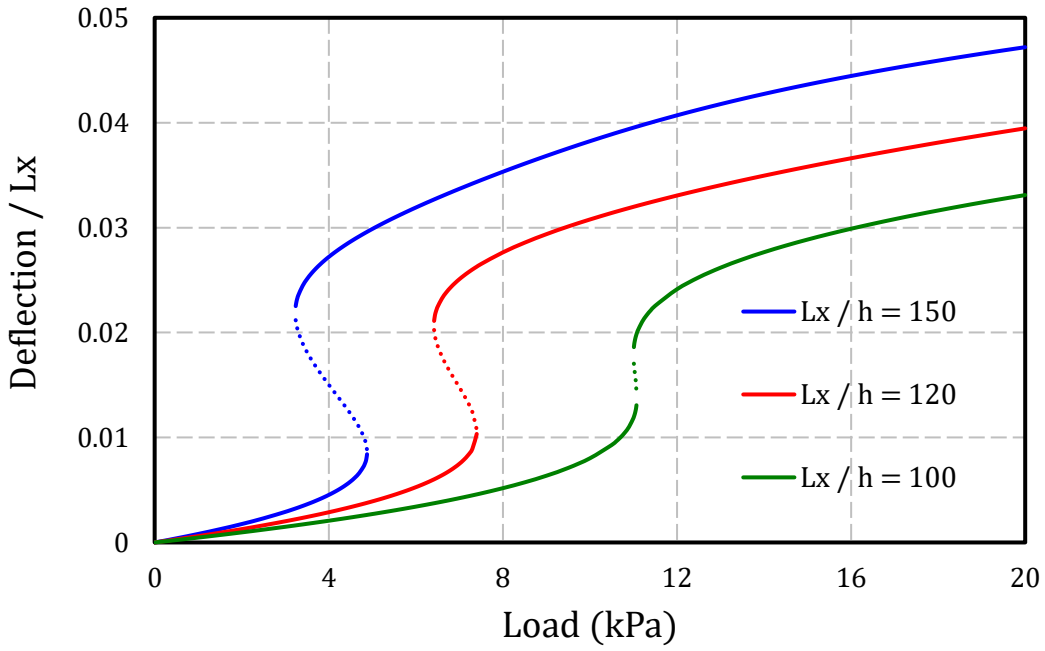


Figure 5.20: The nonlinear load-deflection curves of simply supported unsymmetric [0,0,90,90] spherical shells under a uniformly distributed load for various $L_x/h$.

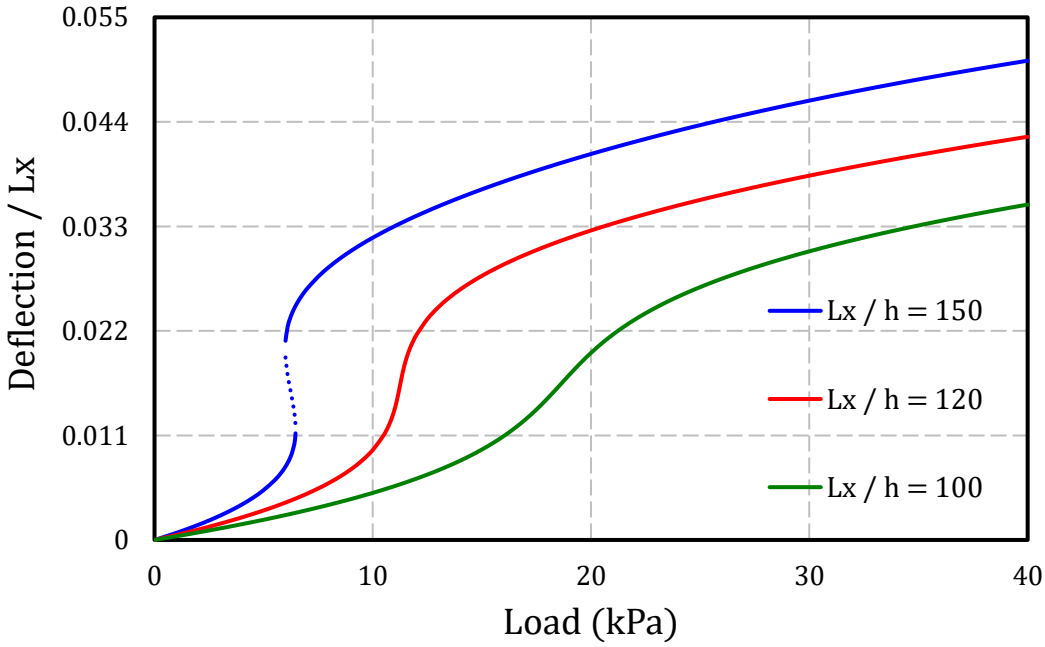


Figure 5.21: The nonlinear load-deflection curves of simply supported antisymmetric [0,90,0,90] spherical shells under a uniformly distributed load for various $L_x/h$.

Table 5.8: The effect of thickness and material on the snapthrough and snapback loads of simply supported spherical shells with dimensions of $L_x = L_y = 60\ cm$, $R_x = R_y = -10L_x$ under a uniformly distributed load.

| Material | $L_x/h$ | Snapthrough Load (Pa) | Snapback Load (Pa) |
|---|---|---|---|
| Aluminum | 150 | 13835 | 8258 |
| | 120 | 21022 | 17028 |
| | 100 | 31461 | 30440 |
| Unidirectional | 150 | 5763 | 5763 |
| $[0_4]$ | 120 | 11259 | 11259 |
| | 100 | 19782 | 19782 |
| Symmetric | 150 | 6861 | 6737 |
| $[0,90]_S$ | 120 | 12436 | 12436 |
| | 100 | 20904 | 20904 |
| Unsymmetric | 150 | 4881 | 3230 |
| [0,0,90,90] | 120 | 7401 | 6416 |
| | 100 | 11078 | 11002 |
| Antisymmetric | 150 | 6463 | 5987 |
| [0,90,0,90] | 120 | 11244 | 11244 |
| | 100 | 18659 | 18659 |

# Chapter 6. Conclusion and Future Work

In this thesis, the nonlinear static bending and snapthrough response of doubly curved laminated shells is investigated. The proposed model is based on the classical lamination shell theory with the von Karman geometric nonlinearity. The equations of motion and the associated boundary conditions are obtained using the Hamilton's principle. By utilizing the nonlinear compatibility equation along with the Airy stress function, the axial displacements are eliminated from equations of motion. Therefore, the three governing equations are reduced to two equations: the compatibility equation and the equation governing the lateral deflection. Afterwards, the two equations of motion are discretized using the Galerkin's approach. The discretized equations are general and apply on different boundary conditions provided that appropriate trial functions are used for the stress function and lateral deflection. The model is validated against the results available in the literature and a good agreement has been obtained. The numerical results for simply supported composite shells under uniformly distributed loads are presented. Namely, unidirectional $[0_4]$, symmetric $[0,90]_S$, unsymmetric $[0,0,90,90]$ and antisymmetric $[0,90,0,90]$ layups were considered. For the sake of comparison, the nonlinear static bending behavior of an isotropic metallic shell made up of Aluminum as a baseline is also presented. A parametric study is performed to examine the influence of three key parameters on the nonlinear bending response of doubly curved composite shells: the radius of curvature-to-length ratio $R_x/L_x$, the ratio of the principal radii of curvature $R_y/R_x$, and the thickness. The results show that as the ratio $R_x/L_x$ increases, the snapthrough load decreases. As the ratio of the radii of curvature $R_y/R_x$ increases, the snapthrough load decreases. As the thickness increases, the snapthrough load increases and the jump phenomenon gets narrowed or disappears. The unsymmetric laminate $[0,0,90,90]$ exhibits the least snapthrough load under different variables considered in this study.

This study could be extended to investigate

- The snapthrough response of FRC doubly curved shells under harmonic loadings.
- The nonlinear dynamics of bi-stable shells.

- The buckling and postbuckling of doubly curved FRC shells.
- The effect of nanoparticles such as carbon nanotubes, graphene nanoplatelets, graphene powder oxide and nanoclays as reinforcement parts for functionally graded reinforced composites on the nonlinear bending behavior.

## References


[1] C. Y. Chia, "Nonlinear analysis of doubly curved symmetrically laminated shallow shells with rectangular planform," *Ingenieur-Archiv,* vol. 58, no. 4, pp. 252-264, 1988, doi: 10.1007/BF00535935.

[2] C.-Y. Chia, "Geometrically Nonlinear Behavior of Composite Plates: A Review," *Applied Mechanics Reviews,* vol. 41, pp. 439-451, 1988.

[3] S. T. Dennis, "A Galerkin solution to geometrically nonlinear laminated shallow shell equations," *Computers & Structures,* vol. 63, no. 5, pp. 859-874, 1997, doi: https://doi.org/10.1016/S0045-7949(96)00380-X.

[4] H.-S. Shen, "Non-linear bending of shear deformable laminated plates under lateral pressure and thermal loading and resting on elastic foundations," *The Journal of Strain Analysis for Engineering Design,* vol. 35, no. 2, pp. 93-103, 2000/02/01 2000, doi: 10.1243/0309324001514053.

[5] H.-S. Shen, "Hygrothermal Effects on the Nonlinear Bending of Shear Deformable Laminated Plates," *Journal of Engineering Mechanics,* vol. 128, no. 4, pp. 493-496, 2002/04/01 2002, doi: 10.1061/(ASCE)0733-9399(2002)128:4(493).

[6] J.-S. Chen, C. Pan, C.-T. Wu, and W. K. Liu, "Reproducing Kernel Particle Methods for large deformation analysis of non-linear structures," *Computer Methods in Applied Mechanics and Engineering,* vol. 139, no. 1, pp. 195-227, 1996/12/15/ 1996, doi: https://doi.org/10.1016/S0045-7825(96)01083-3.

[7] S. Li, W. Hao, and W. K. Liu, "Numerical simulations of large deformation of thin shell structures using meshfree methods," *Computational Mechanics,* vol. 25, no. 2, pp. 102-116, 2000/03/01 2000, doi: 10.1007/s004660050463.

[8] M. Amabili, "Theory and experiments for large-amplitude vibrations of circular cylindrical panels with geometric imperfections," *Journal of Sound and Vibration,* vol. 298, no. 1, pp. 43-72, 2006/11/22/ 2006, doi: https://doi.org/10.1016/j.jsv.2006.04.038.

[9] Y. Nath, M. Prithviraju, and A. A. Mufti, "Nonlinear statics and dynamics of antisymmetric composite laminated square plates supported on nonlinear elastic

subgrade," *Communications in Nonlinear Science and Numerical Simulation,* vol. 11, no. 3, pp. 340-354, 2006/06/01/ 2006, doi: https://doi.org/10.1016/j.cnsns.2004.11.003.

[10] J. Girish and L. S. Ramachandra, "Nonlinear Static Response and Free Vibration Analysis of Doubly Curved Cross-Ply Panels," *Journal of Aerospace Engineering,* vol. 20, no. 1, pp. 45-52, 2007/01/01 2007, doi: 10.1061/(ASCE)0893-1321(2007)20:1(45).

[11] M. Amabili, "Non-linear vibrations of doubly curved shallow shells," *International Journal of Non-Linear Mechanics,* vol. 40, no. 5, pp. 683-710, 2005/06/01/ 2005, doi: https://doi.org/10.1016/j.ijnonlinmec.2004.08.007.

[12] K. M. Liew, X. Zhao, and A. J. M. Ferreira, "A review of meshless methods for laminated and functionally graded plates and shells," *Composite Structures,* vol. 93, no. 8, pp. 2031-2041, 2011/07/01/ 2011, doi: https://doi.org/10.1016/j.compstruct.2011.02.018.

[13] H.-S. Shen, *A Two-Step Perturbation Method in Nonlinear Analysis of Beams, Plates and Shells,* Hoboken: Wiley, 2013.

[14] F. Alijani and M. Amabili, "Non-linear static bending and forced vibrations of rectangular plates retaining non-linearities in rotations and thickness deformation," *International Journal of Non-Linear Mechanics,* vol. 67, pp. 394-404, 2014/12/01/ 2014, doi: https://doi.org/10.1016/j.ijnonlinmec.2014.10.003.

[15] M. H. Ghayesh and H. Farokhi, "Nonlinear mechanics of doubly curved shallow microshells," *International Journal of Engineering Science,* vol. 119, pp. 288-304, 2017/10/01/ 2017, doi: https://doi.org/10.1016/j.ijengsci.2017.06.015.

[16] H. Farokhi and M. H. Ghayesh, "Nonlinear mechanical behaviour of microshells," *International Journal of Engineering Science,* vol. 127, pp. 127-144, 2018/06/01/ 2018, doi: https://doi.org/10.1016/j.ijengsci.2018.02.009.

[17] G. Watts, M. K. Singha, and S. Pradyumna, "A numerical study on the nonlinear behavior of corner supported flat and curved panels," *Archive of Applied Mechanics,* vol. 88, no. 4, pp. 503-516, 2018/04/01 2018, doi: 10.1007/s00419-017-1322-1.

[18] G. Watts, M. K. Singha, and S. Pradyumna, "Nonlinear bending and snap-through instability analyses of conical shell panels using element free Galerkin method," *Thin-Walled Structures,* vol. 122, pp. 452-462, 2018/01/01/ 2018, doi: https://doi.org/10.1016/j.tws.2017.10.027.

[19] Y.-X. Zhao, T. Liu, and Z.-M. Li, "Nonlinear bending analysis of a 3D braided composite cylindrical panel subjected to transverse loads in thermal environments," *Chinese Journal of Aeronautics,* vol. 31, no. 8, pp. 1716-1727, 2018/08/01/ 2018, doi: https://doi.org/10.1016/j.cja.2018.03.022.

[20] M. Amabili and J. N. Reddy, "The nonlinear, third-order thickness and shear deformation theory for statics and dynamics of laminated composite shells," *Composite Structures,* vol. 244, p. 112265, 2020/07/15/ 2020, doi: https://doi.org/10.1016/j.compstruct.2020.112265.

[21] J. N. Reddy and W. C. Chao, "Nonlinear bending of bimodular-material plates," *International Journal of Solids and Structures,* vol. 19, no. 3, pp. 229-237, 1983, doi: https://doi.org/10.1016/0020-7683(83)90059-8.

[22] J. N. Reddy and W. C. Chao, "Non-linear bending of thick rectangular, laminated composite plates," *International Journal of Non-Linear Mechanics,* vol. 16, no. 3, pp. 291-301, 1981, doi: https://doi.org/10.1016/0020-7462(81)90042-1.

[23] J. N. Reddy and W. C. Chao, "Large-deflection and large-amplitude free vibrations of laminated composite-material plates," *Computers & Structures,* vol. 13, no. 1, pp. 341-347, 1981, doi: https://doi.org/10.1016/0045-7949(81)90142-5.

[24] A. K. Noor and S. J. Hartley, "Nonlinear shell analysis via mixed isoparametric elements," *Computers & Structures,* vol. 7, no. 5, pp. 615-626, 1977/10/01/ 1977, doi: https://doi.org/10.1016/0045-7949(77)90004-9.

[25] T. Kant and J. R. Kommineni, "Geometrically Non-Linear Analysis of Doubly Curved Laminated and Sandwich Fibre Reinforced Composite Shells with a Higher Order Theory and C° Finite Elements," *Journal of Reinforced Plastics and Composites,* vol. 11, no. 9, pp. 1048-1076, 1992, doi: 10.1177/073168449201100905.

[26] C.-L. Liao and J. N. Reddy, "Analysis of anisotropic, stiffened composite laminates using a continuum-based shell element," *Computers & Structures,* vol. 34, no. 6, pp. 805-815, 1990/01/01/ 1990, doi: https://doi.org/10.1016/0045-7949(90)90351-2.

[27] J. J. Lee, I.-K. Oh, I. Lee, and J. J. Rhiu, "Non-linear static and dynamic instability of complete spherical shells using mixed finite element formulation," *International Journal of Non-Linear Mechanics,* vol. 38, no. 6, pp. 923-934, 2003, doi: https://doi.org/10.1016/S0020-7462(02)00038-0.

[28] Y. X. Zhang and K. S. Kim, "Linear and Geometrically nonlinear analysis of plates and shells by a new refined non-conforming triangular plate/shell element," *Computational Mechanics,* vol. 36, no. 5, pp. 331-342, 2005, doi: 10.1007/s00466-004-0625-6.

[29] K. Y. Sze, X. H. Liu, and S. H. Lo, "Popular benchmark problems for geometric nonlinear analysis of shells," *Finite Elements in Analysis and Design,* vol. 40, no. 11, pp. 1551-1569, 2004, doi: https://doi.org/10.1016/j.finel.2003.11.001.

[30] R. A. Arciniega and J. N. Reddy, "Tensor-based finite element formulation for geometrically nonlinear analysis of shell structures," *Computer Methods in Applied Mechanics and Engineering,* vol. 196, no. 4, pp. 1048-1073, 2007/01/01/ 2007, doi: https://doi.org/10.1016/j.cma.2006.08.014.

[31] Y. Urthaler and J. N. Reddy, "A Mixed Finite Element for the Nonlinear Bending Analysis of Laminated Composite Plates Based on FSDT," *Mechanics of Advanced Materials and Structures,* vol. 15, no. 5, pp. 335-354, 2008/04/15 2008, doi: 10.1080/15376490802045671.

[32] A. Lal, B. N. Singh, and S. Anand, "Nonlinear bending response of laminated composite spherical shell panel with system randomness subjected to hygro-thermo-mechanical loading," *International Journal of Mechanical Sciences,* vol. 53, no. 10, pp. 855-866, 2011/10/01/ 2011, doi: https://doi.org/10.1016/j.ijmecsci.2011.07.008.

[33] M. Rezaiee-Pajand and E. Arabi, "A curved triangular element for nonlinear analysis of laminated shells," *Composite Structures,* vol. 153, pp. 538-548, 2016/10/01/ 2016, doi: https://doi.org/10.1016/j.compstruct.2016.06.052.

[34] M. M. Shokrieh and A. Nouri Parkestani, "Post buckling analysis of shallow composite shells based on the third order shear deformation theory," *Aerospace Science and Technology*, vol. 66, pp. 332-341, 2017/07/01/ 2017, doi: https://doi.org/10.1016/j.ast.2017.01.011.

[35] Ö. Civalek, "Nonlinear analysis of thin rectangular plates on Winkler–Pasternak elastic foundations by DSC–HDQ methods," *Applied Mathematical Modelling*, vol. 31, no. 3, pp. 606-624, 2007/03/01/ 2007, doi: https://doi.org/10.1016/j.apm.2005.11.023.

[36] Ö. Civalek, "Geometrically nonlinear dynamic analysis of doubly curved isotropic shells resting on elastic foundation by a combination of harmonic differential quadrature-finite difference methods," *International Journal of Pressure Vessels and Piping*, vol. 82, no. 6, pp. 470-479, 2005, doi: https://doi.org/10.1016/j.ijpvp.2004.12.003.

[37] A. K. Baltacıoglu, B. Akgöz, and Ö. Civalek, "Nonlinear static response of laminated composite plates by discrete singular convolution method," *Composite Structures*, vol. 93, no. 1, pp. 153-161, 2010/12/01/ 2010, doi: https://doi.org/10.1016/j.compstruct.2010.06.005.

[38] C. W. Bert, S. K. Jang, and A. G. Striz, "Nonlinear bending analysis of orthotropic rectangular plates by the method of differential quadrature," *Computational Mechanics*, vol. 5, no. 2, pp. 217-226, 1989/03/01 1989, doi: 10.1007/BF01046487.

[39] P. Malekzadeh and A. R. Setoodeh, "Large deformation analysis of moderately thick laminated plates on nonlinear elastic foundations by DQM," *Composite Structures*, vol. 80, no. 4, pp. 569-579, 2007/10/01/ 2007, doi: https://doi.org/10.1016/j.compstruct.2006.07.004.

[40] Ö. Kalbaran and H. Kurtaran, "Large Displacement Static Analysis of Composite Elliptic Panels of Revolution having Variable Thickness and Resting on Winkler-Pasternak Elastic Foundation," *Latin American Journal of Solids and Structures*, vol. 16, no. 9, 2019, doi: https://doi.org/10.1590/1679-78255842.

[41] J. Alamatian and J. Rezaeepazhand, "Nonlinear bending analysis of variable cross-section laminated plates using the dynamic relaxation method," *Journal of*

*Mechanical Science and Technology*, vol. 30, no. 2, pp. 783-788, 2016/02/01 2016, doi: 10.1007/s12206-016-0133-6.

[42] M. Mehrabian and M. E. Golmakani, "Nonlinear bending analysis of radial-stiffened annular laminated sector plates with dynamic relaxation method," *Computers & Mathematics with Applications*, vol. 69, no. 10, pp. 1272-1302, 2015/05/01/ 2015, doi: https://doi.org/10.1016/j.camwa.2015.03.021.

[43] J. N. Reddy, *Mechanics of laminated composite plates and shells : theory and analysis*. Boca Raton: CRC Press (in English), 2004.

[44] K. Alhazza and A. Nayfeh, "Nonlinear vibrations of doubly-curved cross-ply shallow shells,"42 AIAA/ASME/AHS/ASC Structures, Structural Dynamics, and Materials Conference and Exhibition, Seattle, WA, 16-19 April 2001, doi: https://doi.org/10.2514/6.2001-1661.

[45] M. Amabili, *Nonlinear Vibrations and Stability of Shells and Plates*. Cambridge: Cambridge University Press, 2008.

[46] R. J. Asaro and V. A. Lubarda, *Mechanics of solids and materials* (Cambridge books online.). Cambridge ;: Cambridge University Press (in English), 2006.

[47] J. N. Reddy, *An Introduction to Continuum Mechanics*. Cambridge: Cambridge University Press, 2013.

[48] I. D. Breslavsky and K. V. Avramov, "Effect of boundary condition nonlinearities on free large-amplitude vibrations of rectangular plates," *Nonlinear Dynamics*, vol. 74, no. 3, pp. 615-627, 2013/11/01 2013, doi: 10.1007/s11071-013-0993-6.

[49] M. Amabili, "Nonlinear vibrations of rectangular plates with different boundary conditions: theory and experiments," *Computers & Structures*, vol. 82, no. 31, pp. 2587-2605, 2004, doi: https://doi.org/10.1016/j.compstruc.2004.03.077.

[50] A. C. Ugural, *Plates and shells : theory and analysis* (CRC Series in Applied and Computational Mechanics). Boca Raton: CRC Press, Taylor & Francis Group (in English), 2018.

[51] R. D. Blevins, *Formulas for Natural Frequency and Mode Shape*. Krieger, 1995.

[52] G. A. Vogl and M. W. Hyer, "Natural vibration of unsymmetric cross-ply laminates," *Journal of Sound and Vibration*, vol. 330, no. 20, pp. 4764-4779, 2011, doi: https://doi.org/10.1016/j.jsv.2011.03.014.

## Appendix. The Galerkin's Discretization

The Galerkin's discretization of terms appear in the equations of motion is outlined in this appendix.

$$\begin{aligned}
&\int_0^{L_x}\int_0^{L_y}\frac{\partial^2 w_0}{\partial x^2}\frac{\partial^2 w_0}{\partial y^2}\psi_i(x)\,\psi_j(y)\,dy\,dx \\
&=\int_0^{L_x}\int_0^{L_y}\left[\sum_{m=1}^{N}\sum_{n=1}^{N}X_m''(x)\,Y_n(y)\,q_{mn}(t)\right] \\
&\times\left[\sum_{p=1}^{N}\sum_{q=1}^{N}X_p(x)\,Y_q''(y)\,q_{pq}(t)\right]\psi_i(x)\,\psi_j(y)\,dy\,dx \\
&=\left[\int_0^{L_x}\sum_{m=1}^{N}\sum_{p=1}^{N}X_m''(x)\,X_p(x)\,\psi_i(x)\,dx\right] \\
&\times\left[\int_0^{L_y}\sum_{n=1}^{N}\sum_{q=1}^{N}Y_n(y)\,Y_q''(y)\,\psi_j(y)\,dy\right]q_{mn}(t)\,q_{pq}(t)
\end{aligned} \tag{A.1}$$

$$\int_0^{L_x}X_m''(x)\,X_p(x)\,\psi_i(x)\,dx=a_{mpi}^{\phi x} \tag{A.2}$$

$$\int_0^{L_y}Y_q''(y)\,Y_n(y)\,\psi_j(y)\,dy=a_{qnj}^{\phi y} \tag{A.3}$$

Thus we have

$$\begin{aligned}
&\int_0^{L_x}\int_0^{L_y}\frac{\partial^2 w_0}{\partial x^2}\frac{\partial^2 w_0}{\partial y^2}\psi_i(x)\,\psi_j(y)\,dy\,dx \\
&=\sum_{m=1}^{N}\sum_{n=1}^{N}\sum_{p=1}^{N}\sum_{q=1}^{N}a_{mpi}^{\phi x}\,a_{qnj}^{\phi y}\,q_{mn}(t)\,q_{pq}(t)
\end{aligned} \tag{A.4}$$

$$\int_0^{L_x}\int_0^{L_y}\frac{\partial^4\phi}{\partial x^4}\psi_i(x)\,\psi_j(y)\,dy\,dx$$

$$=\int_0^{L_x}\int_0^{L_y}\sum_{m=1}^{N}\sum_{n=1}^{N}\psi_m''''(x)\,\psi_n(y)\,F_{mn}(t)\,\psi_i(x)\,\psi_j(y)\,dy\,dx$$

$$=\left[\int_0^{L_x}\sum_{m=1}^{N}\psi_m''''(x)\,\psi_i(x)\,dx\right]\left[\int_0^{L_y}\sum_{n=1}^{N}\psi_n(y)\,\psi_j(y)\,dy\right]F_{mn}(t) \tag{A.5}$$

$$\int_0^{L_x}\psi_m''''(x)\,\psi_i(x)\,dx=k_{mi}^{\phi x} \tag{A.6}$$

$$\int_0^{L_y}\psi_n(y)\,\psi_j(y)\,dy=d_{nj}^{\phi y} \tag{A.7}$$

Thus we have

$$\int_0^{L_x}\int_0^{L_y}\frac{\partial^4\phi}{\partial x^4}\psi_i(x)\,\psi_j(y)\,dy\,dx=\sum_{m=1}^{N}\sum_{n=1}^{N}k_{mi}^{\phi x}\,d_{nj}^{\phi y}\,F_{mn}(t) \tag{A.8}$$

$$\int_0^{L_x}\int_0^{L_y}\frac{\partial^4\phi}{\partial y^4}\psi_i(x)\,\psi_j(y)\,dy\,dx$$

$$=\int_0^{L_x}\int_0^{L_y}\sum_{m=1}^{N}\sum_{n=1}^{N}\psi_m(x)\,\psi_n''''(y)\,F_{mn}(t)\,\psi_i(x)\,\psi_j(y)\,dy\,dx$$

$$=\left[\int_0^{L_x}\sum_{m=1}^{N}\psi_m(x)\,\psi_i(x)\,dx\right]\left[\int_0^{L_y}\sum_{n=1}^{N}\psi_n''''(y)\,\psi_j(y)\,dy\right]F_{mn}(t) \tag{A.9}$$

$$\int_0^{L_x}\psi_m(x)\,\psi_i(x)\,dx=d_{mi}^{\phi x} \tag{A.10}$$

$$\int_0^{L_y}\psi_n''''(y)\,\psi_j(y)\,dy=k_{nj}^{\phi y} \tag{A.11}$$

Thus we get

$$\int_0^{L_x}\int_0^{L_y}\frac{\partial^4\phi}{\partial y^4}\psi_i(x)\,\psi_j(y)\,dy\,dx=\sum_{m=1}^{N}\sum_{n=1}^{N}d_{mi}^{\phi x}\,k_{nj}^{\phi y}\,F_{mn}(t) \tag{A.12}$$

$$\int_0^{L_x}\int_0^{L_y}\frac{\partial^4\phi}{\partial x^2\partial y^2}\psi_i(x)\,\psi_j(y)\,dy\,dx$$

$$=\int_0^{L_x}\int_0^{L_y}\sum_{m=1}^{N}\sum_{n=1}^{N}\psi_m''(x)\,\psi_n''(y)\,F_{mn}(t)\,\psi_i(x)\,\psi_j(y)\,dy\,dx$$

$$=\left[\int_0^{L_x}\sum_{m=1}^{N}\psi_m''(x)\,\psi_i(x)\,dx\right]\left[\int_0^{L_y}\sum_{n=1}^{N}\psi_n''(y)\,\psi_j(y)\,dy\right]F_{mn}(t) \tag{A.13}$$

$$\int_0^{L_x}\psi_m''(x)\,\psi_i(x)\,dx=r_{mi}^{\phi x} \tag{A.14}$$

$$\int_0^{L_y}\psi_n''(y)\,\psi_j(y)\,dy=r_{nj}^{\phi y} \tag{A.15}$$

Thus we have

$$\int_0^{L_x}\int_0^{L_y}\frac{\partial^4\phi}{\partial x^2\partial y^2}\psi_i(x)\,\psi_j(y)\,dy\,dx=\sum_{m=1}^{N}\sum_{n=1}^{N}r_{mi}^{\phi x}\,r_{nj}^{\phi y}\,F_{mn}(t) \tag{A.16}$$

$$\int_0^{L_x}\int_0^{L_y}\frac{\partial^4 w_0}{\partial x^4}\psi_i(x)\,\psi_j(y)\,dy\,dx$$

$$=\int_0^{L_x}\int_0^{L_y}\sum_{m=1}^{N}\sum_{n=1}^{N}X_m''''(x)\,Y_n(y)\,q_{mn}(t)\,\psi_i(x)\,\psi_j(y)\,dy\,dx$$

$$=\left[\int_0^{L_x}\sum_{m=1}^{N}X_m''''(x)\,\psi_i(x)\,dx\right]\left[\int_0^{L_y}\sum_{n=1}^{N}Y_n(y)\,\psi_j(y)\,dy\right]q_{mn}(t) \tag{A.17}$$

$$\int_0^{L_x}X_m''''(x)\,\psi_i(x)\,dx=e_{mi}^{\phi x} \tag{A.18}$$

$$\int_0^{L_y} Y_n(y)\,\psi_j(y)\,dy = g_{nj}^{\phi y} \tag{A.19}$$

Thus we get

$$\int_0^{L_x}\int_0^{L_y} \frac{\partial^4 w_0}{\partial x^4}\psi_i(x)\,\psi_j(y)\,dy\,dx = \sum_{m=1}^{N}\sum_{n=1}^{N} e_{mi}^{\phi x}\, g_{nj}^{\phi y}\, q_{mn}(t) \tag{A.20}$$

$$\int_0^{L_x}\int_0^{L_y} \frac{\partial^4 w_0}{\partial y^4}\psi_i(x)\,\psi_j(y)\,dy\,dx$$

$$= \int_0^{L_x}\int_0^{L_y} \sum_{m=1}^{N}\sum_{n=1}^{N} X_m(x)\,Y_n''''(y)\,q_{mn}(t)\,\psi_i(x)\,\psi_j(y)\,dy\,dx$$

$$= \left[\int_0^{L_x} \sum_{m=1}^{N} X_m(x)\,\psi_i(x)\,dx\right]\left[\int_0^{L_y} \sum_{n=1}^{N} Y_n''''(y)\,\psi_j(y)\,dy\right] q_{mn}(t) \tag{A.21}$$

$$\int_0^{L_x} X_m(x)\,\psi_i(x)\,dx = g_{mi}^{\phi x} \tag{A.22}$$

$$\int_0^{L_y} Y_n''''(y)\,\psi_j(y)\,dy = e_{nj}^{\phi y} \tag{A.23}$$

Thus we have

$$\int_0^{L_x}\int_0^{L_y} \frac{\partial^4 w_0}{\partial y^4}\psi_i(x)\,\psi_j(y)\,dy\,dx = \sum_{m=1}^{N}\sum_{n=1}^{N} g_{mi}^{\phi x}\, e_{nj}^{\phi y}\, q_{mn}(t) \tag{A.24}$$

$$\int_0^{L_x}\int_0^{L_y} \frac{\partial^4 w_0}{\partial x^2\partial y^2}\psi_i(x)\,\psi_j(y)\,dy\,dx$$

$$= \int_0^{L_x}\int_0^{L_y} \sum_{m=1}^{N}\sum_{n=1}^{N} X_m''(x)\,Y_n''(y)\,q_{mn}(t)\,\psi_i(x)\,\psi_j(y)\,dy\,dx$$

$$= \left[\int_0^{L_x} \sum_{m=1}^{N} X_m''(x)\,\psi_i(x)\,dx\right]\left[\int_0^{L_y} \sum_{n=1}^{N} Y_n''(y)\,\psi_j(y)\,dy\right] q_{mn}(t) \tag{A.25}$$

$$\int_0^{L_x} X_m''(x)\,\psi_i(x)\,dx = h_{mi}^{\phi x} \tag{A.26}$$

$$\int_0^{L_y} Y_n''(y)\,\psi_j(y)\,dy = h_{nj}^{\phi y} \tag{A.27}$$

Thus we get

$$\int_0^{L_x}\int_0^{L_y} \frac{\partial^4 w_0}{\partial x^2 \partial y^2}\psi_i(x)\,\psi_j(y)\,dy\,dx = \sum_{m=1}^{N}\sum_{n=1}^{N} h_{mi}^{\phi x}\,h_{nj}^{\phi y}\,q_{mn}(t) \tag{A.28}$$

$$\int_0^{L_x}\int_0^{L_y} \frac{\partial^2 w_0}{\partial y^2}\psi_i(x)\,\psi_j(y)\,dy\,dx$$

$$= \int_0^{L_x}\int_0^{L_y} \sum_{m=1}^{N}\sum_{n=1}^{N} X_m(x)\,Y_n''(y)\,q_{mn}(t)\,\psi_i(x)\,\psi_j(y)\,dy\,dx$$

$$= \left[\int_0^{L_x} \sum_{m=1}^{N} X_m(x)\,\psi_i(x)\,dx\right]\left[\int_0^{L_y} \sum_{n=1}^{N} Y_n''(y)\,\psi_j(y)\,dy\right] q_{mn}(t) \tag{A.29}$$

Based on the equations (A.22) and (A.27) we will obtain

$$\int_0^{L_x}\int_0^{L_y} \frac{\partial^2 w_0}{\partial y^2}\psi_i(x)\,\psi_j(y)\,dy\,dx = \sum_{m=1}^{N}\sum_{n=1}^{N} g_{mi}^{\phi x}\,h_{nj}^{\phi y}\,q_{mn}(t) \tag{A.30}$$

$$\int_0^{L_x}\int_0^{L_y} \frac{\partial^2 w_0}{\partial x^2}\psi_i(x)\,\psi_j(y)\,dy\,dx$$

$$= \int_0^{L_x}\int_0^{L_y} \sum_{m=1}^{N}\sum_{n=1}^{N} X_m''(x)\,Y_n(y)\,q_{mn}(t)\,\psi_i(x)\,\psi_j(y)\,dy\,dx$$

$$= \left[\int_0^{L_x} \sum_{m=1}^{N} X_m''(x)\,\psi_i(x)\,dx\right]\left[\int_0^{L_y} \sum_{n=1}^{N} Y_n(y)\,\psi_j(y)\,dy\right] q_{mn}(t) \tag{A.31}$$

Based on the equations (A.19) and (A.26) we will obtain

$$\int_0^{L_x}\int_0^{L_y}\frac{\partial^2 w_0}{\partial x^2}\psi_i(x)\,\psi_j(y)\,dy\,dx=\sum_{m=1}^{N}\sum_{n=1}^{N}h_{mi}^{\phi x}\,g_{nj}^{\phi y}\,q_{mn}(t) \tag{A.32}$$

$$\begin{aligned}&\int_0^{L_x}\int_0^{L_y}\frac{\partial^2 w_0}{\partial x^2}\frac{\partial^2 \phi}{\partial y^2}X_i(x)\,Y_j(y)\,dy\,dx\\&=\int_0^{L_x}\int_0^{L_y}\left[\sum_{m=1}^{N}\sum_{n=1}^{N}X_m''(x)\,Y_n(y)\,q_{mn}(t)\right]\\&\times\left[\sum_{p=1}^{N}\sum_{q=1}^{N}\psi_p(x)\,\psi_q''(y)\,F_{pq}(t)\right]X_i(x)\,Y_j(y)\,dy\,dx\\&=\left[\int_0^{L_x}\sum_{m=1}^{N}\sum_{p=1}^{N}X_m''(x)\,\psi_p(x)\,X_i(x)\,dx\right]\\&\times\left[\int_0^{L_x}\sum_{n=1}^{N}\sum_{q=1}^{N}Y_n(y)\,\psi_q''(y)\,Y_j(y)\,dx\right]q_{mn}(t)\,F_{pq}(t)\end{aligned} \tag{A.33}$$

$$\int_0^{L_x}X_m''(x)\,\psi_p(x)\,X_i(x)\,dx=a_{mpi}^{wx} \tag{A.34}$$

$$\int_0^{L_x}\psi_q''(y)\,Y_n(y)\,Y_j(y)\,dx=b_{qnj}^{wy} \tag{A.35}$$

Thus we have

$$\begin{aligned}&\int_0^{L_x}\int_0^{L_y}\frac{\partial^2 w_0}{\partial x^2}\frac{\partial^2 \phi}{\partial y^2}X_i(x)\,Y_j(y)\,dy\,dx\\&=\sum_{m=1}^{N}\sum_{n=1}^{N}\sum_{p=1}^{N}\sum_{q=1}^{N}a_{mpi}^{wx}\,b_{qnj}^{wy}\,q_{mn}(t)\,F_{pq}(t)\end{aligned} \tag{A.36}$$

$$\int_0^{L_x}\int_0^{L_y}\frac{\partial^2 w_0}{\partial y^2}\frac{\partial^2 \phi}{\partial x^2}X_i(x)\,Y_j(y)\,dy\,dx$$

$$=\int_0^{L_x}\int_0^{L_y}\left[\sum_{m=1}^{N}\sum_{n=1}^{N}X_m(x)\,Y_n''(y)\,q_{mn}(t)\right]$$

$$\times\left[\sum_{p=1}^{N}\sum_{q=1}^{N}\psi_p''(x)\,\psi_q(y)\,F_{pq}(t)\right]X_i(x)\,Y_j(y)\,dy\,dx$$

$$=\left[\int_0^{L_x}\sum_{m=1}^{N}\sum_{p=1}^{N}X_m(x)\,\psi_p''(x)\,X_i(x)\,dx\right]$$

$$\times\left[\int_0^{L_x}\sum_{n=1}^{N}\sum_{q=1}^{N}Y_n''(y)\,\psi_q(y)\,Y_j(y)\,dx\right]q_{mn}(t)\,F_{pq}(t) \qquad \text{(A.37)}$$

$$\int_0^{L_x}\psi_p''(x)\,X_m(x)\,X_i(x)\,dx=b_{pmi}^{wx} \qquad \text{(A.38)}$$

$$\int_0^{L_x}Y_n''(y)\,\psi_q(y)\,Y_j(y)\,dx=a_{nqj}^{wy} \qquad \text{(A.39)}$$

Thus we get

$$\int_0^{L_x}\int_0^{L_y}\frac{\partial^2 w_0}{\partial y^2}\frac{\partial^2 \phi}{\partial x^2}X_i(x)\,Y_j(y)\,dy\,dx$$

$$=\sum_{m=1}^{N}\sum_{n=1}^{N}\sum_{p=1}^{N}\sum_{q=1}^{N}b_{pmi}^{wx}\,a_{nqj}^{wy}\,q_{mn}(t)\,F_{pq}(t) \qquad \text{(A.40)}$$

$$\int_0^{L_x}\int_0^{L_y}\frac{\partial^2 w_0}{\partial x\partial y}\frac{\partial^2 \phi}{\partial x\partial y}X_i(x)\,Y_j(y)\,dy\,dx$$
$$=\int_0^{L_x}\int_0^{L_y}\left[\sum_{m=1}^{N}\sum_{n=1}^{N}X'_m(x)\,Y'_n(y)\,q_{mn}(t)\right]$$
$$\times\left[\sum_{p=1}^{N}\sum_{q=1}^{N}\psi'_p(x)\,\psi'_q(y)\,F_{pq}(t)\right]X_i(x)\,Y_j(y)\,dy\,dx$$
$$=\left[\int_0^{L_x}\sum_{m=1}^{N}\sum_{p=1}^{N}X'_m(x)\,\psi'_p(x)\,X_i(x)\,dx\right]$$
$$\times\left[\int_0^{L_x}\sum_{n=1}^{N}\sum_{q=1}^{N}Y'_n(y)\,\psi'_q(y)\,Y_j(y)\,dx\right]q_{mn}(t)\,F_{pq}(t) \qquad \text{(A.41)}$$

$$\int_0^{L_x}X'_m(x)\,\psi'_p(x)\,X_i(x)\,dx=c_{mpi}^{wx} \qquad \text{(A.42)}$$

$$\int_0^{L_x}Y'_n(y)\,\psi'_q(y)\,Y_j(y)\,dx=c_{nqj}^{wy} \qquad \text{(A.43)}$$

Thus we have

$$\int_0^{L_x}\int_0^{L_y}\frac{\partial^2 w_0}{\partial x\partial y}\frac{\partial^2 \phi}{\partial x\partial y}X_i(x)\,Y_j(y)\,dy\,dx$$
$$=\sum_{m=1}^{N}\sum_{n=1}^{N}\sum_{p=1}^{N}\sum_{q=1}^{N}c_{mpi}^{wx}\,c_{nqj}^{wy}\,q_{mn}(t)\,F_{pq}(t) \qquad \text{(A.44)}$$

$$\int_0^{L_x}\int_0^{L_y}\frac{\partial^2 w_0}{\partial t^2}\,X_i(x)\,Y_j(y)\,dy\,dx$$
$$=\int_0^{L_x}\int_0^{L_y}\sum_{m=1}^{N}\sum_{n=1}^{N}X_m(x)\,Y_n(y)\,\ddot{q}_{mn}(t)\,X_i(x)\,Y_j(y)\,dy\,dx$$
$$=\left[\int_0^{L_x}\sum_{m=1}^{N}X_m(x)\,X_i(x)\,dx\right]\left[\int_0^{L_y}\sum_{n=1}^{N}Y_n(y)\,Y_j(y)\,dy\right]\ddot{q}_{mn}(t) \qquad \text{(A.45)}$$

$$\int_0^{L_x} X_m(x)\, X_i(x)\, dx = d_{mi}^{wx} \tag{A.46}$$

$$\int_0^{L_y} Y_n(y)\, Y_j(y)\, dy = d_{nj}^{wy} \tag{A.47}$$

Thus we obtain

$$\int_0^{L_x}\int_0^{L_y} \frac{\partial^2 w_0}{\partial t^2}\, X_i(x)\, Y_j(y) dy\, dx = \sum_{m=1}^{N}\sum_{n=1}^{N} d_{mi}^{wx}\, d_{nj}^{wy}\, \ddot{q}_{mn}(t) \tag{A.48}$$

$$\int_0^{L_x}\int_0^{L_y} \frac{\partial^4 \phi}{\partial x^4} X_i(x)\, Y_j(y)\, dy\, dx$$

$$= \int_0^{L_x}\int_0^{L_y} \sum_{m=1}^{N}\sum_{n=1}^{N} \psi_m''''(x)\, \psi_n(y)\, F_{mn}(t)\, X_i(x)\, Y_j(y)\, dy\, dx$$

$$= \left[\int_0^{L_x} \sum_{m=1}^{N} \psi_m''''(x)\, X_i(x)\, dx\right]\left[\int_0^{L_y} \sum_{n=1}^{N} \psi_n(y)\, Y_j(y)\, dy\right] F_{mn}(t) \tag{A.49}$$

$$\int_0^{L_x} \psi_m''''(x)\, X_i(x)\, dx = e_{mi}^{wx} \tag{A.50}$$

$$\int_0^{L_y} \psi_n(y)\, Y_j(y)\, dy = g_{nj}^{wy} \tag{A.51}$$

Thus we have

$$\int_0^{L_x}\int_0^{L_y} \frac{\partial^4 \phi}{\partial x^4} X_i(x)\, Y_j(y)\, dy\, dx = \sum_{m=1}^{N}\sum_{n=1}^{N} e_{mi}^{wx}\, g_{nj}^{wy}\, F_{mn}(t) \tag{A.52}$$

$$\int_0^{L_x}\int_0^{L_y}\frac{\partial^4\phi}{\partial y^4}X_i(x)\,Y_j(y)\,dy\,dx$$

$$=\int_0^{L_x}\int_0^{L_y}\sum_{m=1}^{N}\sum_{n=1}^{N}\psi_m(x)\,\psi_n''''(y)\,F_{mn}(t)\,X_i(x)\,Y_j(y)\,dy\,dx$$

$$=\left[\int_0^{L_x}\sum_{m=1}^{N}\psi_m(x)\,X_i(x)\,dx\right]\left[\int_0^{L_y}\sum_{n=1}^{N}\psi_n''''(y)\,Y_j(y)\,dy\right]F_{mn}(t) \tag{A.53}$$

$$\int_0^{L_x}\psi_m(x)\,X_i(x)\,dx=g_{mi}^{wx} \tag{A.54}$$

$$\int_0^{L_y}\psi_n''''(y)\,Y_j(y)\,dy=e_{nj}^{wy} \tag{A.55}$$

Thus we get

$$\int_0^{L_x}\int_0^{L_y}\frac{\partial^4\phi}{\partial y^4}X_i(x)\,Y_j(y)\,dy\,dx=\sum_{m=1}^{N}\sum_{n=1}^{N}g_{mi}^{wx}\,e_{nj}^{wy}\,F_{mn}(t) \tag{A.56}$$

$$\int_0^{L_x}\int_0^{L_y}\frac{\partial^4\phi}{\partial x^2\partial y^2}X_i(x)\,Y_j(y)\,dy\,dx$$

$$=\int_0^{L_x}\int_0^{L_y}\sum_{m=1}^{N}\sum_{n=1}^{N}\psi_m''(x)\,\psi_n''(y)\,F_{mn}(t)\,X_i(x)\,Y_j(y)\,dy\,dx$$

$$=\left[\int_0^{L_x}\sum_{m=1}^{N}\psi_m''(x)\,X_i(x)\,dx\right]\left[\int_0^{L_y}\sum_{n=1}^{N}\psi_n''(y)\,Y_j(y)\,dy\right]F_{mn}(t) \tag{A.57}$$

$$\int_0^{L_x}\psi_m''(x)\,X_i(x)\,dx=h_{mi}^{wx} \tag{A.58}$$

$$\int_0^{L_y}\psi_n''(y)\,Y_j(y)\,dy=h_{nj}^{wy} \tag{A.59}$$

Thus we obtain

$$\int_0^{L_x}\int_0^{L_y}\frac{\partial^4\phi}{\partial x^2\partial y^2}X_i(x)\,Y_j(y)\,dy\,dx=\sum_{m=1}^{N}\sum_{n=1}^{N}h_{mi}^{wx}\,h_{nj}^{wy}\,F_{mn}(t) \tag{A.60}$$

$$\int_0^{L_x}\int_0^{L_y}\frac{\partial^4 w_0}{\partial x^4}\,X_i(x)\,Y_j(y)\,dy\,dx$$

$$=\int_0^{L_x}\int_0^{L_y}\sum_{m=1}^{N}\sum_{n=1}^{N}X_m''''(x)\,Y_n(y)\,q_{mn}(t)\,X_i(x)\,Y_j(y)\,dy\,dx$$

$$=\left[\int_0^{L_x}\sum_{m=1}^{N}X_m''''(x)\,X_i(x)\,dx\right]\left[\int_0^{L_y}\sum_{n=1}^{N}Y_n(y)\,Y_j(y)\,dy\right]q_{mn}(t) \tag{A.61}$$

$$\int_0^{L_x}X_m''''(x)\,X_i(x)\,dx=k_{mi}^{wx} \tag{A.62}$$

Based on the equation (A.47) we will get

$$\int_0^{L_x}\int_0^{L_y}\frac{\partial^4 w_0}{\partial x^4}\,X_i(x)\,Y_j(y)\,dy\,dx=\sum_{m=1}^{N}\sum_{n=1}^{N}k_{mi}^{wx}\,d_{nj}^{wy}\,q_{mn}(t) \tag{A.63}$$

$$\int_0^{L_x}\int_0^{L_y}\frac{\partial^4 w_0}{\partial y^4}\,X_i(x)\,Y_j(y)\,dy\,dx$$

$$=\int_0^{L_x}\int_0^{L_y}\sum_{m=1}^{N}\sum_{n=1}^{N}X_m(x)\,Y_n''''(y)\,q_{mn}(t)\,X_i(x)\,Y_j(y)\,dy\,dx$$

$$=\left[\int_0^{L_x}\sum_{m=1}^{N}X_m(x)\,X_i(x)\,dx\right]\left[\int_0^{L_y}\sum_{n=1}^{N}Y_n''''(y)\,Y_j(y)\,dy\right]q_{mn}(t) \tag{A.64}$$

$$\int_0^{L_y}Y_n''''(y)\,Y_j(y)\,dy=k_{nj}^{wy} \tag{A.65}$$

Based on the equation (A.46) we will obtain

$$\int_0^{L_x}\int_0^{L_y}\frac{\partial^4 w_0}{\partial y^4}\,X_i(x)\,Y_j(y)\,dy\,dx=\sum_{m=1}^{N}\sum_{n=1}^{N}d_{mi}^{wx}\,k_{nj}^{wy}\,q_{mn}(t) \tag{A.66}$$

$$\int_0^{L_x}\int_0^{L_y}\frac{\partial^4 w_0}{\partial x^2\partial y^2}X_i(x)\,Y_j(y)\,dy\,dx$$

$$=\int_0^{L_x}\int_0^{L_y}\sum_{m=1}^{N}\sum_{n=1}^{N}X_m''(x)\,Y_n''(y)\,q_{mn}(t)\,X_i(x)\,Y_j(y)\,dy\,dx$$

$$=\left[\int_0^{L_x}\sum_{m=1}^{N}X_m''(x)\,X_i(x)\,dx\right]\left[\int_0^{L_y}\sum_{n=1}^{N}Y_n''(y)\,Y_j(y)\,dy\right]q_{mn}(t) \tag{A.67}$$

$$\int_0^{L_x}X_m''(x)\,X_i(x)\,dx=r_{mi}^{wx} \tag{A.68}$$

$$\int_0^{L_y}Y_n''(y)\,Y_j(y)\,dy=r_{nj}^{wy} \tag{A.69}$$

Thus we get

$$\int_0^{L_x}\int_0^{L_y}\frac{\partial^4 w_0}{\partial x^2\partial y^2}X_i(x)\,Y_j(y)\,dy\,dx=\sum_{m=1}^{N}\sum_{n=1}^{N}r_{mi}^{wx}\,r_{nj}^{wy}\,q_{mn}(t) \tag{A.70}$$

$$\int_0^{L_x}\int_0^{L_y}\frac{\partial^2\phi}{\partial y^2}X_i(x)\,Y_j(y)\,dy\,dx$$

$$=\int_0^{L_x}\int_0^{L_y}\sum_{m=1}^{N}\sum_{n=1}^{N}\psi_m(x)\,\psi_n''(y)\,F_{mn}(t)\,X_i(x)\,Y_j(y)\,dy\,dx$$

$$=\left[\int_0^{L_x}\sum_{m=1}^{N}\psi_m(x)\,X_i(x)\,dx\right]\left[\int_0^{L_y}\sum_{n=1}^{N}\psi_n''(y)\,Y_j(y)\,dy\right]F_{mn}(t) \tag{A.71}$$

Based on the equations (A.54) and (A.59) we will have

$$\int_0^{L_x}\int_0^{L_y}\frac{\partial^2\phi}{\partial y^2}X_i(x)\,Y_j(y)\,dy\,dx=\sum_{m=1}^{N}\sum_{n=1}^{N}g_{mi}^{wx}\,h_{nj}^{wy}\,F_{mn}(t) \tag{A.72}$$

$$\int_0^{L_x}\int_0^{L_y}\frac{\partial^2\phi}{\partial x^2}X_i(x)\,Y_j(y)\,dy\,dx$$

$$=\int_0^{L_x}\int_0^{L_y}\sum_{m=1}^{N}\sum_{n=1}^{N}\psi_m''(x)\,\psi_n(y)\,F_{mn}(t)\,X_i(x)\,Y_j(y)\,dy\,dx$$

$$=\left[\int_0^{L_x}\sum_{m=1}^{N}\psi_m''(x)\,X_i(x)\,dx\right]\left[\int_0^{L_y}\sum_{n=1}^{N}\psi_n(y)\,Y_j(y)\,dy\right]F_{mn}(t) \qquad \text{(A.73)}$$

Based on the equations (A.51) and (A.58) we will obtain

$$\int_0^{L_x}\int_0^{L_y}\frac{\partial^2\phi}{\partial x^2}X_i(x)\,Y_j(y)\,dy\,dx=\sum_{m=1}^{N}\sum_{n=1}^{N}h_{mi}^{wx}\,g_{nj}^{wy}\,F_{mn}(t) \qquad \text{(A.74)}$$

## Vita

Hooman Aminipour was born in 1991, in Shiraz, Fars province, Iran. He received his primary and secondary education in Shiraz, Iran. He received his B.Sc. degree in Mechanical Engineering from the Islamic Azad University, Marvdasht Branch in 2015. From 2015 to 2018, he worked as a research assistant and co-authored 2 articles which were published in ISI international journals. In January 2019, he joined the Mechanical Engineering master's program in the American University of Sharjah as a graduate teaching assistant. During his master's study, he co-authored 2 articles which were published in ISI international journals. His research interests are in linear and nonlinear static, dynamics and wave propagation analysis of plates and shells, micro/nano-mechanics and size dependent behavior of plates and shells and functionally graded reinforced materials.